CLONING AND EXPRESSION OF A FUNCTIONALLY ACTIVE TRUNCATED *N*-GLYCOSYLATED KSHV COMPLEMENT REGULATORY PROTEIN AND IMMUNOHISTOCHEMICAL STUDIES WITH THE ANTI-KCP PEPTIDE ANTIBODY

By

Neuza Alexandra Gomes Pereira

GMSNEU001

SUBMITTED TO THE UNIVERSITY OF CAPE TOWN

In fulfilment of the requirements for the degree of

MSc (Med)

Masters in Medical Virology

Faculty of Health Sciences

UNIVERSITY OF CAPE TOWN

2005

Supervisor: Prof. GJ Kotwal, Division of Medical Virology,

University of Cape Town

DECLARATION

I, Neuza Alexandra Gomes Pereira, hereby declare that the work on which this dissertation is based is my original work (except where acknowledgements indicate otherwise) and that neither the whole work nor any part of it has been, is being, or is to be submitted for another degree in this or any other university.

I empower the university to reproduce for the purpose of research either the whole or any potion of the contents in any manner whatsoever.

Signed by candidate

Signature: ... signature removed

Date: ...14th March 2005.....

ACKNOWLEDGEMENTS

A special thanks to **Professor Girish J. Kotwal,** my project supervisor, for all his time and advice relating to my work in his laboratory.

Prof. C Boshoff of the University College London, UK is gratefully acknowledged for KSHV DNA from PEL.

I would like to thank **Associate Prof. Edward Sturrock** (IIDMM, University of Cape Town) and his collaborators in Brazil for the synthesis of the peptide used to produce the anti-KCP antibody.

Prof. D Govender (Division of Anatomical Pathology, University of Cape Town) is thankfully acknowledged for providing me with coded human tissue samples. I also thank him for advice relating to the immunohistochemical studies.

I would like to acknowledge **Heather McLeod** for all the work and enthusiasm she put into the immunohistochemical studies. I also thank her for introducing me to **Dr Krish Mafke**, to whom I'm very grateful for taking the time to proof-read my dissertation and for all the great discussions.

I would especially like to thank **Dr Khati Makobetsa** (Shoez) for allowing me to use his Western blot apparatus on many occasions during my research.

I thank GJK, the Poliomyelitis Research Foundation (PRF) and the National Research foundation (NRF) for funding during this project.

I also would like to acknowledge our lab manager **Mr Abdu Mohamed** and my fellow students in the lab, particularly **Yohannes Ghebremariam** for showing me how to carry out the hemolysis assay.

Last but not least a very special thank you to **Dr Odutayo Odunuga** (Tayo) for his unfailing support, advice and most of all for his friendship.

ABSTRACT

Kaposi sarcoma herpes virus (KSHV) is a typical DNA virus that is associated with a number of proliferative diseases including Kaposi's sarcoma. The KSHV open reading frame (ORF) 4 encodes a complement regulatory protein (Kaposi complement-binding protein, KCP) that binds complement proteins and inhibits the complement-mediated lysis of cells infected by the virus, thus providing a strategy for evasion of the host complement system. Kaposi's sarcoma is an angiogenic skin lesion that has been recognized as one of the most abundant tumours found in many parts of Southern Africa and which can occasionally become highly invasive, aggressive and capable of causing death, particularly amongst AIDS patients. It is of major significance to understand how complement control proteins (CCPs) such as KCP perform their biological functions at the molecular and structural levels, because of their potentials as therapeutic agents, their implications in the pathology and importance in the etiology of many disease conditions. This study was therefore undertaken to characterise the structure-function relationship of KCP. Based on primary sequence analysis and comparison to other functionally and structurally similar proteins, oligonucleotide primers were designed to amplify by PCR, three regions of the predicted ORF 4 from human herpes virus-8 (HHV-8) DNA isolated from a primary effusion lymphoma cell line. The PCR products were inserted by ligation into the expression vector pPIC9 to generate three recombinant plasmids for heterologous expression in the yeast, *Pichia pastoris* and to produce separately, the 4 N-terminal Sushi domains (KCP-S, small), KCP protein lacking the putative transmembrane binding domain (KCP-M, medium) and the full-length protein (KCP-F, full). Expression of the viral proteins was confirmed by SDS-PAGE and Western blot analyses using a rabbit polyclonal antibody directed against a selected peptide region that is common to all three recombinant KCPs. All the KCP proteins migrated electrophoretically as higher bands compared to their expected sizes. The lower mobilities of the proteins may be due to glycosylation since there are potential *N*- and *O*-glycosylation sites in the protein's primary sequence. Also, diffused bands were obtained in all the electrophoretic gels and Western blots carried out, which is characteristic of glycoproteins. Furthermore, the antibody recognized several larger

and smaller bands that may represent aggregates and/or degradation products respectively. Both partially purified KCP-S and KCP-S directly from expression media were able to inhibit complement-mediated lysis of sensitized sheep erythrocytes by approximately 60% in a hemolysis assay. This result confirms previous reports that recombinant KCP is twice more efficient in inhibiting the classical pathway-mediated lysis of erythrocytes than the vaccinia virus complement control protein (VCP), which also contains 4 Sushi domains. The KCP-F and KCP-M proteins did not show any significant complement inhibitory activities. Preliminary immunohistochemical studies using the same antibody were carried out to determine the expression and distribution of KCP proteins in Kaposi's sarcoma.

TABLE OF CONTENTS

DECLARATION i

ACKNOWLEDGEMENTS ii

ABSTRACT iii

TABLE OF CONTENTS v

LIST OF FIGURES x

LIST OF TABLES xiii

LIST OF SYMBOLS xiv

LIST OF ABBREVIATIONS xv

CHAPTER ONE: INTRODUCTION 1

1.1 KAPOSI'S SARCOMA ASSOCIATED HERPESVIRUS 1

1.1.1 KSHV Classification and Structure 2

1.1.2 The KSHV Genome 4

1.1.3 KSHV Lytic Replication and Latent Infection 6

1.1.4 *In Vitro* cultivation of KSHV 8

1.1.5 KSHV: A Model for Viral Oncogenesis 9

1.1.5.1 The Cell Division Cycle and its Control System 9

1.1.5.2 KSHV Oncogenic Proteins target the Cell Cycle 10

1.2 KSHV-RELATED PROLIFERATIVE DISORDERS 13

1.2.1 PEL and MCD 13

1.2.2 Kaposi's Sarcoma 14

1.2.2.1 Clinical Variants of Kaposi's Sarcoma 15

1.2.2.2 Histology of Kaposi's sarcoma 15

1.2.2.3 Current Therapy for KS 16

1.3 COMPLEMENT SYSTEM AND INFLAMMATORY RESPONSES 17

1.3.1 Host Complement Inhibitory/ Regulatory proteins 20

1.3.1.1 The C4-Binding Protein (C4BP) 21

1.3.1.2 Other Host Complement Inhibitor-An Overview 21

1.3.2 Viral Strategies of Immune System Evasion 23

1.3.3 Immunomodulators of Viral Infection 24

1.3.3.1 Examples of KSHV Chemokine Homologs 24
1.3.3.2 Examples of KSHV Cytokine Homologs 26
1.3.3.3 Examples of Complement Regulatory Proteins 26
1.3.4 The KSHV Complement Regulatory Protein 27

1.4 STATEMENT OF HYPOTHESIS 32
1.4.1 Broad Hypothesis 32
1.4.2 Specific Hypothesis 32

1.5 AIMS AND OBJECTIVES 32

CHAPTER TWO: MATERIALS AND METHODS 33

2.1 PREPARATION OF THE KSHV ORF 4 DNA CONSTRUCTS 33
2.1.1 Primer Design 33
2.1.2 PCR amplification of the KSHV ORF 4 genes from KSHV DNA 34
2.1.3 Purification of the PCR products 36
2.1.4 Measurement of DNA concentration 37
2.1.5 Preparation of competent bacterial cells 37
2.1.6 Vector pGEMT-easy DNA ligation 38
2.1.7 Transformation of competent bacterial cells 39
2.1.8 Small-scale plasmid DNA preparation 39
2.1.9 DNA sequencing of the KCP gene encoded by KSHV ORF 4 40
2.1.10 Restriction enzyme analysis of the pGEMT-easy constructs 41
2.1.11 Agarose Gel Electrophoresis 42
2.1.12 Directional analysis of the cloned genes by RE digestion 42
2.1.13 Small-scale isolation and RE analysis of pPIC9 plasmid 44
2.1.14 pGEMT DNA isolation from low-melt 1% agarose gel 44
2.1.15 Vector pPIC9 DNA ligation 45
2.1.16 RE digestion analysis of the pPIC9 DNA constructs 45

2.2 TRANSFORMATION OF *P. PASTORIS* AND SELECTION OF POSITIVE CLONES 46
2.2.1 Linearization of pPIC9 and pPIC9/KSHV ORF 4 constructs 46
2.2.2 Plasmid pPIC9 DNA isolation from low-melt 1% agarose gel 47
2.2.3 Preparation of yeast competent cells 47
2.2.4 Transformation of competent yeast cells 47
2.2.5 Isolation of genomic DNA from *Pichia* yeast transformants 48
2.2.6 Screening for Mut^+ and Mut^S transformants 49

2.2.7 PCR analysis of *Pichia* transformants 50

2.3 EXPRESSION OF THE RECOMBINANT KCPs IN *PICHIA PASTORIS* 52

2.3.1 Small and medium-scale protein expression of recombinant *Pichia* strains 52

2.3.2 Optimisation of methanol-induced production of the recombinant proteins 53

2.3.3 Concentration of the media containing secreted recombinant KCP 54

2.3.4 Small-scale Ammonium Sulphate Protein precipitation 54

2.3.5 Estimation of protein concentration using a Densitometer 55

2.4 DESIGN AND SYNTHESIS OF A POLYCLONAL ANTI-KCP PEPTIDE ANTIBODY 55

2.4.1 Peptide selection for the synthesis of the polyclonal antibody 55

2.4.2 HiTrap protein A-purification of the polyclonal anti-KCP peptide antibody 56

2.4.3 Bio-Rad protein micro assay for antibody quantification 57

2.5 IMMUNOLOGICAL DETECTION, SDS-PAGE AND WESTERN BLOT ANALYSIS 57

2.5.1 Immunological detection of KSHV ORF 4 proteins 57

2.5.2 SDS-PAGE Electrophoresis 58

2.5.3 Western analysis of the expressed KSHV ORF 4 proteins 59

2.5.4 Chemiluminescence-based Immunodetection of the rKCPs 59

2.6 FUNCTIONAL AND STRUCTURAL ANALYSIS OF THE EXPRESSED KSHV ORF 4 RECOMBINANT PROTEINS 60

2.6.1 Biological Activity Test of the secreted proteins 60

2.6.2 *N*-Deglycosylation Analysis of the truncated KCP 62

2.7 IMMUNOHISTOCHEMICAL DETECTION OF THE KCP IN KAPOSI'S SARCOMA 63

2.7.1 Coating of slides with 3-aminopropyltri-ethoxyethylsilane 63

2.7.2 Immunohistochemistry of KS tissue samples with anti-KCP 63

CHAPTER THREE: RESULTS 65

3.1 PREPARATION OF THE KSHV ORF 4 CONSTRUCTS 65

3.1.1 Preparation of the pGEMT/KSHV ORF 4 DNA constructs 65

3.1.2 PCR amplification of the KSHV ORF 4 from KSHV DNA 67

3.1.3 Small-scale preparation of plasmid DNA 68
3.1.4 Restriction enzyme digestion analysis of the pGEMT-easy DNA constructs 68
3.1.5 Directional analysis of the cloned genes by restriction enzyme digestion 70
3.1.6 DNA sequencing results 72
3.1.7 Preparation of the pPIC9/KSHV ORF 4 gene constructs 74
3.1.8 Small-scale isolation and restriction enzyme analysis of the pPIC9 plasmid DNA 75
3.1.9 DNA isolation from low-melt gels 76
3.1.10 Restriction enzyme analysis of the pPIC9 DNA constructs 76

3.2 TRANSFORMATION AND SELECTION FOR POSITIVE CLONES 78
3.2.1 Screening for Mut^+ and Mut^S transformants 78
3.2.2 PCR analysis of *Pichia* transformants 79

3.3 EXPRESSION OF RECOMBINANT KCP IN *PICHIA PASTORIS* 81
3.3.1 Optimisation of methanol-induced production of the rKCPs 81
3.3.2 Estimation of protein concentration in the culture media 82
3.3.3 Small-scale ammonium sulphate precipitation 84

3.4 SYNTHESIS OF A POLYCLONAL ANTI-KCP PEPTIDE ANTIBODY 84
3.4.1 HiTrap protein a purification of the anti-KCP antibody 85
3.4.2 BioRad antibody quantification micro assay 86

3.5 IMMUNOLOGICAL DETECTION, SDS-PAGE AND WESTERN BLOT ANALYSIS 86

3.6 FUNCTIONAL AND STRUCTURAL ANALYSIS OF THE EXPRESSED rKCPs 90
3.6.1 Recombinant KCP-S protein is functional 90
3.6.2 Truncated KCP-S protein is *N*-glycosylated 90

3.7 IMMUNOHISTOCHEMICAL STUDIES OF KS TISSUE WITH POLYCLONAL ANTI-KCP PEPTIDE ANTIBODY 92
3.7.1 Pre-immune and antibody controls of immunostaining 91
3.7.2 Immunohistochemical detection of endogenous KCP in Kaposi's sarcoma 95

CHAPTER FOUR: DISCUSSION 98

4.1 IMMUNOHISTOCHEMICAL DETECTION OF THE KCP PROTEIN IN KAPOSI'S SARCOMA 98

4.2 HETEROLOGOUS PRODUCTION OF KCP IN THE METHYLOTROPHIC YEAST *PICHIA PASTORIS* 102

APPENDIX A: PLASMIDS AND *PICHIA* STRAINS 108

APPENDIX B: LIST OF MATERIALS AND SUPPLIERS 109

REFERENCES 110

LIST OF FIGURES

FIGURE 1: ILLUSTRATED REPRESENTATION OF THE KSHV STRUCTURAL COMPONENTS 2

FIGURE 2: CHARACTERISTICS OF THE MEMBERS OF THEα, β AND γ SUBFAMILIES OF THE HERPESVIRIDAE FAMILY 3

FIGURE 3: THE CELL CYCLE AND ASSOCIATION OF KSHV v-CYCLIN WITH KEY CELL CYCLE REGULATORS 12

FIGURE 4: OVERVIEW OF THE CURRENT UNDERSTANDING OF THE COMPLEMENT PATHWAYS 19

FIGURE 5: CLUSTAL W MULTIPLE SEQUENCE ALIGNMENT OF THE SCRs OF KCP 28

FIGURE 6: PRIMARY STRUCTURAL FEATURES OF THE KSHV COMPLEMENT REGULATORY PROTEIN 29

FIGURE 7: ILLUSTRATION OF THE PREDICTED CRYSTAL STRUCTURE OF THE FOUR SCRs MOTIFS OF KCP 31

FIGURE 8: SCHEMATIC DIAGRAM OF THE RECOMBNANT KSHV ORF 4 TRANSCRIPT MAP 36

FIGURE 9: SIGNIFICANCE OF DETERMINING THE DIRECTION OF THE INSERT WHEN LIGATED INTO p-GEMT-EASY VECTOR 43

FIGURE 10: ILLUSTRATION OF THE PELLICON XL-DEVICE 54

FIGURE 11: CRITERIA FOR THE SELECTION OF A COMMON SUITABLE KCP PEPTIDE 56

FIGURE 12: SCHEMATIC DIAGRAM OF PGNase F *N*-DEGLYCOSYLATION 62

FIGURE 13: RESTRICTION PLASMID MAPS OF THE p-GEMT-EASY VECTOR AND CONSTRUCTS 66

FIGURE 14: AGAROSE GEL ANALYSIS OF THE KSHV ORF 4 PCR PRODUCTS 67

FIGURE 15: AGAROSE GEL ANALYSIS OF THE ISOLATED p-GEMT PLASMID DNA 68

FIGURE 16: AGAROSE GEL ANALYSIS OF THE p-GEMT/KSHV ORF 4 CONSTRUCTS RE ANALYSIS 69

FIGURE 17: AGAROSE GEL OF THE DIRECTIONAL ANALYSIS OF THE INSERTS BY RE DIGESTION 71

FIGURE 18: MULTIPLE SEQUENCE ALIGNMENT OF THE CLONED KCP GENE WITH THE pGEMT PRIMERS DNA SEQUENCING RESULTS 72

FIGURE 19: RECOMBINANT AND WILD TYPE KCP MULTIPLE SEQUENCE ALIGNMENT USING CLUSTAL W 73

FIGURE 20: RESTRICTION PLASMID MAPS OF THE pPIC9 VECTOR AND CONSTRUCTS 74

FIGURE 21: AGAROSE GEL OF THE pPIC9 RESTRICTION ENDONUCLEASE ANALYSIS 75

FIGURE 22: AGAROSE GEL OF THE GENES OF INTEREST RECOVERED FROM LOW-MELT GEL 76

FIGURE 23: AGAROSE GEL OF THE pPIC9/KSHV ORF 4 CONSTRUCTS RE ANALYSIS 77

FIGURE 24: HIS^+ GS115 *PICHIA* TRANSFORMANTS ARE MOSTLY MUT^S PHENOTYPE 78

FIGURE 25: PCR ANALYSIS OF THE pPIC9/KSHV ORF 4 (735) *PICHIA* TRANSFORMANTS 79

FIGURE 26: PCR ANALYSIS OF THE pPIC9/KSHV ORF 4 (1436) *PICHIA* TRANSFORMANTS 80

FIGURE 27: PCR ANALYSIS OF THE pPIC9/KSHV ORF 4 (1581) *PICHIA* TRANSFORMANTS 80

FIGURE 28: COOMASSIE-STAINED SDS-PAGE GEL SCANNED WITH THE DENSIOMETER FOR ESTIMATION OF PROTEIN CONCENTRATION 82

FIGURE 29: STANDARD CURVE USED TO ESTIMATE THE CONCENTRATION OF THE EXPRESSED KCPs PRESENT IN THE CULTURE MEDIA 83

FIGURE 30: SDS-PAGE ANALYSIS OF rKCPs PRECIPITATED FROM THE SUPERNATANT WITH SATURATED AMMONIUM SULPHATE 84

FIGURE 31: SDS-PAGE ANALYSIS OF THE ANTI-KCP ANTIBODY PURIFICATION STAGES 85

FIGURE 32: BSA STANDARD CURVE USED TO DETERMINE ANTI-KCP ANTIBODY CONCENTRATION 86

FIGURE 33: EXPRESSION AND DETECTION OF THE RECOMBINANT KCP-S PROTEIN 87

FIGURE 34: EXPRESSION AND DETECTION OF THE RECOMBINANT KCP-M PROTEIN 88

FIGURE 35: EXPRESSION AND DETECTION OF THE RECOMBINANT KCP-F PROTEIN 89

FIGURE 36: INHIBITION OF THE CLASSICAL PATHWAY-MEDIATED LYSIS OF ssRBC BY RECOMBINANT KCP 90

FIGURE 37: SDS-PAGE ANALYSIS OF THE ENZYMATIC DEGLYCOSYLATION WITH PNGase F SHOWS THAT TRUNCATED KCP-S IS *N*-GLYCOSYLATED 91

FIGURE 38: THE PRIMARY AND SECONDARY ANTIBODY CONTROLS SHOWED NO SPECIFIC STAINING 92

FIGURE 39: THE PRE-IMMUNE CONTROL INDICATES THAT THE STAINING OBTAINED WITH ANTI-KCP PRIMARY ANTIBODY IS MORE SPECIFIC 93

FIGURE 40: POSITIVE CONTROLS SHOWING EXPECTED IMMUNOSTAINING OF THE KS TISSUE 93

FIGURE 41: DIFFERENT STAGES OF KS DISPLAYING HHV-8 NUCLEAR POSITIVITY IN THE LESIONAL SPINDLE CELLS 94

FIGURE 42: IMMUNOHISTOCHEMICAL ANALYSIS OF VARIOUS EARLY PATCH STAGE KS WITH ANTI-KCP PEPTIDE PRIMARY ANTIBODY 95

FIGURE 43: IMMUNOHISTOCHEMICAL ANALYSIS OF VARIOUS INTERMEDIATE PLAQUE STAGE KS WITH ANTI-KCP PEPTIDE PRIMARY ANTIBODY 96

FIGURE 44: IMMUNOHISTOCHEMICAL ANALYSIS OF VARIOUS LATE/ADVANCED NODULAR STAGE KS WITH ANTI-KCP PEPTIDE PRIMARY ANTIBODY 97

LIST OF TABLES

TABLE 1: MAJOR KSHV GENES OF KNOWN PRODUCTS AND THEIR RESPECTIVE FUNCTIONS 5

TABLE 2: OUTLINE OF THE KSHV-RELATED PROLIFERATIVE DISORDERS AND THEIR PROPERTIES 14

TABLE 3: EXAMPLES OF VIRAL IMMUNOMODULATORS OF COMPLEMENT PATHWAYS 25

TABLE 4: DESIGN OF PRIMERS FOR PCR AMPLIFICATION OF KCP FROM KSHV DNA 34

TABLE 5: MASTER MIX COMPONENTS USED IN THE PCR OF THE KSHV ORF4 GENES 35

TABLE 6: THERMOCYCLING PARAMETERS USED IN THE PCR OF THE KSHV ORF4 GENE 35

TABLE 7: COMPONENTS USED IN THE RE ANALYSIS OF THE pGEMT DNA CONSTRUCTS 41

TABLE 8: COMPONENTS USED IN THE *BAMH*I RE DIGESTION DIRECTIONAL ANALYSIS 42

TABLE 9: COMPONENTS USED IN THE *HIND*III AND *PST*I ANALYSIS OF THE pPIC9 PLASMID 44

TABLE 10: COMPONENTS USED IN THE SET UP OF THE pPIC9 LIGATION REACTIONS 45

TABLE 11: COMPONENTS USED IN THE RE ANALYSIS OF THE pPIC9 DNA CONSTRUCTS 46

TABLE 12: COMPONENTS USED IN THE *SAC* I LINEARISATION OF THE pPIC9 CONSTRUCTS 47

TABLE 13: MASTER MIX COMPONENTS USED IN THE PCR OF THE 735 bp GENE FROM *PICHIA* HIS$^+$ TRANSFORMANTS 50

TABLE 14: MASTER MIX COMPONENTS USED IN THE PCR OF THE 1436 AND 1581 bp GENES FROM *PICHIA* HIS$^+$ TRANSFORMANTS 51

TABLE 15: THERMOCYCLING PARAMETERS USED IN THE PCR OF THE *PICHIA* HIS$^+$ TRANSFORMANTS 52

TABLE 16: COMPONENTS USED IN THE PREPARATION OF SDS-PAGE GELS 58

TABLE 17: COMPONENTS USED INT THE SET UP OF THE HEMOLYSIS ASSAY REACTIONS 61

TABLE 18: SDS-PAGE (FIGURE 29) DENSIOMETER SCAN AUTOGRID RESULTS 82

LIST OF SYMBOLS

1.	A_{260}	absorbance at 260 nanometres
2.	bp	base pair
3.	°C	degrees Celsius
4.	cm	centimetre
5.	Da	Dalton
6.	X g	relative centrifugal force (RCF) unit
7.	g	gram
8.	h	hour
9.	kb	kilo bases
10.	kDa	kilodalton
11.	L	litre
12.	m	metre
13.	µg	microgram
14.	µl	microlitre
15.	µm	micrometer
16.	µmol	micromole
17.	mg	milligram
18.	ml	millilitre
19.	mm	millimetre
20.	mm^2	millimetre squared
21.	min	minute
22.	M	molar
23.	mol	mole
24.	nm	nanometre
25.	rpm	revolutions per minute
26.	sec	second
27.	U	units
28.	V	volt
29.	v/v	volume per volume
30.	w/v	weight per volume

LIST OF ABBREVIATIONS

aa	Amino acid
Ab	Antibody
Ag	Antigen
AIDS-KS	Acquired immunodeficiency syndrome- Kaposi's sarcoma
Amp^R gene	Ampicillin Resistant Gene
APES	3-aminopropyltri-ethoxyethylsilane
ATP	Adenosine Triphosphate
BC	Background Control
BCBL-1	Body Cavity-based Lymphoma-1
BCIG (=X-gal)	5-bromo-4-chloro-3-indolyl-β-D-galactopyranoside
BMGY	Buffered Glycerol Complex Medium
BMMY	Buffered Methanol Complex Medium
BSA	Bovine Serum Albumin
CCC	Covalently Closed Circular
CCP	Complement control Protein
CCPH	HVS Complement Control Protein homolog
C4BP	C4-Binding Protein
CDK	Cyclin-dependent Kinase
CDI	CDK inhibitor
cDNA	Complementary DNA
CPV	Cowpox Virus
CR-1	Complement Receptor-1
DAB	3, 3'-diaminobenzidine
DAF	Decay Accelerating Factor
ddH_2O	Double Distilled Water
DMSO	Dimethyl Sulfoxide
DMVEC	Dermal Microvascular Endothelial Cell line
DNA	Deoxyribonucleic Acid
ds	Double-stranded
EBV	Epstein-Barr Virus

EDTA	Ethylenediaminetatraacetic Acid
E. coli	Escherichia coli
FLIP	Fas-ligand-interleukin 2-converting enzyme inhibitor protein
G + C	Guanine and Cytosine
gC-1	glycoprotein C-1
GCRs	G protein-coupled receptors
gDNA	genomic DNA
GPI	Glycosyl Phosphatidylinositol
HAART	Highly Active Antiretroviral Therapy
HCl	Hydrochloric Acid
HCMV	Human Cytomegalovirus
HHV-2	Herpesvirus saimiri
HHV-4	Human Herpesvirus-4
HHV-8	Human Herpesvirus-8
HIER	Heat Induced Epitope Retrieval
HIV	Human Immunodeficiency Virus
HSV	Herpes Simplex Virus
Ig	Immunoglobulin
IgG	Immunoglobulin G
IMP	Inflammation Modulatory protein
IPTG	Isopropyl- β- D- thiogalactoside
KCP	KSHV Complement Control/Regulatory Protein
KLH	Keyhole Limpet Hemocyanin
KS	Kaposi's sarcoma
KSHV	Kaposi's Sarcoma-associated herpesvirus
LANA	Latency-associated Nuclear Antigen
LB	Luria Broth
LUR	Long Unique Region
MAC	Membrane Attack Complex
MCD	Multicentric Castleman's Disease
MCP	Membrane Cofactor Protein
MD	Minimal Dextrose
MHC	Major Histocompatibility Complex

MHV68	Murine Gammaherpesvirus 68
MM	Minimal Methanol
MPF	M- phase promoting factor
Mut^+	Methanol Utilization Plus
Mut^S	Methanol Utilization Slow
NMR	Nuclear Magnetic Resonance
NaOH	Sodium Hydroxide
OD	Optical Density
ORF	Open Reading Frame
PAGE	Polyacrylamide gel electrophoresis
PBS	Phosphate buffered saline
PBS-T	PBS-Tween 20
PCR	Polymerase Chain Reaction
PDB	Protein Database Bank
PEL	Primary Effusion Lymphoma
pH	- log $[H^+]$
PMSF	Phenylmethylsulfonyl fluoride
PNGase	Peptide: *N*-Glycosidase F
POD	Horseradish Peroxidase
pRB	Retinoblastoma protein
RCA	Regulators of Complement Activation
RDA	Representational Difference Analysis
RDB	Regeneration Dextrose medium
RE	Restriction endonuclease
RNA	Ribonucleic acid
RT	Room Temperature
SCR	Short Consensus Repeats
SDS	Sodium dodecyl sulphate or sodium lauryl sulphate
SDS-PAGE	Sodium dodecyl sulphate-polyacrylamide gel electrophoresis
SPR	Surface Plasmon Resonance
ssRBCs	sensitised red blood cells
TBE	Tris- borate-EDTA
TBS	Tris-buffered saline
TBST	Tris- buffered saline/Tween 20

TE	Tris- EDTA buffer
TEMED	N,N,N,N'- tetramethylethylenediamine
TPA	12-O-tetradecanoylphorbol-13-acetate
TR	Terminal Repeat
Tris	Tris- 2-amino- 2-(hydroxymethyl)-1, 3 propandiol
TSP	Thrombospondin-1
UV	Ultraviolet
VCP	Vaccinia Virus Complement Control Protein
vIL6	viral Interleukin 6
vMIP	viral Macrophage Inflammatory Protein
YNB	Yeast Nitrogen Base
YPD	Yeast extract Peptone Dextrose medium

CHAPTER ONE

INTRODUCTION

The literature survey carried out, comprising of a critical review of a large number of previous studies will follow from broad to more project-specific and relevant information. It will initially describe the classification, structure, genome, life cycle and *in vitro* cultivation of Kaposi's sarcoma associated herpesvirus (KSHV) and KSHV as a model for viral oncogenesis. In section 1.2, the chief KSHV-related proliferative disorders such as multicentric castleman's disease (MCD), primary effusion lymphoma (PEL) and Kaposi's sarcoma (KS) will be reviewed with the latter being described in more detail. These sections will be followed by a description of the complement system and inflammatory responses and how viruses have evolved or acquired means to subvert the host immune system in order to succeed as infectious agents. Finally a detailed description of the KSHV complement regulatory protein, its biochemical characterisation and molecular function within the context of the complement system regulation will be presented in this chapter.

1.1 Kaposi's Sarcoma-Associated Herpesvirus

Tumour viruses are presently regarded as essential tools in cancer research as many have led to the discovery of critical cell regulatory proteins such as p53, p300, E2F, just to name a few. KSHV is rapidly becoming one of the chief models of viral transformation because its genome has been sequenced and annotated. KSHV is also known as human herpesvirus 8 (HHV-8) because it is the eighth human herpesvirus identified to date (Russo *et al,* 1996). This viral strain was initially discovered from an acquired immunodeficiency syndrome-Kaposi's sarcoma (AIDS-KS) skin lesion in 1993 by the molecular biological technique, representational difference analysis (RDA). RDA allowed the isolation and identification of two unique herpes-related deoxyribonucleic acid (DNA) fragments present in KS-diseased tissue that were not present in non-diseased tissue from the same individual (Chang *et al,* 1994). In order to detect and quantify the presence of KSHV DNA from a different number of

sources, a convenient and economic polymerase chain reaction (PCR) method has been developed by Curreli *et al* (2003) whereby, a different size DNA fragment has been synthesised to compete with the target viral DNA in a single PCR reaction.

1.1.1 KSHV Classification and Structure

Herpesviruses are typically divided into three main subfamilies namely the large, heterogeneous alphaherpesvirus group, which includes herpes simplex virus (HSV), the betaherpesvirus group, which includes the human cytomegalovirus (HCMV) and finally the gammaherpesvirus group, which consists of herpesviruses that replicate and persist in lymphocytes. The latter induces lymphoproliferation (Albrecht *et al*, 1992) and an example of this group is KSHV, which may also become latent in B-cells (Figure 2). HHV-8 a new human herpesvirus closely related to Epstein-Barr virus (EBV), also known as HHV-4, is a large enveloped double-stranded DNA virus that belongs to the *Rhadinovirus* or gamma-2-herpesvirus genus within the subfamily *Gammaherpesvirinae* (Jenner and Boshoff, 2002). Structurally, KSHV has a target-like ultra structural appearance (Renne *et al*, 1996) with an electron-dense nucleocapsid core surrounded by an amorphous proteinaceous tegument and a lipid bilayer envelope (Moore and Chang, 2001) as represented by Figure 1.

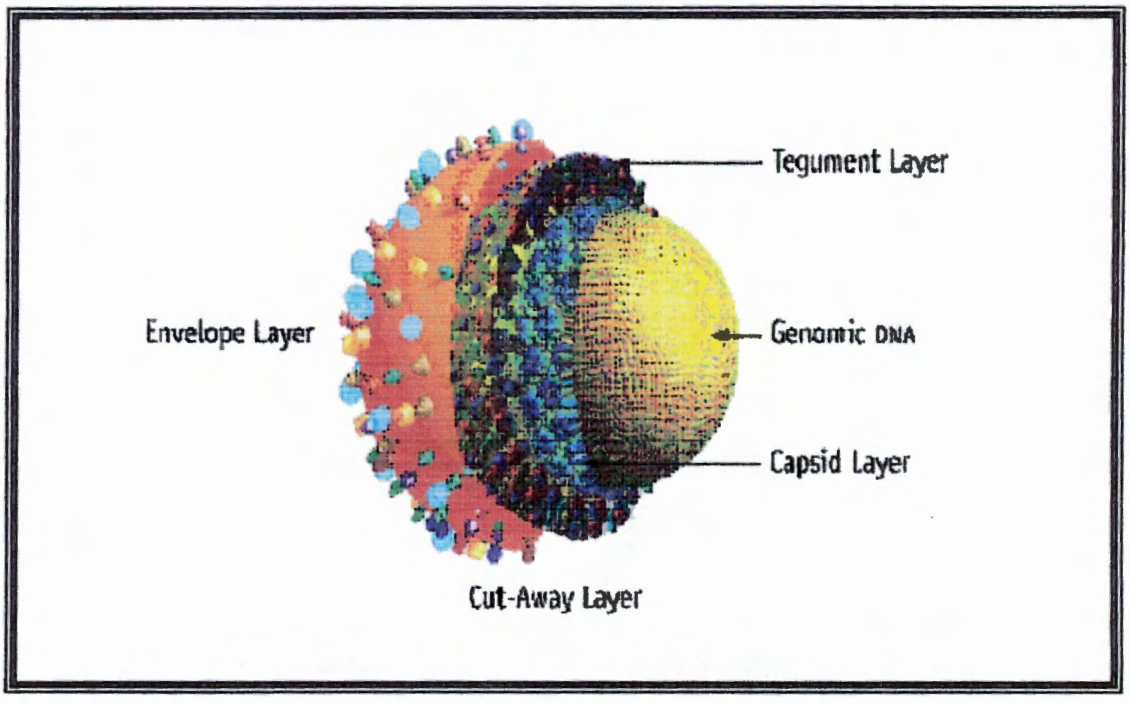

Figure 1. Illustrated representation of the KSHV structural components

KSHV is a large enveloped double-stranded DNA virus composed of a nucleocapsid layer as well as a proteinaceous tegument layer followed by an outer lipid bilayer. (Adapted from Henderson, 2002).

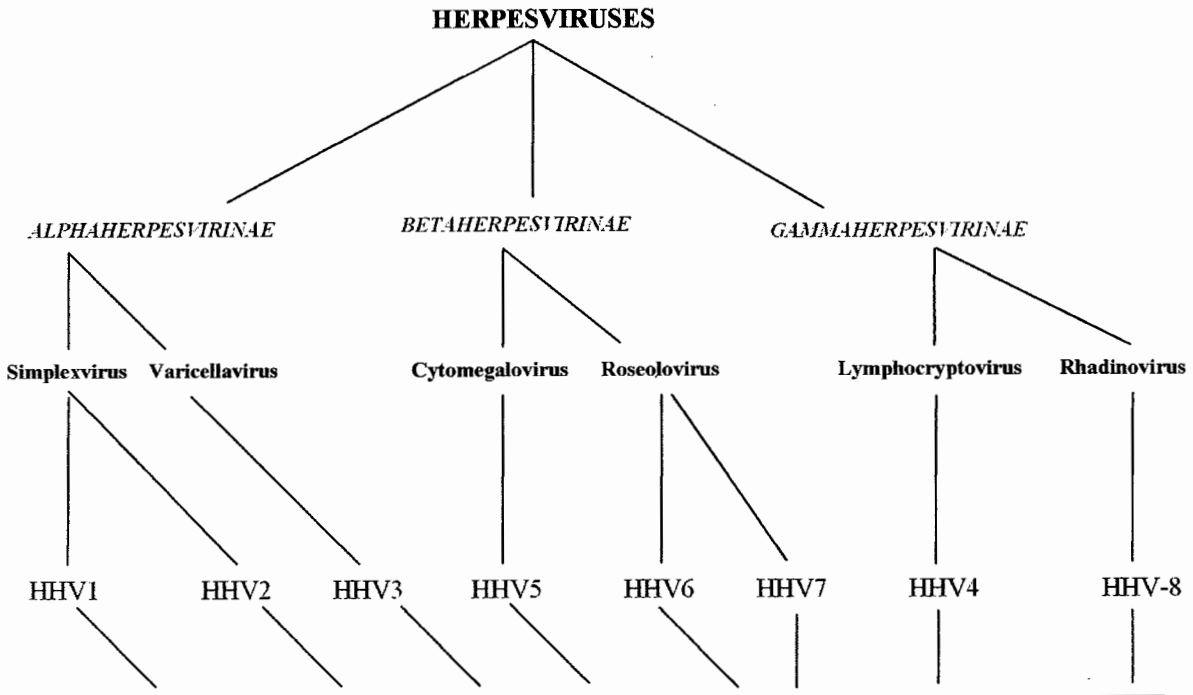

Common Name	**Herpes simplex 1**	**Herpes simplex 2**	**Varicella-virus**	**Cytomegalovirus**	HHV 6 & HHV 7	EBV	KSHV
Growth Cycle	Short	Short	Short	Long	Long	Variable	Variable
Cytopath	Cytolytic	Cytolytic	Cytolytic	Cytomegalic	Lympho Proliferative	Lympho proliferative	Lympho proliferative
Site of Latency	Neurons	Neurons	Neurons	Glands/Kidneys	Lymphoid tissue	Lymphoid tissue	Lymphoid tissue
Prevalence	Ubiquitous	Ubiquitous	Ubiquitous	Ubiquitous	Ubiquitous	Ubiquitous	Obscure
Clinical Presentation"	**Herpes labialis** **Keratocon-junctivitis** **Encephalitis**	**Genital Herpes** **Meningitis**	**Chicken pox** **Shingles**	**Mononucleosis-like syndrome** **Intestinal pneumonitis** **Chorioretinitis**	**Roseola infartum in the case of HHV 6** **Non-specified in the case of HHV 7**	**Mononucleosis** **Nasopharyngeal carcinoma** **Burkitt's lymphoma** **Oral hairy cell leukoplakia** **Diffuse polyclonal lymphomas in AIDS**	**KS** **PEL** **MCD**

Figure 2. Characteristics of the members of the alpha, beta and gamma subfamilies of the herpesvirinae family (Geraminejad *et al,* 2002)

Both KSHV and EBV belong to the gammaherpesvirinae subfamily of herpes viruses, a group recognised for its capacity to sustain latency in lymphocytes. KSHV is the first Rhadinovirus known to actually infect humans. Unlike all the other members of the herpes virus family, KSHV is the only type of herpes virus that may be regarded as very cryptic and highly difficult to undergo transmission.

This virus shares several characteristics of other herpes viruses and based on sequence analysis it is particularly closely related to herpes virus saimiri (HVS-2) of squirrel monkeys (Albrecht *et al,* 1992), known to cause polyclonal T-cell lymphoproliferative disorders in a number of monkey species (Moore *et al,* 1996). Although rhadinoviruses are a rather underexploited model of viral tumorigenesis, they are still regarded as an important and useful group of viruses. Like other rhadinoviruses, KSHV is uniquely suited for studies of virus-cell interactions because of the production of viral homologs to oncoproteins and cell signalling proteins (Russo *et al,* 1996). It is believed that the acquisition of host genes by KSHV places the virus at an advantage, because by interfering with the host cellular defence mechanisms this virus can overcome destructive anti-viral responses (Neipel *et al,* 1997).

1.1.2 The KSHV Genome

Russo *et al* (1996) successfully sequenced the entire genome of KSHV by mapping continuous overlapping virus DNA inserts from body cavity-1 (BC-1) genomic libraries, with the exception of an unclonable repeat region at the right end of the genome. These results led to the definition of the viral genome structure as well as identification of genes that are likely to be responsible for KSHV-related pathogenesis (Russo *et al,* 1996). Encapsulated DNA from KSHV particles isolated from an EBV-negative body cavity based lymphoma-1 (BCBL-1) cell line was analysed by pulsed-field gel electrophoresis and the results showed that the KSHV genome is approximately 165 kb long (Renne *et al,* 1996). On the other hand, KSHV genome derived from a BC-1 infected cell line is approximately 270 kb long due to a duplication of a coding segment, which is inserted into the terminal repeat (TR) region (Russo *et al,* 1996). The structure of BC-1 KSHV genome is characterized by a long unique region (LUR) flanked by 801 bp TR regions, which in addition to having 84.5% guanine and cytosine (G+C) content, also contains putative packaging and cleavage signal sequences. The LUR of the KSHV genome is about 145 kb in length, has a 53.5% G+C content and contains all 90 identified KSHV open reading frames (ORFs) (Russo *et al,* 1996), 66 of which are known to have homologues in the HSV genome, and are therefore numbered based on the HSV nomenclature. However, KSHV genes that are not homologous to HSV genes are given a K prefix such as K1-K15 and include many of the cellular homolog genes (Jenner and Boshoff, 2002)

often coding for cell cycle regulation and signal transduction proteins (Russo *et al,* 1996). Additional sequence analysis of the KSHV genome has revealed the presence of two putative lytic replication origins, which are the theoretical initiation sites for genome replication (Nicholas *et al,* 1998). Furthermore, sequence analysis has also shown that a large section of the KSHV genome is highly conserved among other herpes virus with transforming potential such as murine gammaherpesvirus 68 (MHV68), EBV and HSV (Sarid *et al,* 1998). Conserved ORFs coding for supposed viral structural proteins and enzymes include genes involved in viral DNA replication, regulators of gene expression and five conserved herpes virus structural capsid and glycoprotein genes (Russo *et al,* 1996) as depicted in Table 1. The fourth ORF of the KSHV genome encodes a protein, KSHV complement control protein (KCP) also known as complement regulatory protein (CRP) predicted to have complement regulating activity (Spiller *et al,* 2003a) and it will be further discussed in 1.3.4. Although chimeric genomes have been found, KSHV is an ancient human virus that is transmitted mainly in a regular way with consequently very low recombination rates (Zong *et al,* 2002). Phylogenetic analysis of the ORF 75 gene from 41 HHV-8 DNA samples has shown that in addition to subgroups A/B and C there is a novel subgroup present in South Africa which has been termed N. It is thought that this new subgroup N may have emerged as a result of continuous reactivation of KSHV in patients also affected by AIDS (Alagiozoglou *et al,* 2000).

Many ORFs encoded by the KSHV genome are host cell homologues involved in the regulation of the cell cycle and immune responses in turn contributing to the oncogenesis/virulence of this virus as described in sub-sections 1.1.5 and 1.3.2 respectively.

Table 1. Major KSHV genes of known products and their respective functions

KSHV Gene	Protein Product	Function
ORF K1	**K1ST**	Constitutively activates B-cell signalling pathways through syk; down regulates BCR; Oncogenic
ORF K2	**vIL-6**	Activates gp130 independently of IL-6R; Autocrine growth factor in PEL; Angiogenic
ORF K4	**vMIP-II**	CCR-3 agonist; Broad spectrum cytokine receptor antagonist; Inhibits leukocyte chemotaxis; Angiogenic
ORF K4.1	**vMIP-III**	CCR-4 agonist; Induces T_H2 chemotaxis; Angiogenic
ORF K6	**vMIP-I**	CCR-8 agonist; Induces T_H2 chemotaxis; Angiogenic
ORF K8	**b-ZIP**	Lytic transactivator

ORF 8.1	**gp35-37**	Glycoprotein incorporated into virion
ORF K9	**vIRF-1**	Inhibits interferon signaling; Binds CBP/p300
ORF 10	**vIRF-4**	Blocks IFN- and IRF-mediated transcriptional activation
ORF K10.5	**LANA-2**	IRF-4 homology; Inhibits p53-mediated apoptosis
ORF K12	**Kaposin**	Oncogenenic
ORF K13	**Vflip**	Homolog of cellular apoptosis inhibitor (FLIP)
ORF K15	**LAMP**	Binds TRAF1, 2 and 3
ORF 2	**Dihydrofolate reductase**	Thymidylate production
ORF 4	**Complement Binding Protein (CBP)**	Inhibits complement-mediated lysis
ORF 6	**ssDNA binding protein (SSB)**	DNA replication
ORF 8	**Glycoprotein B**	Glycoprotein incorporated into virion
ORF 9	**DNA polymerase (POL)**	Functional DNA polymerase
ORF 16	**vBcl-2**	Inhibits bax-mediated and virally induced apoptosis
ORF 17	**Pr and AP**	Protease and assembly protein respectively
ORF 21	**Thymidine kinase**	Thymidylate production
ORF 22	**Glycoprotein H**	Glycoprotein
ORF 37	**Alkaline exonuclease**	DNase involved in DNA repair and packaging
ORF 39	**Glycoprotein M**	Glycoproein
ORF 40	**Primase-associated factor (PAF)**	DNA replication
ORF 43	**Minor capsid protein**	Capsid
ORF 50	**ART**	Spliced transactivator that initiates lytic gene expression
ORF 54	**dUTPase**	Thymidylate production
ORF 71	**v-FLIP**	Inhibits Fas-mediated apoptosis; Oncogenic
ORF 72	**vCYC**	Associates with cdk6 to phosphorylate pRB and histone H1
ORF 73	**LANA-1**	Binds to ori-P and maintains viral episome; Inhibits p53 and pRB
ORF 74	**vGCR**	Chemokine receptor homolog; Binds IL-8; Oncogenic

(Jenner and Boshoff, 2002)

1.1.3 KSHV Lytic Replication and Latent Infection

Like all other herpesviruses, KSHV has two distinct modes of replication during its life cycle namely the lytic phase and the latent phase. The latent mode of infection is characterized by entry of the virions into a host cell, re-circularisation of the linear KSHV genome at its terminal repeat region and replication of the circular viral episome together with host cell DNA. The episome is kept in the replicating cell by the latency-associated nuclear antigen (LANA), which binds the episome, possibly through histone H1 interactions (Coscoy and Ganem, 2000) thus allowing equal

segregation of latent viral genomes to daughter cells during mitosis (Ballestas *et al*, 1999). In addition, it has been shown that LANA mediates the replication of plasmid DNAs containing viral TRs. LANA 1 N-terminus is indispensable for chromosome association, DNA replication and episome persistence to take place in uninfected cells (Barbera *et al*, 2004). Key mechanistic features of latent DNA replication have been suggested to be conserved amongst closely related herpes viruses (Grundhoff and Ganem, 2002). Therefore, during latency, KSHV gene expression is minimized and the virus is dependent on the cellular replication machinery for survival. Furthermore, in order to evade the host immune responses, foreign antigen presentation is also minimal by maintaining the viral genes silent. On the other hand, during the lytic mode of replication, viral DNA, which is replicated by the virus-encoded polymerase, is encapsulated into infectious virions (Moore and Chang, 2001). The viral genes needed by the virus to carry out these two processes are sequentially activated by the master transactivator or by secondary transcriptional molecules in a regulated series of early, delayed-early and late patterns of viral gene transcription (Schulz *et al*, 2002). Possible master lytic transactivators include the KSHV gene products, K-bZIP and ART, encoded by ORF K8 and ORF50 respectively. Northern hybridization analysis has shown that ART is likely to first transactivate ORF K8, product of which, subsequently acts on other viral promoters to generate proteins involved in capsid formation (Sun *et al*, 1999), as well as release of infectious virions, thus showing that the lytic cycle is crucial for the spread of KSHV infection (Wang *et al*, 2003). Although human immunodeficiency virus (HIV-1) Tat has formerly been believed to be an activator of KSHV lytic replication, Varthakavi *et al* (2002) showed that Tat alone is incapable of inducing the lytic phase of KSHV and that HIV-1 infection strongly induces this phase through activation of the KSHV Rta promoter. Therefore this group has concluded that in addition to HIV-1 tat, other factors are needed to activate lytic replication of KSHV.

Inflammatory cytokines present in KS lesions are capable of inhibiting spontaneous KSHV lytic gene expression but not the level of infection and this therefore suggests that cytokines add to KSHV pathogenesis by promoting latent KSHV infection of the endothelial cells (Milligan *et al*, 2004).

Patches of unprompted lytic infection rather than just latent infection has been shown to arise within KSHV-infected dermal micro vascular endothelial cell (DMVEC)

lines. As a result, a quantitative assay has been developed by Ciufo *et al* (2001) to directly measure the infectivity of KSHV virion preparations based on varied spindle cell colony and plaque formation.

Although KSHV-infected tissues have been shown to consist primarily of latently infected cells, with only a small percentage of cells in the lytic phase, it has also been revealed that in addition to being essential for viral transmission, lytic viral proteins are also important in causing neoplastic transformations such as Kaposi's sarcoma. Therefore, elucidation and full characterization of the signals and mechanisms which allow the switch from the latent phase into the lytic phase, such as expression of the immediate early Lyta/ORF50 gene believed to be controlled by means of methylation, is an important area of research in order to learn how KSHV regulates its life cycle. According to Laman and Boshoff (2001), this further knowledge may in turn lead to the development of novel antiviral agents.

1.1.4 *In Vitro* Cultivation of KHSV

The BC-1 cell line, which is confected with EBV, was the first reported and characterized KSHV cell line. However, the fact that some cell lines derived from PEL are EBV negative has suggested that EBV co-infection is not necessary for the *in vitro* cultivation of KSHV (Cesarman *et al*, 1995; Renne *et al,* 1996).

KSHV can be directly cultured to high copy number in PEL-derived cell lines, which are B-cell lymphomas latently infected with KSHV. The efficiency of viral transmission to other cell lines and serial propagation of the virus remains extremely difficult to carry out. However, KSHV genome transmission from BC-1 cell line has been detected by PCR analysis (Moore *et al*, 1996) but this strain is still regarded as infection-incompetent (Sarid *et al,* 1998). TR analysis of KSHV in BC-1 under standard growth conditions correlates with the virus being under a tight latent replication control (Russo *et al,* 1996). Transcripts found under these conditions are likely to encode latency-associated proteins which in turn, may be essential for maintaining the latent viral genome and transforming virus-infected cells (Sarid *et al,* 1998).

Infected PEL cell lines carrying multicopy KSHV episomes can be induced into the lytic cycle by chemical agents such as sodium butyrate, which inhibits histone deacetylases involved in transcriptional repression and the phorbol ester, 12-O-

tetradecanoylphorbol-13-acetate (TPA), which induces expression of histone acetyltransferases and activates transcription (Miller *et al*, 1997; Masumi *et al,* 1999). The ability to induce lytic cycle KSHV infection including the production of some mature virions has indeed facilitated the study of the genetics and molecular biology of this virus (Ciufo *et al,* 2001).

1.1.5 KSHV: A Model for Viral Oncogenesis

It is well known that some tumors are often associated with viral infections such as KSHV, which has been shown to be present in 90-95% of KS lesions as demonstrated by DNA and serology-based studies (Gao *et al*, 1997). The growth and division of normal cells is under the control of two types of genes namely the proto-oncogenes, which promote growth and the tumor suppressor genes, which restrain the cellular growth. Therefore, disruption of the normal functioning of any of these two types of genes can cause the cells to grow in an uncontrolled manner thereby leading to tumorigenesis (Madigan *et al*, 2000). Amongst other DNA tumor viruses, KSHV has independently evolved precise mechanisms to evade immune responses, including the synthesis of a complement regulatory homologue amongst many other important cellular proteins. It has also developed strategies to prevent cell cycle shutdown, to interrupt activation of apoptotic pathways and to inhibit the tumor suppressor genes. In general, the study of tumour viruses is of critical significance as properties of oncogenic viruses often lead to a better understanding of non-virally induced cancers.

1.1.5.1 The Cell Division Cycle and its Control system

In each division cycle a cell must replicate its DNA, undergo M phase during which the replicated chromosomes are segregated into separate nuclei by mitosis, must split into two by cytokinesis, and finally the cell must undergo a period of continuous cell growth known as the interphase. The cell cycle is known to be composed of four phases, the gap before DNA replication (G_1), the DNA synthetic phase (S), the gap after DNA replication (G_2) and the mitotic phase, which terminates in cell division (M) as illustrated in Figure 3. In addition, cells in G_1 can enter a specialized resting state, often called the G_0 (Alberts *et al*, 1994). The cell cycle events are well ordered into distinct pathways in which the initiation of late events is dependent on the completion of early events (Hartwell and Weinert, 1989).

Cell division is the fundamental means by which all living things are propagated (Alberts *et al*, 1994) and it is controlled through a complex network of biochemical signals, which regulate specific transitions in the cell cycle (Van den Heuvel and Harlow, 1993). It is speculated that each step of the cell cycle is largely regulated by complexes formed between cyclin-dependent protein kinases (CDK) and members of the cyclin family such that the G1/S transition is regulated by Cdk2/cyclin E, Cdk3/unknown cyclin, Cdk4/ cyclin D1-D3; Cdk6/cyclin D3; the S phase is regulated by Cdk2/cyclin A; G2 phase by Cdc2/cyclin A and G2/M transition by Cdc2/cyclin B (Veseley *et al,* 1994). The control mechanisms that inhibit cell cycle transition after DNA damage consist of multiple signalling pathways and are known as cell cycle checkpoints (Hartwell and Weinert, 1989). One of these checkpoints is present in G1 just before entry into S phase and the other in G_2 at the entry to mitosis (Figure 3).

The proliferation of cells is a highly regulated process that is subject to many external and internal stresses, including viral infections such as KSHV, irradiation, toxic substances and reactive oxygen species, against which several stabilizing and repair mechanisms have been developed by the cells. The cell-cycle control system is based on a set of interacting proteins that induce and regulate the essential processes within the cell thereby allowing the duplication and division of the cell contents to occur (Alberts *et al*, 1994). As previously mentioned, some of the cellular responses to viral infections may result in cell cycle shutdown and induction of apoptosis in order to destroy the virus-infected cells and prevent further propagation of the viral disease. Russo *et al* (1996) has shown that KSHV has a large number of functional homologs to cellular genes that play key roles in interfering and disrupting the cell-cycle control system.

1.1.5.2 KSHV Oncogenic Proteins Target the Cell Cycle

Cell cycle progression is strictly controlled by the expression and activation of regulatory molecules, which can either act as accelerators or suppressors (Sato and Torigoe, 1998). Key molecules of the cell cycle control system include the cyclins, cyclin- dependent protein kinase (CDK) inhibitors (CDI), the retinoblastoma protein (pRB) and the transcriptional factor E2F, all of which play important roles particularly at the starting point of the cell cycle (Sato and Torigoe, 1998).

Like any other DNA virus, KSHV must encourage G1 phase progression and entry into the S-phase of the cell cycle for efficient replication of its genome as depicted in

Figure 3. In the G1 phase, pRB, which is one of the major suppressor molecules capable of regulating the cell cycle, act as a transcriptional repressor in its hypophosphorylated state when it is bound to the E2F family of transcription factors (Sellers and Kaelin, 1996). The E2F family mediates transcription of genes required for DNA synthesis, such as cyclin E, Cyclin A, dihydrofolate reductase, and thymidine kinase (Wang, 1997).

One of the few proteins that are expressed in latently infected cancer cells is the KSHV v-cyclin encoded by ORF 72. Godden-Kent *et al* (1997) showed that in tissue culture cells, this viral protein forms a complex with CDK 6 thereby promoting the phosphorylation and inactivation of the pRB suppressor protein. This in turn, causes the retinoblastoma protein to release E2F leading to activation of the S-phase genes and progression of the cell cycle from the G1 phase to the S phase. In addition, v-cyclin-CDK 6 complex is resistant to the physiological inhibitors of the cell cycle p16, p21 and p27 (Swanton *et al*, 1997), which under normal circumstances inhibit the cyclin D2-CDK6 complex (Mann *et al*, 1999). Furthermore, CDK 6 activated by v-cyclin phosphorylates histone H1 implying that the kinase activity initiated by this viral cyclin may abrogate cell cycle checkpoints as there may be a change in substrate partiality (Godden-Kent *et al*, 1997).

Other viral oncogenes acknowledged being widely expressed in the latent state of KSHV infection and assumed to be essential for the transforming ability of this virus are the fas-ligand-interleukin 2-converting enzyme inhibitor protein (FLIP) which can inhibit Fas- mediated apoptosis and LANA encoded by ORF 71 and ORF 73, respectively. Fujimuro *et al* (2003) showed that the LANA C-terminus has sequence homology to the Axin GSK-3β binding domain, and that LANA stabilizes β-catenin leading to a cell cycle-dependant nuclear accumulation of GSK-3β, which is in turn, associated with entry into the S phase. Therefore, this study provided further convincing proof that LANA also contributes to the proliferative- stimulatory properties of KSHV. Among a number of other important established functions, LANA also has the capacity to avert the tumour suppressor p53 from inducing cell death (Friborg *et al*, 1999).

It is interesting to note that the KSHV oncogenic group of LANA, v-cyclin and v-FLIP are encoded on a tricistronic transcript and the function of one protein may therefore allow another to play a key role in the development of the tumour. In addition to these main oncogenic proteins, KSHV also produces homologues to the

interferon regulatory factor and interleukin- 6, which may also induce tumour formation via deregulation of growth signalling pathways or through evasion strategies of the host immune system (Boshoff, 2003) and the latter will be further discussed in **section 1.3.2**. Tomlinson and Damania (2004) have recently demonstrated that activation of the Akt signalling pathway by the KSHV K1 protein phorphorylates and inhibit members of the fork head (FKHR) transcription factor family, which are also major regulators of the cell cycle.

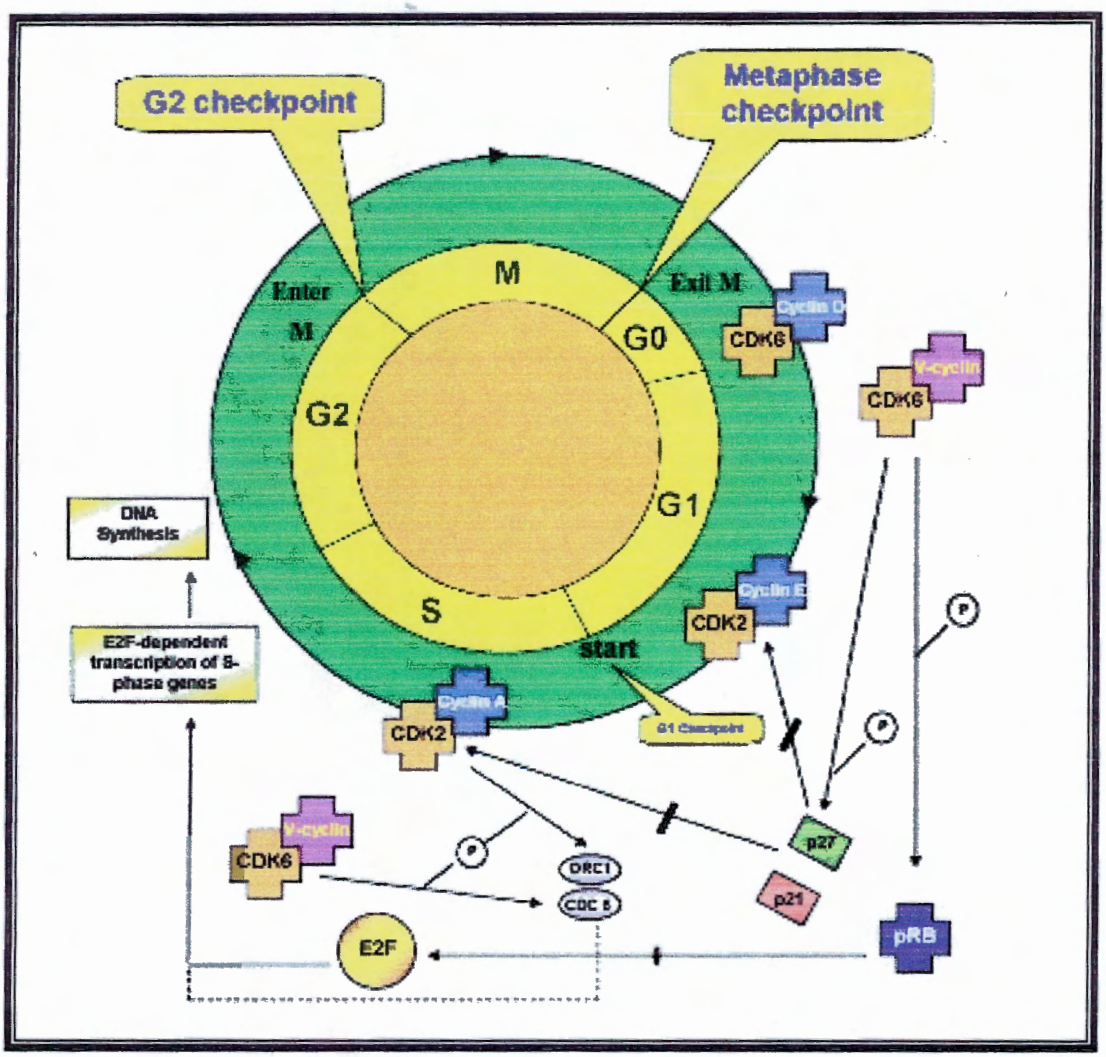

Figure 3. The cell cycle and association of KSHV v-cyclin with key regulators

The KSHV v-cyclin performs the function of 3 separate cyclin-CDK complexes: (1) exit from G0 (Cyclin D-CDK 6) whereby it phosphorylates and inactivates pRB causing the release of E2F leading to DNA synthesis; (2) through G1 (Cyclin E-CDK 2) whereby it phosphorylates and inactivates p27 alleviating its inhibitory effect on cyclin E-CDK 2 and cyclin A-CDK 2 and finally (3) entry into S-phase (Cyclin A-CDK 2) whereby it interacts and phosphorylates proteins of the origin recognition complex (ORC1 and CDC6) which are involved in DNA replication. (Adapted from Alberts *et al*, 1994 and Boshoff and Weiss, 2002).

As reviewed here, KSHV seems capable of discovering and interfering with almost all established cancer pathways in order to induce tumor formation as Boshoff (2003) described it.

1.2 KSHV-Related Proliferative Disorders

At present, the proliferative diseases unmistakably related to KSHV infection include a tumor of endothelial cell origin known as Kaposi's sarcoma (KS), some plasma cell forms of multicentric Castleman's disease (MCD) which is a B-cell lymphoproliferative disorder, and a body cavity-based or primary effusion lymphoma (BCBL or PEL) which also infects B-cells (Moore and Chang, 2001). Up to a study carried out by Pan *et al* (2001) KSHV was controversially associated with multiple myeloma but through the optimization of PCR protocols used for the detection of KSHV DNA, this group has acquired strong supportive data pinpointing that KSHV is not associated with the latter. It is now believed that KSHV is essential however, not sufficient for the development of these proliferative disorders because these diseases are most commonly found in transplant recipients that were already HHV-8 positive before they were transplanted, and AIDS-patients showing that immunosuppression is the leading cause of tumor development in the presence of the virus (Geraminejad *et al,* 2002).

1.2.1 PEL and MCD

As previously mentioned, KSHV is found in the rare form of lymphoma, PEL, which is thought to originate from post-germinal center B-cells due to the presence of hyper mutated immunoglobulin genes (Matolcsy *et al,* 1998) as well as markers of late stage B-cell differentiation (Gaidano *et al,* 1997). Also unusual is MCD, which is a non-malignant lymphoproliferative disorder, characterized by atypical polyclonal B-cells, in a microenvironment of intrleukin-6 (IL-6) excess (Parravinci *et al,* 1997) lymphadenopathy, fever and splenic infiltration and is more common in HIV-infected patients where it often becomes an aggressive disease (Jenner and Boshoff, 2002) just like KS. The mechanism by which KSHV causes these proliferative disorders is not yet well understood but is thought to involve several molecular events, the study of which should expand our knowledge of viral related cancers (Geraminejad *et al,* 2002).

Table 2. Outline of the KSHV-related proliferative disorders & their properties

Disorder	Characteristics	Degree of association
KS	AIDS- associated, African endemic, classical or Mediterranean and transplant-associated	**Very strong:** clearly fulfils commonly used criteria for causality
PEL	A subset of body cavity lymphomas, often EBV co-infection, most common in HIV patients, aggressive disease with poor prognosis	**Strong** but not as well-defined as KS above; likely to be detected by association with EBV
MCD	Most common in HIV patients, sometimes PEL or KS- associated	**Moderate:** Same as above; disorder can develop in the absence of KSHV, particularly in HIV-negative patients
Febrile rash illness	Found in children	**Moderate:** few cases reported
Acute bone marrow failure	Uncommon- reported in 3 transplant recipients to date	**Moderate:** few cases reported
Multiple myeloma	4-5 new cases/100 000 persons/year Progressive hematologic disease Excessive no of abnormal plasma cells	**Weak:** suggested association not yet substantiated by sufficient laboratory and epidemiological data

(Cannon *et al*, 2003)

1.2.2 Kaposi's sarcoma

KS is a malignant neoplasm of the blood vessels with rather erratic behaviour and outcome and it is characterized by prominent angiogenesis because of a discrepancy between promoters and inhibitors. Thrombospondin-1 (TSP), a physiological inhibitor of angiogenesis was shown to inhibit endothelial cell proliferation induced by both KS supernatants and Tat, a product of HIV-1 with angiogenic potential and most likely associated with AIDS-KS pathogenesis (Taraboletti *et al*, 1999).

KS was first described by Moritz Kaposi, a Hungarian dermatologist, in 1872 as an "idiopathic multiple pigment-sarcoma of the skin". For an entire century, it was regarded as an indolent tumor, a rare disorder of older men typically of Eastern European, Mediterranean or Jewish origin (Geraminejad *et al*, 2002). However with the onset of the AIDS epidemic it is now considered an aggressive tumor capable of dissemination and even causing death particularly amongst male homosexuals (Geraminejad *et al*, 2002; Zong *et al*, 2002).

1.2.2.1 Clinical Variants of Kaposi's sarcoma

There are four main variants of KS namely the classic form, the endemic KS, the iatrogenic variant and finally the epidemic type. Classic KS is the type that occurs more prevalently in older men of Eastern European, Mediterranean or Jewish origin. It is characterized by the slow formation of benign nodules, which result from the coming together of the lesions. The endemic KS variant which is also often referred to as African KS can in turn be subdivided into four clinical subvariants: a) nodular which is similar to the classic type; b) florid and c) infiltrative, both of which are more aggressive and d) lymphadenopathic form which unlike all other types of KS is very common amongst children particularly young South African Bantu children. On the other hand, the iatrogenic variant of KS is closely related to severe immunosuppression. Therefore it is the type most commonly found in organ transplant recipients who had to take high doses of immunosuppressant drugs, however, the lesions tend to develop only a few years later after the organ transplant. Finally the epidemic type, also known as AIDS-associated KS, is considered the most common proliferative disorder related to AIDS and unlike the classic type, early lesions tend to emerge on the face as reddish to pink papules which in prolonged cases form larger plaques (reviewed in Geraminejad *et al*, 2002).

1.2.2.2 Histology of Kaposi's sarcoma

The progression of KS can be divided into three distinct stages namely the patch or early, the plaque or intermediate stage and the nodular or late stage. During the initial stage of KS (Figure 42 A 1-4), very few spindle cells characteristic of the nodule can actually be visualized. There is instead a large degree of jagged and dilated vascular empty spaces, which take place mostly in the reticular dermis layer of the skin tissue and sometimes may surround normal blood vessels (Jenner and Boshoff, 2002). The patch stage is also characterized by flat elongated endothelial cells lining these clear slit-like spaces and infusing through dermal collagen bundles. Other morphological characteristics of the patch phase include the incidence of perivascular infiltrate of lymphocytes together with plasma cells. Furthermore, a few scattered extravasated erythrocytes and hemosiderin deposits (which are formed because of the break down of hemoglobulin present in the red blood cells) can also be present. The initial stage of

KS is at times hard to diagnose but because HHV-8 infection has been shown to occur mainly in this phase of the disease, the early immunohistochemical detection of HHV-8 with an anti-LANA monoclonal antibody is regarded as a potentially useful tool in the diagnosis of KS (Hong *et al*, 2003).

Following the patch stage is the intermediate plaque stage of KS disease progression, which is characterized by an elevated number of elongated endothelial cells, as well as, by a further development of the spindle-cell proliferation, showing signs of slit-like blood vessel formation within the deeper section of the dermis. As a result, during this phase, almost the entire thickness of the dermis becomes occupied by the more profound vascular proliferation (Figure 43 A 1-3).

At the late and most advanced nodular stage of the vascular tumor (Figure 44 A 1-4) there is hardly any dermal collagen present and the lesion is now characterized by proliferating fascicles of spindle cells growing in all directions, connecting with one another and forming large nodules in the upper half of the dermis, which can clearly be visualized at lower microscopic magnification. These proliferating fascicles are characterized by slit-like blood vessels, extravasated erythrocytes, fibroblasts, inflammatory cells including lymphocytes and plasma cells, and large deposits of haemosiderin pigment within the tumor cells as well as macrophages (Chor and Santa Cruz, 1992). Furthermore, another prominent feature of nodular KS is the presence of hyaline bodies/globules, which are speculated to be defeated or phagocytosed red blood cells (RBC) and these can be seen as light pink eosinophilic structures. Nearly all the tumor (spindle) cells are latently infected by KSHV suggesting that paracrine mechanisms are involved in the progression of the disease (Dupin *et al,* 1999). Studies have shown that KSHV TR sequences in the late stage lesions display all patterns of clonality (Judde *et al*, 2000) implying that KS starts as a polyclonal hyperplasia and that through oligoclonality, develops into a true monoclonal malignancy (Jenner and Boshoff, 2002).

1.2.2.3 Current Therapy for Kaposi's sarcoma

At present, there is no known curative therapy for KS but solely a number of treatments capable of preventing tumor development or reducing KS pathogenesis. Most of the existent treatments will target either cell proliferation or angiogenesis type of mechanisms implicated in tumor growth. Combined chemotherapy, interferon

administration and radiotherapy are some of the commonly used anti-proliferative means of treating KS. Interferons possess anti-angiogenic properties, which have been shown to be related with the baseline $CD4^+$ cell implying that interferons may act through the immune responses in controlling KS. Administration of IFN-α is a systemic therapy for KS and it should only be used in patients with disseminated tumour, particularly when involving visceral organs (reviewed in Hermans, 2000). Recent *in vitro* studies conducted by Pozharshkaya *et al* (2004) indicated that both IFN-γ and IFN-α induced the expression of cellular antiviral genes in HHV-8 infected BCBL-1 cells, it enhanced cell death and decreased the production of infectious virus.

In Western countries and the USA, where highly active anti-retroviral therapy (HAART) is widely used to treat HIV infection, there has been a staged decrease in the occurrence of both KS and other AIDS-associated malignancies, which are often caused by secondary viral infections. The enhancement of the immune system during therapy with HAART is evidently very significant and therefore a useful approach for the immune-prevention of KS. The fact that post-transplant KS lesions regress upon cessation of immunosuppressive treatment imply that cellular immune responses are undoubtedly significant in keeping KSHV infection under control thereby preventing the onset of KS (Bower *et al*, 1999). In conclusion, the main approach in treating KS is undoubtedly by finding means of keeping the immune system boosted.

1.3 Complement System and Inflammatory Responses

Inflammatory responses are characterized by an influx of immune cells, which can be mediated by chemoattractants or chemotactic factors (Kotwal, 2000). The complement system is part of the innate immune defence system, composed of a group of approximately 30 serum proteins, which interact with each other in a cascade-type reaction that splits subsequent proteins into fragments (Walport, 2001). The explosive nature of the complement system, either in the presence or absence of antibodies, can lead to virus neutralization and opsonisation, lysis of virus-infected cells and amplification of inflammatory and specific immune responses (Rother and Till, 1988) as depicted in Figure 4. The usual activation of complement makes up the first line of defence often leading to the release of potent chemotactic complement factors such as C3a, C4a and C5a (Blue box, Figure 4), also known as anaphylotoxins

which are responsible for attracting inflammatory cells thereby causing an inflammatory response at the site of infection (Kotwal, 1997).

The complement amplification events can be initiated via three distinct pathways as shown in Figure 4:

a) The classical pathway, which is activated by an antigen-antibody reaction that starts with the binding of the C1 complex via C1q to the Fc region of immunoglobulin (Ig) (McGeer and McGeer, 1992)

b) Spontaneously (alternative pathway) as a result of differences in envelope or membrane composition compared to the host (Spiller *et al*, 2003a) as well as an inherent flux of the most copious complement factor, C3 and finally c) the lectin pathway which recognises a number of saccharide molecules mostly mannose, generally only present on the surface of microorganisms (Blom, 2004).

Irrespective of the complement activation pathway, a membrane attack complex (MAC) is formed at the end of the complement cascade. MAC is a large complex of proteins that in many cases causes a pore in the membrane of the pathogen leading to osmotic differences and therefore lysis of the infectious agent (Muller-Eberhard, 1986). Activation of bound C1 leads to sequential cleavages of C4 and C2, forming C4b2a, the classical pathway C3 convertase. Cleavage of the bound convertase in turn, activates the terminal lytic mechanism, characteristic of both the classical and the alternative pathway (Kotwal *et al*, 1990).

Complement protein C3 is a fundamental molecule whose activation is vital for all the important roles carried out by the complement system (Sahu and Lambris, 2001), which in turn also requires the formation of the C3 and C5 complement convertase enzymatic complexes (Spiller *et al*, 2003a). In addition, C3 promotes phagocytosis as MAC-resistant pathogens are opsonised with C3b and iC3b fragments which bind to the complement receptor 1 (CR1) and complement receptor 2,3 and 4 (CR2, CR3 and CR4) respectively, found on the surface of phagocytes such as macrophages and neutrophils. In addition to triggering immune adherence and phagocytosis, these receptor-ligand associations also facilitate B cell signalling and promote antigen (Ag) localisation (reviewed in Nielsen *et al*, 2000). On the contrary, factor I-mediated enzymatic degradation of C4b results only in the covalent attachment of C4d fragment on the target, referred to as an immunological scar as unlike iC3b, the biological activity of C4d has not yet been identified (Barilla- LaBarca, 2002).

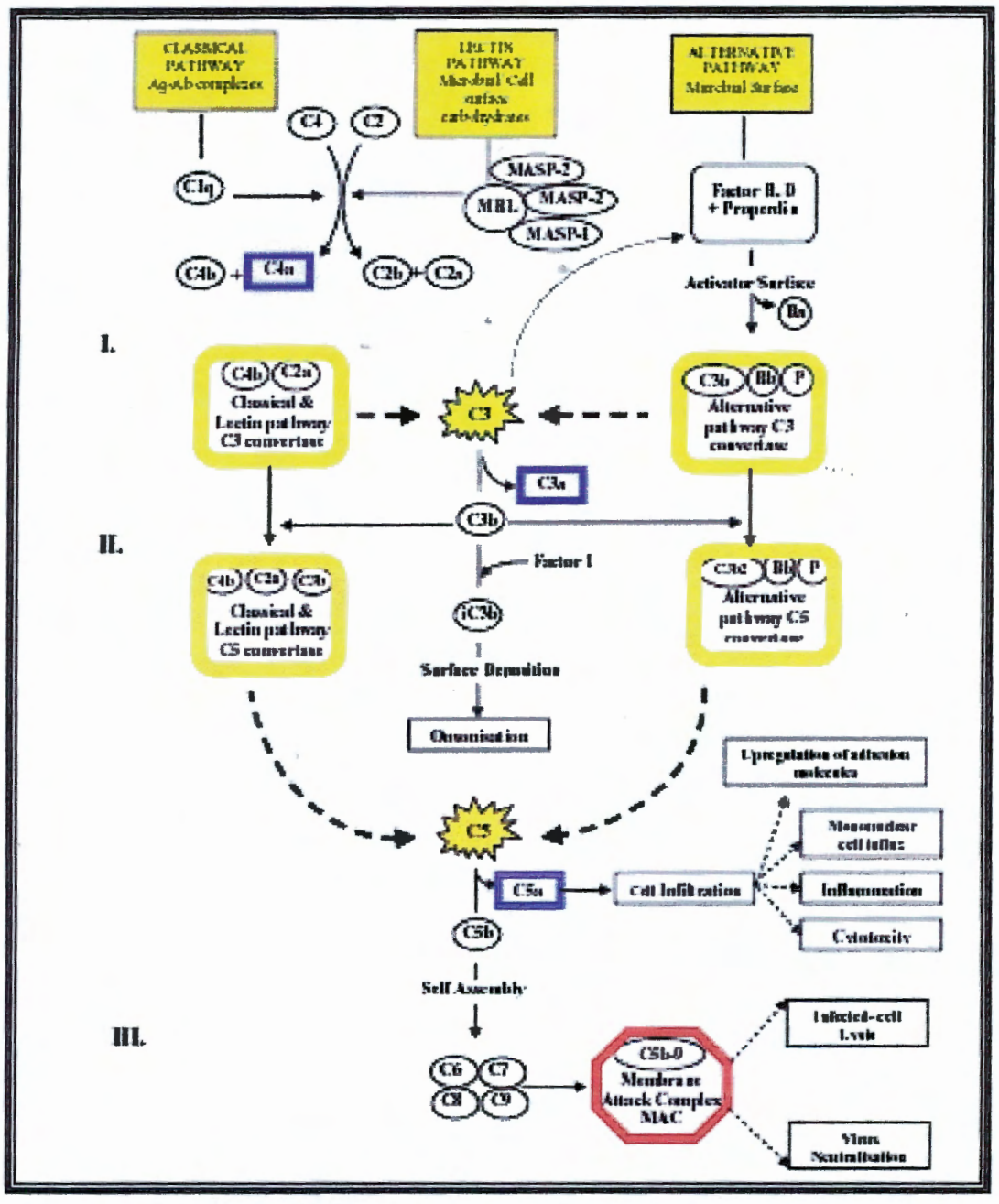

Figure 4. Overview of the current understanding of the complement pathways

The complement system is activated by means of three distinct pathways: The classical, alternative and the lectin pathway. Complement activation can take place on the surface of antigen: antibody complexes (classical), in the absence of antibody on microbial surfaces (alternative) or on cell surface carbohydrates (lectin). The complement system can be divided into three key cascade-like events: **I.** The formation of the C3 convertase (yellow box); **II.** The formation of the C5 convertase (orange box) and finally **III.** The formation of the membrane attack complex (MAC) (red box). The anaphylotoxins, C3a, C4a and C5a (blue boxes) attract inflammatory cells to the site of infection leading to an inflammatory response (Adapted from Kotwal *et al*, 1997).

Furthermore, C3 supports local inflammatory responses against pathogens and instructs the adaptive immune response to select the suitable antigens, for a humoral response. The downfalls of this molecule however, is that its unregulated activation can lead to host cell damage and its interactions with viral proteins for example, may provide a mechanism by which viruses evade the complement system (Sahu and Lambris, 2001).

The fact that patients suffering from the lack of complement components are subject to recurring infections sometimes with detrimental consequences, clearly show the significance of complement as our first line of immune defence. Therefore, it can be concluded that the complement system plays a critical role in innate immunity, which provides a rapid response against a majority of pathogens without the requirement of a previous exposure. In addition, it also plays an important part in forewarning the adaptive immunity of a draw near combat.

1.3.1 Host Complement-Inhibitory/Regulatory Proteins

Considering the volatile and potentially destructive nature of the complement proteins which do not have the ability to differentiate between self and non-self and therefore destroy any cell including host cells (Sahu and Lambris, 2001), there is an evident need for the presence of inhibitors/regulators of the complement system in the host tissues.

In vivo, complement activation is regulated by a family of structurally and functionally related proteins referred to as mediators/regulators of complement activation (RCA) (Lambris *et al*, 1998) that are encoded by a gene cluster present in chromosome 1 (Hourcade *et al*, 1992). These proteins are characterised by the presence of 4-35 common structural motifs called the short consensus repeats (SCRs) or the complement control protein (CCP) domains (Hourcade *et al*, 1989 Kirkitadze and Barlow, 2001). Each CCP module is comprised of approximately 60 amino acids and it is characterised by a conserved motif made up of four disulphide-linked cysteins, prolines, tryptophan and many other residues which together form a compact hydrophobic core in a bead-like structure (Barlow *et al*, 1993).

This family of proteins exist in a balanced manner and include:

(i) The plasma proteins, C4-binding protein (C4BP), which is the major soluble inhibitor, of both the classical and lectin pathways and factor H, which inhibits mainly the alternative complement activation pathway;

(ii) the membrane-bound regulatory proteins, CD35 or CR1, CD55 or decay-accelerating factor (DAF) and CD46 or membrane cofactor protein (MCP), which are generally present at various ratios on all human cells.

On the whole, all these complement inhibitors act at the level of C3 and C4 and function either by accelerating the decay of the C3- and C5-convertases or by enhancing the serine protease factor I (FI)-mediated proteolytic degradation of C3b or C4b complement fragments (Sahu *et al*, 2000). The plasma proteins, factor H and C4BP are specific for C3b and C4b respectively, while MCP and CR1 are cofactor proteins for both C3b and C4b (Barilla- LaBarca *et al*, 2002).

1.3.1.1 The C4-Binding Protein (C4BP)

C4BP is a 570 kDa protein made up of seven alike α-chains containing eight CCP modules. It is also comprised of a single β-chain, which contains three CCP domains and all these structural chains are linked via disulfide bridges. With the use of electron microscopy, two decades ago, Dahlabäck and Müller-Eberhard, (1984) described the conformation of this CRP as spider-like whereby the seven α-chains appear as extended tentacles. Blom *et al* (1999) have identified a cluster of positively charged amino acids which are essential for C4b binding and FI cofactor function. C4BP prevents the deposition of C4b and the assembly of the classical C3-convertase. In turn, it can also accelerate the decay of this convertase and it can serve as a cofactor in the FI-mediated cleavage of C4b and C3b (reviewed in Blom, 2004). In the case of a pathogenic infection, the functions of C4BP mentioned here, lead to decreased opsonisation of the virus particles or other pathogens with C3b therefore discouraging phagocytosis. Furthermore, it also leads to a diminished level in the formation of MAC, in other words, level of lysis and/or neutralisation of the infectious agent.

1.3.1.2 Other Host Complement Inhibitors- An Overview

The functions of CD35/CR1 include:

(i) Cofactor activity for the FI-mediated degradation of C3b;

(ii) Binding of C4b thereby enhancing its cleavage into other C4 complement factors, C4c and C4d;

(iii) Obstruction of the complement cascade by accelerating the decay of both the C3 and C5- convertases;

(iv) Binding of all complexes that are opsonised with C3b and C4b resulting in phagocytosis by the CR1-containing cells (reviewed in Fishelson *et al*, 2003).

CD46/MCP is an extensively dispersed type 1 transmembrane glycoprotein that regulates complement activation, basically, in the same way as CD35 for the exception that this particular regulator of complement does not possess decay-accelerating activity (Kojima *et al*, 1993). Liszewskin and collaborators (2000) have predicted the crystal structure of MCP and shown that it consists of four extracellular adjacent CCP modules all of which contain sites that are important for the complement inhibitory ability of this molecule.

CD55/DAF is an integral membrane protein attached to the cell surface by a glycosyl phosphatidylinositol (GPI)-anchor (Medof *et al*, 1986) and as implied by its name, DAF enhances the decay of both C3 and C5 convertases (Nicholson-Weller and Wang, 1994).

It is worthwhile mentioning that there is an additional host complement inhibitor known as CD59, even though at the DNA level it does not share significant homology to the other complement regulators (Sawada *et al*, 1990) reviewed above. CD59 is very important however, because it provides the last line of defence against undesirable complement activation on host tissues as it interferes with the formation of MAC by preventing C9 polymerisation (Meri *et al*, 1990).

Viruses are compulsory intracellular parasites and ultimately depend on the cell machinery of the host to survive and propagate. Since the complement proteins implicated in the cascade activation process are not able to discriminate between self and non-self, viruses are highly vulnerable to the complement system upon evading the host. Therefore, during co-evolution, viruses have developed and acquired cleaver means of overcoming the complement system of the host, which will be described in the section to follow.

1.3.2 Viral Strategies of Immune System Evasion

In order to combat the host defence mechanisms and succeed as pathogens, certain viruses, including KSHV have developed/acquired strategies of defence against the complement system and other host defence mechanisms (Spiller *et al*, 2003a). These strategies can be divided into two main categories, namely active strategies, in which the virus has obtained immunomodulatory genes, and passive strategies during which error-prone replication allows for rapid antigenic evolution and therefore, consequent evasion of the host immune system (Chaston *et al,* 2001).

One of the mechanisms of immune system evasion by viruses is the sequestering or modulation of the expression of host complement inhibitors by capturing CCPs from the RCA loci of the host. As an example, Spiller *et al* (1996) showed that human cytomegalovirus-infected cells were encouraged to inhibit the complement system when compared to virus-free cells. In the presence of the virus there was an increase in the cell surface expression of host membrane-bound complement inhibitors like DAF and MCP. Like human cytomegalovirus, HIV and vaccinia virus incorporate in their envelope host complement control proteins when they are being released from infected cells. In this way they prevent their opsonization by inhibiting the effects of complement on them (Montefiori *et al*, 1994 and Vanderplasschen *et al*, 1998).

On the other hand, members of the herpesvirus (KSHV, HSV-1, HVS) and poxvirus (vaccinia, cowpox, smallpox) family have developed the ability to encode their own homologues of complement regulatory proteins, capable of binding key complement subunits and inhibiting the complement-mediated destruction of infected cells (Dietz, 2000). Indeed, sequence analysis of these DNA viruses has confirmed the presence of genes with remarkable homology to complement control proteins containing short consensus repeats (SCRs) (Sahu *et al,* 1998a). Furthermore, certain viruses benefit from the complement system by using host complement receptors to infect a range of cells (Sahu *et al*, 1998b).

The protein products of viral "pirated genes", the immunomodulators, distinctively subvert the immune response by targeting specific cellular signal pathways, and thus facilitating pathogenesis and persistent viral infection within the host (Sahu *et al,* 1998a). In addition to causing persistent infections, herpesviruses tend to modulate more strongly the specific secondary host responses aimed at them, for example by blocking antibody attack or antigen presentation to major histocompatibility complex

(MHC) molecules (Hengel *et al,* 1998; Nagashunmugan, 1998). It has been shown recently that KSHV also uses the mechanism of auto-activation to regulate the expression of a viral transforming protein thereby efficiently evading host tumour suppressor pathways (Wang and Gao, 2003).

In conclusion, certain viral genes, which are likely to have been captured from host cells during viral evolution, have undoubtedly been modified to confer an advantage in viral replication, transmission and survival (Dietz, 2000).

1.3.3 Immunomodulators of Viral Infection

Immunomodulators (Table 3) have the ability to conserve the virus by blocking apoptosis until the virus has replicated to high titers and found a new host, and by protecting it against damage from the inflammatory response (Kotwal, 2000).

Many DNA virus produce two major groups of proteins that take place in evasion of the host's immune responses, namely the cell-associated cytokine response-modifying proteins or serpin-related proteins (Kotwal and Moss, 1989) and the secreted proteins also known as virokines (Kotwal and Moss, 1988). In addition, the virokine family consists of a number of cytokine-chemokine-binding proteins or viroreceptors (Upton *et al*, 1992), a neurovirolence factor (Kotwal *et al*, 1989) and a complement control protein (Kotwal and Moss, 1988). Virokines which are often homologous to host proteins are very small and potent virally encoded proteins that are secreted from infected host cells. These are capable of modulating several features of the host immune system, thus creating a favourable habitat for viral replication (Smith and Kotwal, 2001).

1.3.3.1 Examples of KSHV Chemokine Homologs

Virokines include the chemokines, which are significant chemoattractants that play a major role in the initial host immune response to infection and injury (Dietz, 2000).

KSHV encodes a number of proteins homologous to many cellular chemokines for example, the viral macrophage inflammatory protein, vMIP-II, which exhibits broad-spectrum chemokine receptor binding ability (Smith and Kotwal, 2001). Chemokine vMIP-II binds predominantly to the CC-chemokine receptor (CCR-3) causing human eosinophil activation as measured by intracellular calcium mobilization and chemotaxis (Moore *et al,* 1996; Boshoff *et al,* 1997). It has also been shown, that this

particular chemokine can prevent the entry of several strains of HIV-1 into cells by blocking the virus chemokine coreceptor (Luttichau *et al,* 2000).

Table 3. Examples of Viral Immunomodulators of Complement Pathways

Virus	Virokine	Host homologue	Functional activity
KSHV	Kaposica/ CRP/KCP	CCPs: CR1, C4bBP, Factor H, DAF	Enhances the decay of classical C3 convertases; acts as a cofactor for factor I-mediated C4b & C3b cleavage; Inhibits C3b deposition
HVS	ORF4 (CCPH)	C4bBP, DAF, MCP	Inhibits C-mediated lysis, regulates activation of C9
HVS	ORF15/ ORF-LS	CD59	Inhibits C-mediated lysis; regulates activation of C9
HSV	gC1 and gC2	CR1, DAF	Binds to C3b & iC3b; accelerates decay of ACP C3 convertase
HSV 1/2	gE/ gI	Fc receptors	Binds Fc & decreases detection of bound Ab by complement
EBV	gp 335/ 220	C3d	Competes with C3d for binding to CR2
HIV	gp41	C3	Incorporates CD59, DAF, factor H and properdin on surface; prevents complement activation, binds C1
Vaccinia	VCP	CR1, C4bBP, Factor H	Binds C3b & C4b, Cleaves C3b in presence of factor I; inhibits formation & speeds up the decay of C3 convertases
Cowpox	IMP	CCPs	Inhibits complement- mediated lysis & decreases inflammatory response
Myxoma	T2	TNF receptor	Reduces inflammation

(Kotwal, 1997)

It is believed that viral chemokines add to mechanisms that block the host defence and contribute to virus-induced cellular transformation resulting in the development of proliferative disorders such as KS (Dietz, 2000). In addition, KSHV encodes chemokine receptor homologs also known as G-protein-coupled receptors (GCRs), a category of proteins thought to attract macrophages and monocytes via the chemokines bound to their surface. This in turn, results in viral entry and subsequent induced viral replication as well as dissemination of the virus throughout the host (Kotwal, 2000).

1.3.3.2 Examples of KSHV Cytokine Homologs

The first line of defence following KSHV infection in an immunocompetent host is the activation of complement, the influx of immune cells and ultimately the secretion of cytokines, which are responsible for the recruitment of even larger numbers of cells to the infected site. The cytokine receptor-like virokines regulate the improved macrophage influx resulting from proinflammatory cytokines secreted by the initial immune response (Kotwal, 2000). In 1994 Chang *et al*, discovered that KSHV encodes viral interleukin 6 (vIL-6) with 25% amino acid identity with its human homolog, which has been associated with the development of several lymphoproliferative disorders as IL-6 is known to enhance B-cell survival, differentiation and proliferation of lymphatic cells (Hideshima *et al,* 2000). Therefore, it is thought, that the expression of this viral gene is involved in the pathogenesis of KSHV-related diseases namely MCD and PEL (Geraminejad *et al,* 2002).

1.3.3.3 Examples of Complement Regulatory Proteins

The most well studied example of a viral homologue to the family of complement regulatory proteins is the vaccinia virus complement control protein, best well known as VCP, which is a 35 kDa soluble protein composed of four CCP modules (Kotwal and Moss 1988). The crystal structure of VCP was successfully elucidated by Murthy *et al* (2001) and it revealed an extremely extended molecule with the ability to bind heparin and regulate complement activation simultaneously, as shown by surface plasmon resonance (SPR) studies of recombinantly expressed VCP (rVCP) constructs (Smith *et al*, 2003). Nuclear magnetic resonance (NMR) analysis of VCP after exposure to a number of adverse conditions demonstrated that VCP is a very robust complement regulatory protein most likely because of its structural conformation (Smith *et al,* 2002). Functionally, VCP has been shown to inhibit the classical pathway-arbitrated lysis of sheep erythrocytes, to bind C3b and C4b and to function as a cofactor for their FI-mediated cleavage. In addition, VCP also plays a role in the acceleration of the decay of both the classical and alternative pathway C3 convertase complexes (Mckenzie *et al*, 1992). Furthermore, the ability of VCP to bind heparin sulphate proteoglycans on the surface of human endothelial cells enables this protein to inhibit specific antibody binding to MHC class I molecules (Smith *et al*, 2000).

The cowpox virus (CPV) homologue of VCP is called the inflammatory modulatory protein (IMP) and like VCP it has been shown to down-regulate chemotactic

complement factors, C3a, C4a and C5a, thereby resulting in diminished cellular influx and inflammation. This function of IMP was demonstrated by injecting the footpad of BALB/c mice with CPV expressing IMP (Miller *et al,* 1997 and Kotwal *et al,* 1998).

In addition to the two poxviruses examples reviewed above, a number of herpesviruses are known to encode for regulators of the complement system. The first herpesvirus complement regulatory protein identified was glycoprotein C of HSV-1 (gC-1) (Friedman *et al,* 1984) which has also been most extensively studied. Similarly, HSV-2 also encodes for a gC-2. Interestingly none of these two glycoproteins are homologous to the proteins of the RCA family suggesting that in general their mechanisms through which they inhibit complement activation must be peculiarly diverse from the RCA molecules. On the other hand, HVS encodes for a protein with remarkable homology to VCP and other RCA proteins, the HVS complement control protein homolog (CCPH), which due to differential splicing of the primary transcript exists as a membrane and secretory form (Albrecht and Fleckentein, 1992). In addition, HVS also encodes a CD59 homologue capable of interfering with the assembly of MAC (Rother *et al,* 1994). Furthermore, like KSHV, the murine gammaherpesvirus-68 (MHV-68) also possesses an ORF 4, which encodes for a CCP with the ability to regulate both the classical and alternative pathways of complement activation (Kapadia *et al,* 1999).

1.3.4 The KSHV Complement Regulatory Protein (KCP)

As mentioned above, KSHV encodes several proteins that potentially contribute to the disruption of the immune response. One of these virokines was determined by sequence analysis to be encoded by ORF 4 since it shares homology with the cellular proteins known as RCAs (Russo *et al,* 1996).

KSHV ORF 4 is a secondary lytic gene (Jenner *et al,* 2001), which is expressed on the surface of KSHV infected cells (Spiller *et al,* 2003a). Analysis of the primary sequence as deduced from the ORF 4 revealed that the KCP is predicted to be 551 amino acid (aa) residues in size including a 15 aa signal peptide (Figure 6).

KCP is a type 1 membrane-bound protein and structural analysis based on bioinformatics revealed that KCP is comprised of a number of distinct regions: (i) four N-terminal tandemly repeating CCP domains projecting into the extracellular space, which are present within the first 270 aa (Figure 5). The presence of these CCP

domains, therefore render this protein homologous to members of the RCA family, particularly to human DAF.

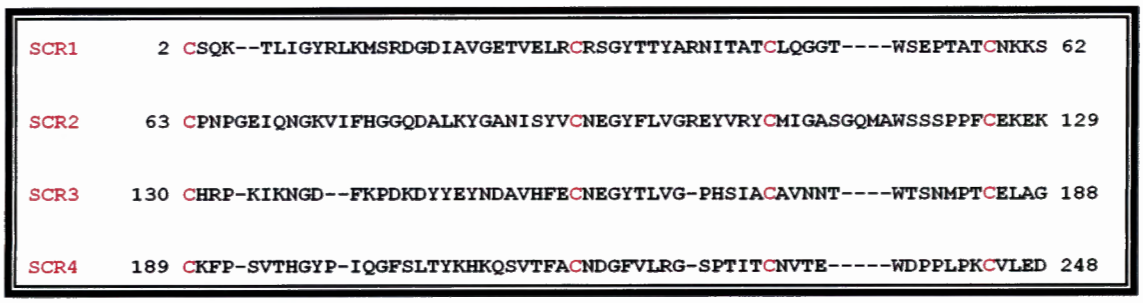

Figure 5. Clustal W multiple sequence alignment of the SCRs of KCP

Each SCR module is comprised of approximately 60 amino acids and it is characterised by a conserved motif made up of four disulphide-linked cysteins.

Immediately after the SCR region is a (ii) proline-rich region of about 70 aa ending in a dicysteine motif which is in turn (iii) followed by a 202 aa serine/threonine rich region speculated to be heavily *O*-glycosylated. Finally, (iv) a carboxy terminal hydrophobic region of 26 aa was identified as a putative transmembrane domain that anchors the protein to the cell membrane (Figure 6).

Spiller *et al* (2003a) showed that transfected mammalian cell lines expressed the KSHV ORF 4 gene as a full-length transcript and as two alternatively spliced transcripts, all of which were shown to only differ in length between the CCP domains and the potential transmembrane region. In other words, the three isoforms maintained the conserved SCR motifs needed for complement regulation as well as the putative transmembrane region. According to this research, the KSHV ORF 4 is the most complex spliced gene encoding a viral complement regulatory protein described to date. On this note, recombinant KCP proteins were produced corresponding to the naturally expressed isoforms as both membrane-bound and soluble truncated fusion proteins with the Fc region of human immunoglobulin, which were in turn conveniently purified by affinity chromatography.

Spiller *et al* (2003a) demonstrated that the three KCP isoforms inhibit C3b deposition on the surface of cells under complement-activating conditions thereby preventing lysis of the infected cells.

Figure 6. Primary Structural Features of KSHV complement regulatory protein

Conserved motifs of the primary structure of KCP are depicted in Figure 6. The four conserved SCR domains are underlined and the disulphide-linked cysteines are shown in bold and red. The signal peptide and the putative transmembrane domain are highlighted in pastel pink and yellow boxes respectively. The potential *N*-glycosylation sites as determined by primary sequence analysis are represented in blue. The 5 proline residues within the proline rich region are bold and italicised in black. Immediately following the proline-rich region is an S/T region containing 26 serines and 38 threonine residues shown in bold and two different shades of green respectively.

KCP expression at the cell surface and on the virion itself is likely to contribute to the viral evasion of the complement component of the innate immune response, facilitate KSHV infection, persistence and pathogenesis and finally aid in targeting KSHV to one of its host reservoirs, since C3d is a ligand for complement receptor 2 present on B-cells (Spiller *et al*, 2003a).

Additionally, Spiller *et al* (2003b) showed that all three forms of KCP-Fc strongly enhanced the decay of classical C3 convertase and in spite of KCP's ability to bind both C3b and C4b its affinity for C4b was shown by SPR to be 10-fold higher. This finding correlates with the fact that KCP is a more efficient inhibitor of the classical than the alternative pathway of complement activation. Furthermore, all cell-bound and soluble forms of KCP in this study were generally comparable in their performance as cofactors for FI-mediated cleavage of both C4b and C3b into C4d and iC3b (further cleaved into C3d) respectively.

On the other hand, Mullick *et al* (2003) have called the KSHV inhibitor of complement, kaposica which they expressed as a recombinant shorter secreted form (encompassing SCRs 1-4 only) in the yeast *Pichia pastoris* expression system. Similarly, this study confirmed the KCP-dependent mechanism by which KSHV can subvert complement attack by the host as the purified protein was shown to (i) repress human complement-mediated lysis of erythrocytes, (ii) prevent the deposition of C3b on the cell surface and (iii) act as a cofactor for FI-mediated cleavage of C3b and C4b. The latter reveals that the KSHV inhibitor of the complement cascade regulates the formation of C3 convertase by turning its subunits, C3b and C4b, into their inactive forms. Furthermore, hemolysis assays carried out by Mullick *et al* (2003) revealed that KCP is twice as efficient in inhibiting the classical pathway-mediated lysis of erythrocytes and approximately five times stronger than VCP in inhibiting the alternative pathway-mediated lysis of erythrocytes.

Most recently, in order to characterise the structure-function relationship of KCP, Mark *et al* (2004) carried out a broad analysis of the CCP domains at the amino acid level by generating twelve mutants, which were in turn analysed for their ability to bind C3b and C4b, act as FI cofactors and to accelerate the decay of convertase complexes. According to Mark *et al* (2004), KCP has undoubtedly evolved in such a way as to maintain the spatial structure of its functional sites, particularly the positively charged regions which are similar to the functional sites present in other common human regulators of the complement system (Figure 7).

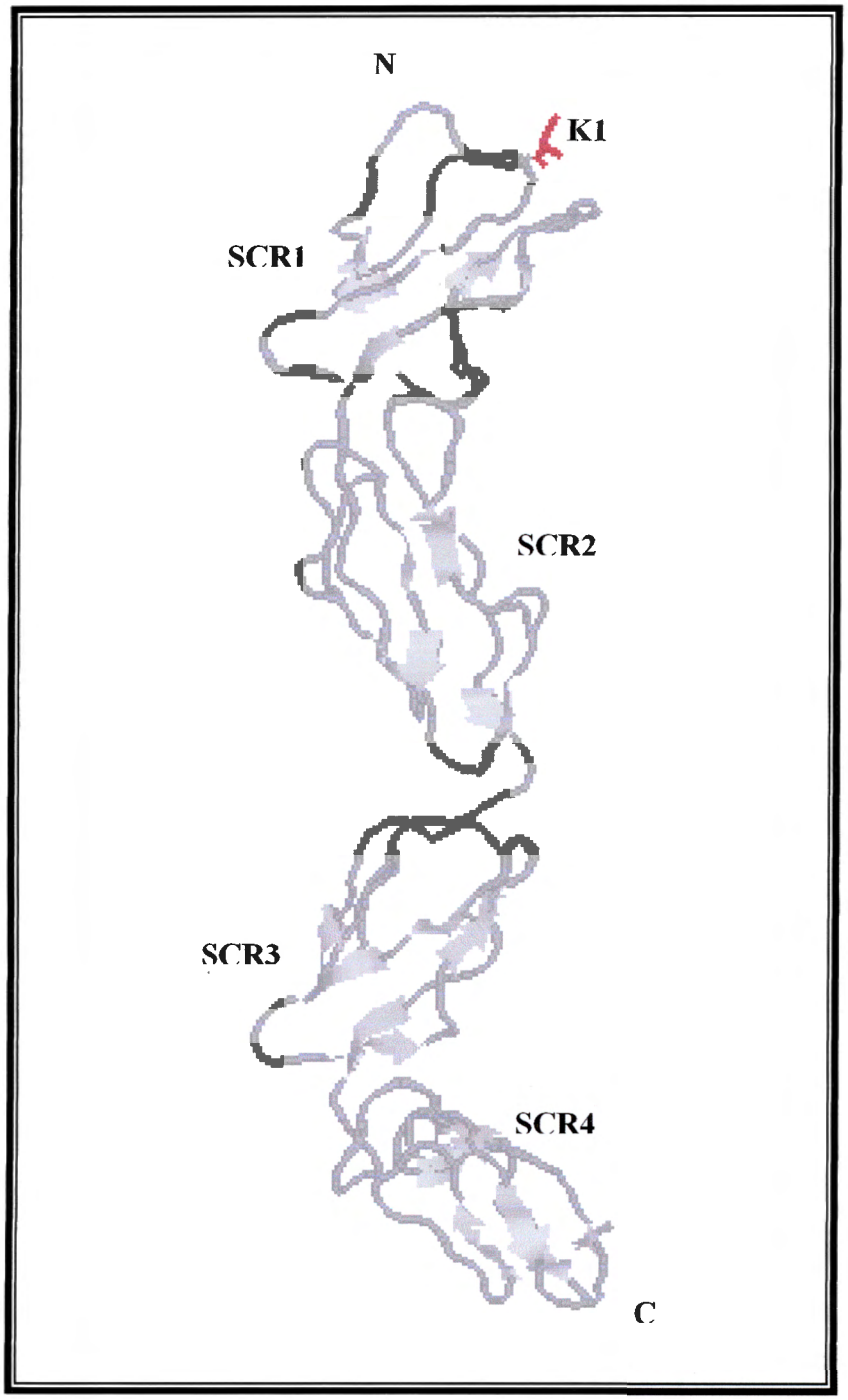

Figure 7. Illustration of the predicted Crystal Structure of the four SCR motifs of KCP

The tertiary structure model of KCP was predicted by homology modelling using the VCP crystal structure contained in the PDB (Protein Data Bank) as a template. The 3D structure of the four SCR motifs of KCP was created using the freely available RasMol software. The amino acid at the N-terminus shown as a red stick represents the first amino acid of CCP where the signal peptide was cleaved off, and it is labelled using the single letter code plus the number that relates to its position in the primary amino acid sequence.

1.4 STATEMENT OF HYPOTHESIS

1.4.1 Broad Hypothesis:

The KSHV (HHV-8) complement regulatory protein (CRP) is involved in the establishment of the viral infection leading to Kaposi's sarcoma in HIV patients.

1.4.2 Specific Hypothesis:

The KSHV (HHV-8) putative complementary ORF4 encodes a functional protein that has an *in vivo* role in the complement inhibition strategy of the virus immune system evasion.

1.5 AIMS AND OBJECTIVES

The primary objective of this work was to characterise the structure-function relationship of KCP. In order to undertake these studies, the following specific aims were pursued:

1) To produce three recombinant versions of KCP, namely a soluble truncated protein comprising of the 4 CCP domains (KCP-S, small), KCP protein lacking the putative transmembrane binding domain (KCP-M, medium) and the full-length ORF 4 protein (KCP-F, full) using the methylotrophic yeast *P. pastoris* expression system;
2) To confirm the secreted expression of the viral proteins by SDS-PAGE, Immunodetection and Western blot analysis;
3) To synthesised a polyclonal anti-KCP antibody directed against a selected peptide region that is common to all three recombinant KCPs;
4) To test the partially purified proteins of interest in a hemolytic assay for complement binding function;
5) To carry out preliminary immunohistochemical studies using the same antibody in order to determine if there's a link between KCP and KS.

CHAPTER TWO

MATERIALS AND METHODS

Materials

Plasmids and *P. pastoris* strains used in this study can be found in **Appendix A**. All materials and their respective suppliers are listed in **Appendix B.**

2.1 Preparation of the KSHV ORF 4 DNA Constructs

For easy cloning of the genes of interest as well as for possible future site-directed mutagenesis work, the KSHV ORF 4 gene products were first inserted into the expression vector pGEMT-easy (Promega) to generate three recombinant plasmids, pGEMT/KSHV ORF 4 (735), pGEMT/KSHV ORF 4 (1436) and pGEMT/KSHV ORF 4 (1581), coding for a soluble protein containing the 4 Sushi domains (735 bp), the whole extra cellular domain (1436 bp) and the full ORF 4 containing the putative transmembrane domain (1581 bp) respectively (Figure 8).

The *Escherichia coli* strain XL-1 blue was used for transformation and propagation of the recombinant plasmids. *E. coli* is the most frequently used prokaryotic host for recombinant DNA technology because it is easy to grow and manipulate in large quantities in a controlled manner. In addition, it has been both genetically, and biochemically unravelled, thus providing a favourable alternative for the effective cloning of the genes of interest.

For the heterologous production of the KSHV ORF 4 complement regulatory protein (KCP) in *P. Pastoris*, the KSHV ORF 4 gene products were then inserted into the yeast expression vector pPIC9 to generate three recombinant plasmids as described above.

2.1.1 Primer Design

Oligonucleotide primers (Table 4) for the *in vitro* amplification of KSHV ORF 4 genes by PCR were carefully designed using the computer software Gene Runner. A sequence-specific forward and three consequent reverse primers were designed and

analysed for the PCR. The G/C content and the melting temperatures (Tm) values of the selected primers were automatically calculated.

Table 4. Design of primers for PCR amplification of KCP from KSHV DNA

Restriction endonuclease sites are indicated underlined and stop codons are in boldface.

Primer	Primer sequence	Tm (°C)	Conc (OD/ml)	Mw
Fwd 03-0668	5'-GAATTCAAGTGTTCCCAAAAAACC-3'	68.8	501.7	7393.9
Rev 1 03-0669	5'-GCGGCCGC**TTA**CAAAACACACTTAGG-3'	78.9	548.5	8029.3
Rev 2 03-0670	5'-GCGGCCGCCGATTTTTAGACGC**TTA**CGGTGGCCTG-3'	96.4	614.7	10851.1
Rev 3 03-0671	5'-GCGGCCGC**CTA**ACGAAAGAACAG-3'	78.4	494.8	7156.7
Fwd 03-1420	5'-TGGCCAGGACAATGAAAAGTGTTCCC-3'	78.7	699.7	8084.3
Rev 03-1421	5'-CTAACGAAAGAACAGATAGTGAAATAAGG-3'	69.1	590.80	9105.0

2.1.2 PCR amplification of KSHV ORF 4 gene from KSHV DNA

The three ORF 4 proteins (Figure 8) encompassing SCRs 1 to 4 were amplified from KSHV DNA isolated from a KSHV-infected PEL cell line (kindly provided by Prof. Chris Boshoff, University college London, UK), with specific primers (Fwd) 5'-GAATTCAAGTGTTCCCAAAAAACC-3' (*Eco*RI site is underlined), (Rev1) 5'-GCGGCCGC**TTA**CAAAACACACTTAGG-3', (Rev2) 5'-GCGGCCGCCGATTTTTAGACGC**TTA**CGGTGGCCTG-3' and (Rev3) 5'-GCGGCCGC**CTA**ACGAAAGAACAG-3' (*Not*I site is underlined and stop codon is in boldface) as represented by Figure 8. The PCR amplification of the KSHV ORF 4 genes was carried out using an enzyme mix containing thermostable *Taq* DNA polymerase and *Tgo* DNA polymerase, which has proof reading activity [Expand^{TM} High Fidelity PCR System (Roche)].

Two separate master mixes were prepared on ice, the components of which are described in Table 5. The master mixes were thoroughly mixed on ice and centrifuged briefly to collect the samples at the bottom of each tube. Master mix 2 [25µl] was added to each one of the master mix 1 [25µl] on ice and mixed thoroughly in order to produce a homogenous reaction. The samples were then placed in a thermocycler (ThermoHybaid cycler) and thermocycling was performed using the parameters described in Table 6.

Table 5. Master Mix Components used in the PCR of the KSHV ORF 4 genes

Master Mix 1 Components	Rxn" 1	Rxn"2	Rxn"3	Rxn"4	**Final Conc"**
$dddH_2O$	22.7	22.7	22.7	22.7	-
dNTP mix (10mM each)	1	1	1	1	200 µM each
KSHVORF 4-specific Fwd primer (100 pmol/µl)	0.5	0.5	0.5	0.5	50 pmol/µl
KSHVORF 4-specific Rev primers (100 pmol/µl)	0.5	0.5	0.5	0.5	50 pmol/µl
KSHV DNA template (360 ng/µl)	0.3	0.3	0.3	0.3	100ng/µl
Total Volume (µl)	25	25	25	25	-

Master Mix 2 Components	Volume added (µl)	**Final Concentration**
$dddH_2O$	77	-
10xExpand High fidelity buffer with 15 mM $MgCl_2$	20	1x
Enzyme mix (3.5 U/µl)	0.75x4 = 3	2.6U/ 50µl reaction
Total Volume (µl)	100/4= 25	-

Table 6. Thermo cycling parameters used in the PCR of the KSHV ORF 4 genes

Step	**Temperature (°C)**	**Time**	**Number of Cycles**
Hot Start	94	2 min	1x
Denaturation	94	30 s	30x
Annealing	56	1 min	
Extension	72	2 min	
Final Extension	72	7 min	1x

The KSHV ORF 4 PCR products were purified using the Wizard® SV system (Promega), which is a silica membrane-based system designed to extract and purify DNA fragments directly from PCR reactions or agarose gels.

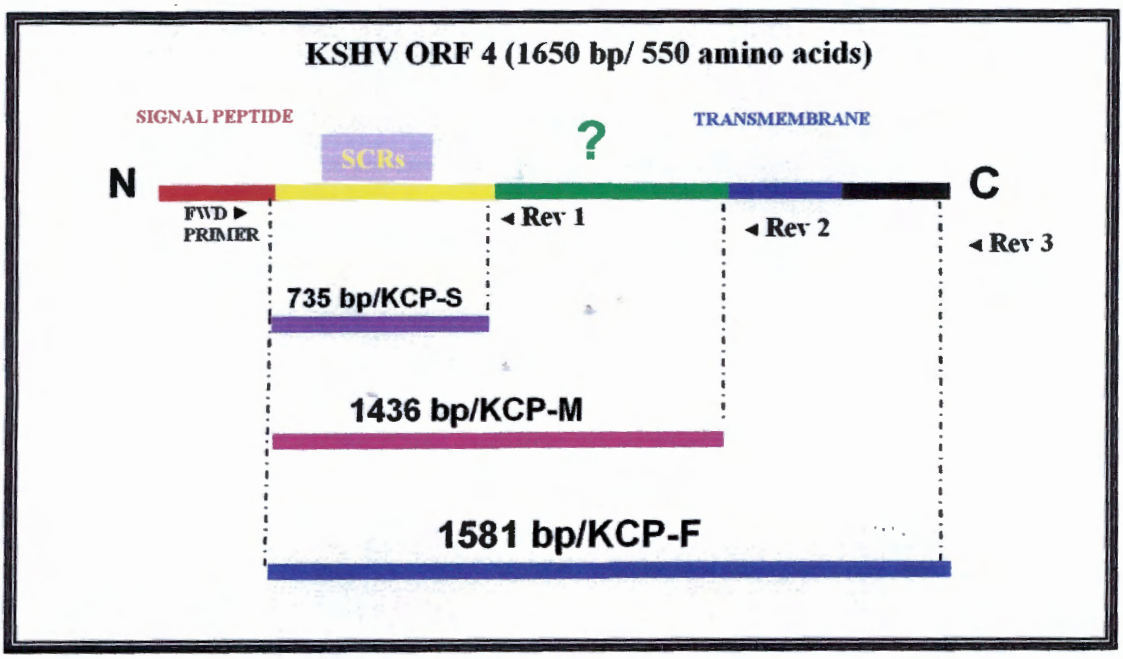

Figure 8. Schematic diagram of the recombinant KSHV ORF 4 transcript map

This figure represents the KSHV ORF 4 gene showing the N and C-terminus as well as the signal peptide (red), the SCRs-containing region (yellow) and the putative transmembrane region (blue). Three sets of primers were carefully designed consisting of a sequence-specific forward and three consequent reverse primers in order to flank three different sized DNA fragments, as represented by the purple, magenta and navy blue transcripts.

2.1.3 Purification of the PCR products

The KSHV ORF 4-specific PCR products were purified with the Wizard® SV system. One SV minicolumn was placed in a collection tube for each PCR reaction above. The prepared PCR products were then transferred to each respective minicolumn followed by incubation at room temperature for one minute. The SV minicolumns were centrifuged in a micro centrifuge at 10 000 x g for 1 minute and the flow-through was then discarded. The columns were washed by adding 700 µl of the membrane wash solution [10 mM potassium acetate pH 5.0, 16.7 µM ethylenediaminetetraacetic acid (EDTA) pH 8.0], which was initially diluted with 95% ethanol to a final concentration of 80% ethanol. The SV minicolumns were centrifuged and the flow-through discarded as before. The wash step was repeated with 500 µl of membrane wash solution followed by centrifugation of the columns for 5 min at 10 000 x g. The flow-through was discarded and the columns were centrifuged for an additional minute. The minicolumns were then carefully transferred to a clean 1.5 ml microcentrifuge tube and the bound DNA was eluted in Tris-2-

amino-2-(hydroxymethyl)-1, 3 propandiol (Tris)-EDTA (TE) buffer [50 µl] (10 mM Tris-HCL pH 8.0 and 1 mM EDTA) and after incubating at room temperature for 5 min, the tubes were microcentrifuged at 10 000 x g for 1 minute. The minicolumns were discarded and the microcentrifuge tubes containing the purified PCR products were stored at 4°C until later use.

2.1.4 Measurement of DNA concentration

The concentration of the above eluted DNA was determined by UV spectrometry using disposable Ultravette® cuvettes (Merk). The DNA was diluted 1:60 in TE buffer and the DNA concentration was calculated using the following formula:

DNA concentration (µg/ml) = A_{260} x 50 x dilution factor

Where, **1 A_{260} unit of dsDNA = 50 µg/ml = 0.15 mM (in nucleotides)**

The absorbance at 280 nm was also measured and the A_{260}: A_{260} ratio calculated in order to assess the purity of the DNA preparation. A ratio less than 1.8 is indicative of protein or phenol contamination of the nucleic acid.

2.1.5 Preparation of competent bacterial cells

Preparation of competent bacterial cells lacking an antibiotic resistance selectable marker was carried out in the absence of antibiotics such as ampicillin. Competent *E. coli* XL-1 Blue cells [genotype: F' Tn 10 $proA^{+}B^{+}$ $lacI^{q}$ Δ(lacZ) M15/recA1 gyrA96 (Nal^{r}) thi hsdR17 ($r_k^{-}m_k^{+}$) supE44 relA1 lac] were prepared by diluting an overnight culture [5 ml] 1: 200 in sterile Luria Broth (LB) liquid media [50 ml] (16 M tryptone, 10 M yeast extract and 5 M NaCl) in a flask 10 x the culture volume. The cells were grown until they reached the early exponential growth phase as determined by the measurement of the optical density (OD) of the culture at 600 nm (OD_{600}) to be between 0.3 and 0.6. The cells were then transferred to 2 x 50 ml [25 ml culture] pre-chilled falcon tubes and the cultures were cooled to 0°C by incubation on ice for 5-10 min. The cells were recovered by centrifugation (4000 rpm, 15 min, 4°C) and kept ice-cold for all subsequent steps. All solutions used for the preparation of the competent bacterial cells namely 0.1M $CaCl_2$, 0.1M $MgCl_2$ and 20% Glycerol were

sterile and pre-cooled to 4°C. The cells were resuspended in one culture volume [25 ml each] of ice-cold 0.1M $MgCl_2$ and left on ice for 20 min. The cells were collected as before and resuspended in half culture volume [12.5 mls each] of ice-cold 0.1M $CaCl_2$ followed by incubation on ice for 5 h (30 min minimum) as efficiency of transformation depends on prolonged $CaCl_2$ exposure. The cells were recovered as before and gently resuspended in1/10 of initial culture volume [25 ml] of ice-cold 0.1M $CaCl_2$ solution [2.5 ml]. The cells were dispensed into 250 µl aliquots and competent cells were prepared by adding one volume [250 µl] ice-cold sterile 20% (v/v) glycerol to the resuspended cells and mixing gently, followed by freezing at 70°C.

2.1.6 pGEMT-easy DNA ligation

The Wizard® SV-purified *Eco RI/Not I* KSHV ORF 4 PCR products were ligated into the pGEMT-easy vector. This vector is prepared by linearization of Promega's pGEM®-T easy vector with *Eco* RV at base 60 of the vector's DNA sequence, and addition of a 3'terminal thymidine to both ends. It is these 3'-T overhangs at the insertion site, which greatly improves the efficiency of ligation of the gene of interest or PCR product into the plasmid, as it prevents re-circularization of the vector. Furthermore, these single 3'-T overhangs provide a compatible overhang for PCR products generated by certain thermostable polymerases as these enzymes often add a single deoxyadenosine to the 3'-ends of the amplified fragments, independent of the template used.

The chosen ratio of insert to vector used in the ligation reation was 8: 1 as it has been successfully used. The appropriate amount of PCR product (insert) used in the ligation reaction was calculated as the follows:

$$\frac{\textbf{(ng of vector x kb size of insert)}}{\textbf{(Kbp size of vector}} \quad \textbf{X (insert: vector molar ratio) = ng of insert}$$

The ligation reactions were mixed on ice and made up to volume with ddH_2O and the components of the reaction were added in the following order: 2 x rapid ligation buffer containing adenosine triphosphate (ATP) was added to a 1 x working concentration, followed by the addition of 50 ng of vector DNA, and the appropriate

amount (ng) of the insert DNA. Lastly, bacteriophage T4 DNA ligase (10 Weiss units/ml) was added to each one of the ligation reactions, which were then incubated overnight at 4°C. In order to assess the activity of the T4 ligase and therefore the efficiency of the ligation reaction, a control insert DNA was used in place of the PCR product. In addition, a background control ligation reaction was also set up with 50 ng of the vector and no insert in order to compare the number of background colonies resulting from non-t-tailed or undigested vector alone to the number of successful transformants. The ligation reactions were transformed into competent *E. coli* XL 1-Blue cells.

2.1.7 Transformation of competent bacterial cells

Each ligation reaction [2 µl] were added to 100 µl of competent XL 1-Blue cells, which were gently thawed on ice. The tubes were gently flicked to mix the contents and incubated on ice for 30 min. A separate transformation reaction in which ddH_2O [2 µl] was added instead of the ligation reaction, was carried out in order to assess the transformation efficiency of the competent cells as well as for sterility of the transformation. The cells were then heated-shocked for 45 seconds-1 minute in a water bath at exactly 42°C followed by incubation on ice for 2 min. Pre-heated (37°C) sterile LB liquid culture media [0.9 ml] was added to the cells followed by incubation for 1 h at 37°C with shaking allowing for further growth of the cells as well as for expression of β-lactamase. This enzyme is expressed by the Amp^R gene present in the pGEMT-easy vector and has the ability of cleaving the ampicillin rings conferring the cells with ampicillin antibiotic resistance. The tubes were microcentrifuged and 900 µl of the medium discarded while the cell pellet was resuspended in the remaining 100 µl of the culture medium. The cells were then plated onto LB agar plates containing the appropriate antibiotic for selection of the successful transformants. Therefore, the *Eco* RI/*Not* I fragments ligated into pGEMT-easy and transformed into competent *E. coli* XL 1-Blue cells were selected with ampicillin (100 µg/ml).

2.1.8 Small-scale preparation of plasmid DNA

Purified preparations of pGEMT/KSHV ORF 4 (735), pGEMT/KSHV ORF 4 (1436) and pGEMT/KSHV ORF 4 (1581) plasmid DNA (labelled A1-4, B1-4 and C1-4 respectively) were obtained using a modified alkaline lysis procedure (Qiagen

miniprep plasmid isolation kit). Single colonies of each plasmid DNA transformed *E. coli* cells were inoculated overnight into sterile LB liquid culture media [5 ml] containing ampicillin (0.1 mg/ ml) in a shaker with agitation at 250 rpm. Aliquots of each overnight cell culture [3 ml] were centrifuged at 9000 x g for 1 minute, and the bacterial cell pellets were resuspended in 250 µl suspension buffer P1 (50 mM Tris-HCl pH 8.0, 10 mM EDTA, 0.1 mg/ ml Rnase A). 250 µl lysis buffer P2 (0.2 M NaOH and 1% SDS) was added and the suspension gently mixed by inversion and incubated for 5 min at room temperature (RT). 350 µl chilled binding buffer N3 (4 M guanidine hydrochloride and 0.5 M potassium acetate pH 4.2) was added and the suspension immediately mixed gently by inversion followed by microcentrifugation for 10 min at 13 000 x g. The pellets were discarded and the supernatants transferred to silica ion- exchange columns (QIAprep column), which were in turn microcentrifuged for 1 min at 13 000 x g. The unbound fraction was discarded and 500 µl wash buffer PB (5 M guanidine hydrochloride, 20 mM tris- HCl pH 6.6) was added and the filter tube columns were microcentrifuged for 1 minute at 13 000 x g. The unabsorbed fraction was discarded and the columns were washed with 750µl wash buffer PE (20 mM NaCl, 2 mM Tris- HCl pH 7.5) and centrifuged as before. Finally, the bound plasmid DNA was eluted in 50 µl TE buffer (10 mM Tris-HCl pH 8.0 and 1 mM EDTA) and the tubes were microcentrifuged at 13 000 x g for 1 minute. The concentration of the purified plasmid DNA was determined by UV spectrometry as described above in section 2.1.4 followed by storage at - 20°C until later analysis.

2.1.9 DNA sequencing of the KCP gene encoded by KSHV ORF 4

Sequencing of the KSHV ORF 4 gene was carried out in Stellenbosch using the ABI PRISM big dye terminator cycle sequencing reaction kit (Applied Biosystems), which is based on the dideoxy chain-terminating method (Sanger *et al*, 1977). The sequencer used was the ABI PRISM 3100 genetic analyser, based on capillary electrophoresis. The sequencing samples were carefully prepared for optimum results. For cycle sequencing, 5 µl of QIAGEN-purified pGEMT/KSHV ORF 4 (1581) plasmid DNA (100 ng/µl) and 1.1 pmol/µl primer were used. In addition to the pGEMT forward and reverse primer, the sequence-specific primers used for the PCR reaction (section 2.1.2), Fwd and Rev 3, were also used for sequencing of the complete KSHV ORF 4

gene. The cycle sequencing reaction was carried out by 25 cycles of 96°C for 10 seconds, 50°C for 5 seconds and 60°C for 4 min, according to the ABI PRISM big dye terminator cycle sequencing protocol.

2.1.10 RE digestion analysis of the pGEMT-easy constructs

Plasmid DNA isolated from *E. coli* transformants as described in section 2.1.8 was screened for the constructs pGEMT/KSHV ORF 4 (735), pGEMT/KSHV ORF 4 (1436) and pGEMT/KSHV ORF 4 (1581) by double-restriction endonuclease digestion with *Eco* RI and *Not* I. All the DNA fragments were analysed by 1% agarose gel electrophoresis. The diagnostic digestion of the double-stranded (ds) DNA was performed using purified plasmid DNA in the range of 100-500 ng and in each digestion the volume of DNA to be digested did not exceed 10% (v/v) of the total reaction volume. All the required components to carry out the restriction endonuclease digest were mixed on ice in the following order:

Table 7. Components used in the RE analysis of the pGEMT DNA constructs

Reagents / DNA	A1	A2	A3	A4	B1	B2	B3	B4	C1	C2	C3	C4	Final Conc"
ddd H_2O	15.3	1.4	14.4	15.1	15.1	11	15.6	15.6	15.3	14	10	12.4	up to total vol of 20 µl
10x restriction buffer	2	2	2	2	2	2	2	2	2	2	2	2	1x
Plasmid DNA	1.7	3.0	2.6	1.9	1.9	6	1.4	1.4	1.7	3.0	7	4.6	~400ng /µl
Eco RI (15 U/µl)	0.5	0.5	0.5	0.5	0.5	0.5	0.5	0.5	0.5	0.5	0.5	0.5	7.5U
Not I (10 U/µl)	0.5	0.5	0.5	0.5	0.5	0.5	0.5	0.5	0.5	0.5	0.5	0.5	5U
Total Vol (µl)	20	20	20	20	20	20	20	20	20	20	20	20	-

The DNA restriction digests were incubated overnight at 37°C in a heating block apparatus. The digestion of the plasmid DNA was stopped by the addition of the appropriate volume of 6x gel loading buffer [0.25% (w/v) bromophenol blue and 30% (v/v) glycerol].

2.1.11 Agarose Gel Electrophoresis

Agarose gel electrophoresis analysis was performed according to standard protocol (Sambrook *et al*, 2001). The DNA (100-500 μg) was resolved by 1% agarose gel electrophoresis in 1 x Tris-Borate EDTA (TBE) buffer (0.045 M Tris base, 0.045 M borate and 0.001 M EDTA) at 1-10 V/cm of gel until the bromophenol blue dye front migrated to the bottom of the gel. In order to visualize the position of the DNA fragments, ethidium bromide (1 mg/ml) was incorporated in the agarose gel mixture prior to gel solidification, to a final concentration of 0.5 μg/ml. Ethidium bromide chelates to the DNA nucleotide bases and fluoresces under a short wavelength UV transluminator.

2.1.12 Directional analysis of the cloned genes by RE digestion

GeneRunner software was used to determine which restriction endonuclease cuts the insert once within the first 735 bp (short soluble portion of the protein of interest). The RE selected was *Bam* HI which is ideal for a quick check of any of the inserts' direction with respect to the vector. This enzyme cuts the insert at position 643 bp and does not cut the pGEMT-easy vector. Similarly, the RE *Eco* RV was the selected enzyme that can cut the vector once at position 60 but does not cut any of the three inserts anywhere in their DNA sequence.

The restriction digest reactions were treated exactly as per section 2.1.10.

Table 8. Components used in the *Bam* HI restriction digest analysis

Reagents / **DNA**	A2	B2	B4	C2	C3	C4	**Final Concentrat'**
ddd H_2O	14	11	16.1	14.5	11.5	14.5	up to total vol of 20 μl
10x restr. buffer	2	2	2	2	2	2	1x
Plasmid DNA	3	6	1.4	3	6	3	~400ng/μl
Bam HI or	0.5	0.5	0.5	0.5	0.5	0.5	5 U
Eco RV	0.5	0.5	0.5	0.5	0.5	0.5	7.5 U
Total Vol (μl)	20	20	20	20	20	20	-

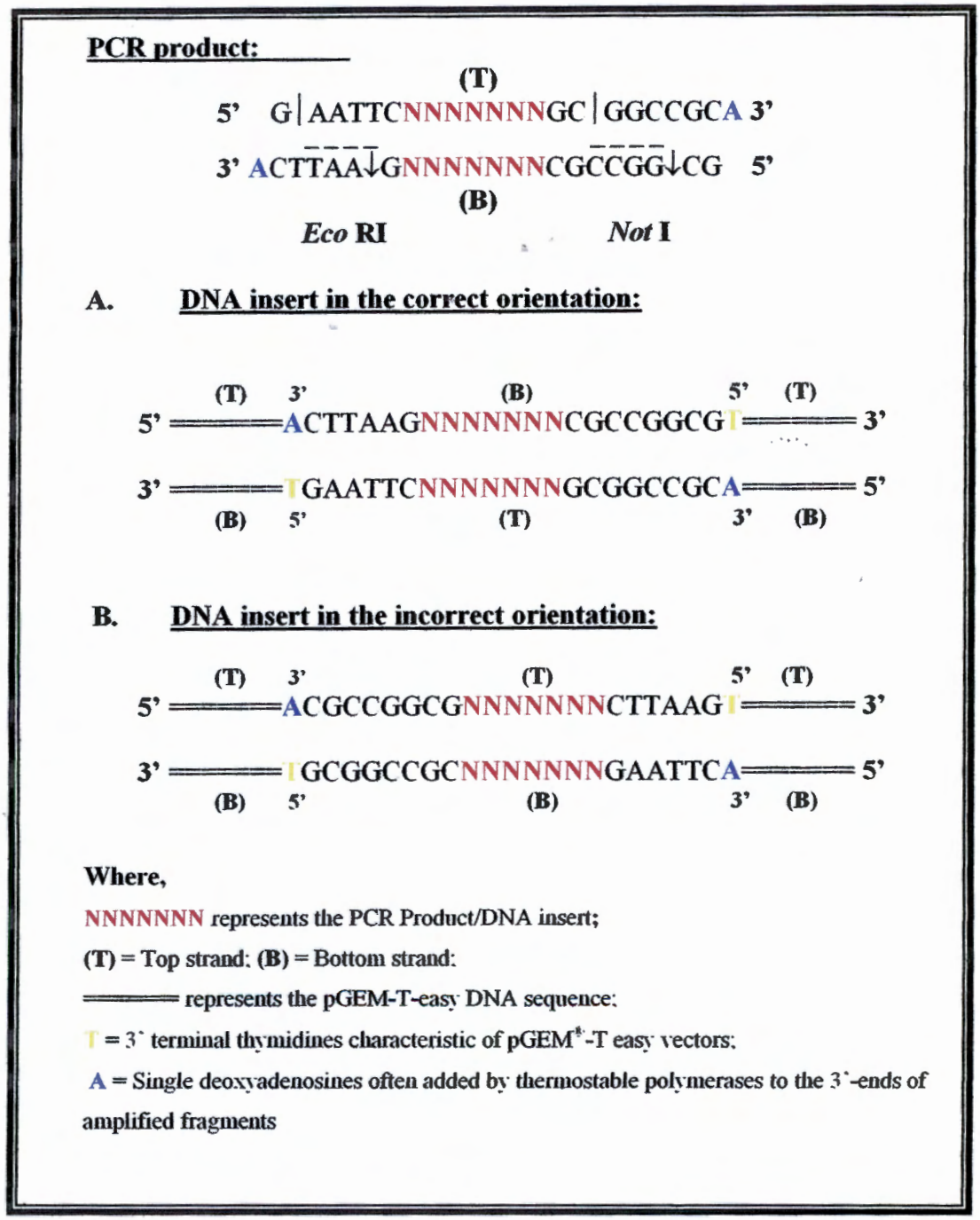

Figure 9. Significance of determining the direction of the insert when ligated into the pGEMT-easy vector

In case **A** above, the top strand of the insert goes from 5'→ 3' therefore restriction sites are recognised by the *Eco* RI & *Not* I REs. As a result, in addition to obtaining a 2981bp DNA fragment, the correct size insert with cohesive *Eco* RI & *Not* I ends is also released upon RE digestion of the pGEMT constructs. However, in case **B** above, the top strand of the insert goes from 3'→ 5' therefore restriction sites are no longer recognised by the *Eco* RI & *Not* I REs. As a result, in addition to obtaining a 2981bp DNA fragment, an insert with cohesive *Eco* RI & *Not* I ends is also released but with additional DNA sequence from the vector itself.

2.1.13 Small-scale isolation and RE analysis of pPIC9 plasmid

Individual XL 1-blue cell colonies transformed with pPIC9 were inoculated into sterile LB liquid culture media [4ml] containing the appropriate antibiotic for selection of the plasmid DNA. The cells were grown overnight with agitation at 225 rpm in a 37°C incubator room. The pPIC9 plasmid DNA was obtained and its concentration determined as per sections 2.1.4. In order to confirm that the DNA isolated was indeed pPIC9 plasmid DNA, in other words, the authenticity of the plasmid, two restriction endonuclease digests, using suitable REs readily available in the laboratory (*Hind* III and *Pst* I), were carried out. The DNA restriction digests were treated exactly as per section 2.1.10.

Table 9. Components used in the *Hind* III and *Pst* I analysis of pPIC9 plasmid

Reagents / DNA	pPIC9 pasmid DNA (275 ng/µl)	pPIC9 pasmid DNA (700 ng/µl)	pPIC9 pasmid DNA (925 ng/µl)	Final Concentration
ddd H_2O	15.5	16.4	16.6	up to total vol of 20 µl
10x restriction buffer	2	2	2	1 x
Plasmid DNA	1.5	0.6	0.4	~400 ng/µl
Hind III or *Pst* I	1	1	1	5 U or 7.5 U
Total Volume (µl)	20	20	20	-

2.1.14 pGEMT DNA Isolation from low-melt 1% agarose gel

Successful pGEMT-easy clones containing the DNA fragments of interest were digested with *Eco* RI and *Not* I as described in section 2.1.10. The *Eco RI/Not I* KSHV ORF 4 DNA fragments were recovered from a low melting temperature agarose gel using the Wizard® SV system. Post electrophoresis the agarose gel was briefly exposed to long wavelength UV radiation in order to detect the DNA of interest. The DNA fragments of the correct molecular mass were excised from the agarose gel using a sterile scalpel blade. The gel slices containing the DNA fragments of interest were transferred to pre-weighed 1.5 ml microcentrifuged tubes. Membrane binding solution (4.5M guanidine isothiocynate, 0.5M potassium acetate pH 5.0) was added at a ratio of 10 µl of solution per 10mg of agarose slice, followed by incubation

at 65°C for 10 min or until the gel slice was completely dissolved. The solution was centrifuged at RT to ensure that all the contents were at the bottom of the tubes and the DNA was recovered and its concentration determined as described in section 2.1.4

2.1.15 Vector pPic 9 DNA ligation

The gel purified *Eco* RI/*Not* I KSHV ORF 4 DNA fragments were ligated into the *Eco* RI/*Not* I-digested yeast expression vector pPIC9. The ligation reactions were mixed on ice and made up to volume with ddH_2O and the components of the reaction were added in the following order:

Table 10. Components used in the set up of the pPIC9 ligation reactions

Reagents / DNA	KSHV ORF 4 (735 bp) gene	KSHV ORF 4 (1436 bp) gene	KSHV ORF 4 (1581 bp) gene	Background control	**Final Concentration**
2x rapid ligation buffer	5	5	5	5	1x
pPIC9 vector	1	1	1	1	384 ng/µl
Insert DNA	3	3	3	-	~1000 ng/µl
T4 DNA ligase	1	1	1	1	10 weiss units/ml
ddH_20	-	-	-	3	up to total vol of 10µl
Total Volume (µl)	10	10	10	10	-

All 4 ligation reactions were incubated overnight at 4°C. In order to compare the number of background colonies resulting from non-t-tailed or undigested vector alone to the number of successful transformants, a background control ligation reaction was also set up with ddH_20 instead of DNA insert. The ligation reactions were transformed into competent *E. coli* XL 1-Blue cells and the plasmid DNA of interest obtained as described in section 2.1.7 and 2.1.8 respectively.

2.1.16 RE digestion analysis of the pPIC9 DNA constructs

Plasmid DNA isolated from *E. coli* transformants as per section 2.1.8, was screened for the constructs pPIC9/KSHV ORF 4 (735), pPIC9/KSHV ORF 4 (1436) and pPIC9/KSHV ORF 4 (1581), by double-restriction endonuclease digestion with *Eco* RI and *Not* I using standard reaction conditions as described in section 2.1.10. All the

required components to carry out the restriction endonuclease digest were mixed on ice in the following order:

Table 11. Components used in the RE analysis of the pPIC9 DNA constructs

Reagents / DNA	A1	A2	A3	B1	B2	B3	C1	C2	C3	Final Conc"
ddd H_2O	15.2	14.87	14.83	15.63	15.78	13.1	14.78	15.02	15.36	up to total vol of 20 µl
10x restriction buffer	2	2	2	2	2	2	2	2	2	1x
Plasmid DNA	1.7	3.0	2.6	1.9	6	1.4	1.7	3.0	7	~400ng/µl
Eco RI	0.5	0.5	0.5	0.5	0.5	0.5	0.5	0.5	0.5	7.5U
Not I	0.5	0.5	0.5	0.5	0.5	0.5	0.5	0.5	0.5	5U
Total Vol (µl)	20	20	20	20	20	20	20	20	20	-

2.2 Transformation of *P. pastoris* and Selection for Positive Clones

Integration of the three different sized KSHV ORF4 genes into the *P.* pastoris genome was carried out by homologous recombination with pPIC9/KSHV ORF4 DNA constructs (Figure 20). Before the transformation procedure, the yeast expression vector pPIC9 was digested with *Sac* I and the expected product was visualised by agarose gel electrophoresis and used to transform *P. pastoris* GS115 competent cells.

2.2.1 Linearization of pPIC9 and pPIC9/KSHV ORF 4 constructs

After successfully cloning the genes of interest, the pPIC9 parental plasmid as well as the pPIC9/KSHVORF 4 constructs, were linearised with the RE *Sac* I in order to encourage homologous recombination during the transformation step. The DNA restriction digests were carried out as described in section 2.1.10. All the required components to carry out the linearization of the plasmid were mixed on ice in the following order:

Table 12. Components used in the *Sac* I RE linearisation of pPIC9 constructs

Reagents / DNA	A1: pPIC9/ KSHV ORF 4 (735)	B2: pPIC9/ KSHV ORF 4 (1436)	C3: pPIC9/ KSHV ORF 4 (1581)	pPic 9 parental plasmid	Uncut pPIC9 vector	Final Conc"
ddd H_2O	0	3.5	0.2	1.5	16	Up to final vol of 20 µl
10x restriction buffer	2	2	2	2	2	1x
Plasmid DNA	14.5	11	14.3	13	2	3500 ng/µl
Sac I (10 U/µl)	3.5	3.5	3.5	3.5	-	35 U
Total Vol (µl)	20	20	20	20	20	-

2.2.2 pPIC9 plasmid DNA isolation from low-melt 1% agarose gel

The *Sac* I linearised pPIC9 DNA was recovered from a low melting temperature agarose gel using the DNA purification kit (Amersham) exactly as described in section 2.1.8 for the exception that a different kit based on the same DNA purification principle was used.

2.2.3 Preparation of yeast competent cells

Competent *Pichia pastoris* GS115 competent cells were prepared by diluting an overnight culture [10 ml] to an OD_{600} of 0.1-0.2 in 10 ml of yeast extract peptone dextrose medium (YPD) [1% yeast extract, 2% peptone, 2% dextrose (glucose)]. The cells were grown for a further 4-6 h at 28°C-30°C in a shaking incubator until the OD_{600} reached 0.6-1.0. The cells were recovered by centrifugation (500 x g, 5 min, RT). The cell pellet was then resuspended in 1 ml of solution I [1M sorbitol, 1mM bicine, 3% ethylene glycol, 5% dimethyl sulfoxide (DMSO), pH 8.0]. The competent cells were dispensed into 50 µl aliquots and slowly frozen at -80°C wrapped in several layers of paper towels.

2.2.4 Transformation of competent yeast cells

One tube of competent yeast cells prepared as described in section 2.2.3 was thawed at room temperature for each transformation reaction. *Sac* I-linearised pPIC9 vector DNA (3 µg) recovered from a low-melt agarose gel was added to the competent cells.

In this transformation reaction the volume of the DNA should not exceed 5 µl therefore the cells were gently centrifuged (5000 x g, 5 min, RT) and 50 µl of the supernatant was discarded before the addition of the necessary DNA volume (µl). Solution II [1 ml] was added to the DNA/cell mixture and all the components were mixed by vortexing. The transformation reactions were then incubated for 1 h at 30°C in a water bath or incubator. During the incubation period, each transformation reaction was mixed every 15 min by vortexing for a few seconds. After incubation, the cells were heat shocked at 42°C in a water bath for 10 min. The cells were recovered (3000 x g, 5 min, RT) and the supernatant was discarded. The cells were resuspended in solution III [1 ml] because transformation was carried out with the pPIC9 expression vector. The cells were once again recovered as above and finally the cell pellet was resuspended in 100-150 µl of solution III. The transformation reactions were then plated onto appropriate selection plates such as regeneration dextrose (RDB) agar plates [1 M sorbitol, 1% dextrose, 1.34% YNB (13.4% yeast nitrogen base with ammonium sulphate without amino acids), 4 x 10^{-5} biotin, 0.005% amino acid mix containing glutamic acid, methionine, lysine, leucine and isoleucine], which were then incubated for 4 days at 30°C.

2.2.5 Isolation of genomic DNA from *Pichia* yeast transformants

Genomic DNA from the desired His^+ recombinant *Pichia* strains obtained in the transformation procedure was isolated using the DNeasy® DNA purification kit (QIAGEN). This case is based on an advanced silica-gel-membrane technology, which allows for rapid and efficient recovery of genomic DNA. The *Pichia* transformants under investigation were grown at 30° C to an OD_{600} of 5-10 in 10 ml buffered glycerol-complex medium [(BMGY) 1% yeast extract, 2% peptone, 100 mM potassium phosphate buffer, pH 6.0, 1.34% YNB, 4 x 10^{-5} biotin, 1% glycerol]. A maximum of 5 x 10^7 cells [1 ml] were harvested (5000 x g, 10 min, RT) and the supernatant discarded. The cell pellet was resuspended in 600 µl freshly prepared sorbitol buffer [1 M sorbitol, 100 mM EDTA, 14 mM β-mercaptoethanol], followed by the addition of 84 µl (200 units) 10 x lyticase stock solution. The reaction samples were incubated at 30°C for 1 h and the spheroplasts were then recovered by centrifugation (300 x g, 10 min, RT). Buffer ATL [180 µl] was used to resuspend the spheroplasts. Proteinase K [20 µl] was added to each reaction sample, which were

then incubated at 55°C overnight in a water bath. The samples were then subjected to RNase treatment by adding 40 µl of the enzyme (10 mg/ml), vortexing and incubating at RT for 2 min. After this short incubation, the tubes were vortexed for 15 seconds and buffer AL [200 µl] was added followed by immediate thorough mixing of the samples by vortexing. All samples were incubated at 70°C for 10 min in a heat block and then 200 µl ethanol (96%) was added and the samples mixed as above. Each mixture was transferred to a DNeasy mini spin column placed in a 2 ml collection tube that was then centrifuged at 8000 rpm for 1 minute and the flow-through was discarded. The columns were placed in the same collection tubes and buffer AW1 [500 µl] was added to each column followed by centrifugation as above. The columns were then placed in new tubes and buffer AW2 [500 µl] was added to each column. The samples were centrifuged at maximum speed (13 000 rpm) for 3 min and the flow-through as well as the collection tubes were discarded. Finally, the columns were placed in clean 1.5 ml eppendorf tubes and buffer AE [100 µl] was pipetted directly onto the membrane and the columns were incubated for approximately 30 min at room temperature. To elute the yeast genomic DNA in the AE buffer, the tubes were centrifuged at 8000 rpm for 1 minute. This elution step was repeated and the second DNA eluates were collected in a series of new eppendorf tubes in order to prevent dilution of the first eluate.

2.2.6 Screening for Mut$^+$ and Mut^S transformants

The phenotype of the transformed *P. pastoris* colonies was investigated in order to discriminate between the types of recombination that can take place: integration at the *HIS4* gene yields a functional *AOX1* gene that will give a methanol utilisation phenotype (Mut$^+$), whereas integration at the *AOX1* gene produces either a functional *AOX*1 gene (Mut$^+$) or *AOX2* gene that will give a slow methanol utilisation phenotype (Mut^S). Therefore, growth rates in the presence of methanol were tested for a large number of His$^+$ colonies picked from the RDB selection plates and streaked in a regular pattern on both a minimal methanol (MM) (1.34% YNB, $4x10^{-5}$% biotin, 0.5% methanol) and minimal dextrose (MD) (1.34% YNB, $4x10^{-5}$% biotin, 2% dextrose) agar plates. A new sterile loop was used for each transformant and the MM plates were always streaked first. Furthermore, to differentiate Mut$^+$ from the Mut^S phenotype, a patch for each of the controls, GS115/His$^+$ Mut^S Albumin and

GS115/His$^+$ Mut$^+$ β-galactosidase, was carried out onto the MD and MM plates. All the plates were incubated at 30°C for 2 or longer days after which, the plates were analysed. The Mut$^+$ transformants should grow well on both plates, while the Mut^S transformants should only grow well on MD plates but show little or no growth on the MM plates.

2.2.7 PCR analysis of *Pichia* transformants

All the *Pichia* transformants were analysed by PCR to determine if the respective genes of interest integrated into the *Pichia* genome. Genomic DNA was isolated from the His$^+$ clones as described in section 2.2.5 using the DNeasy® DNA purification kit. The genes under investigation were then amplified by PCR with 5'-GACTGGTTCCAATTGACAAGC- 3' and 5'- GCAAATGGCATTCTGACATCC-3' specific for the *AOX1* promoter and terminator sequences respectively. In the reactions where KSHV DNA from PEL was used as PCR positive controls, the genes of interest were amplified by priming with the forward primer 03-0668 (F) and reverse primers 03-0669 (R1), 03-0670 (R2) and 03-0671 (R3) for the 735, 1436 and 1581 bp PCR products respectively.

Table 13. Master mix components used in the PCR of the 735bp gene from *Pichia* transformants

Master Mix 1 Components	8 x pPIC9/ KSHV ORF 4 (735) *Pichia* recombinants	GS115/ pPIC9 (no insert) =BC	pPIC9 + 735 bp gene	pPIC9 alone	KSHV DNA	**Final Conc"**
$dddH_2O$	18	18	22.54	22.86	22.7	up to final vol of 25 µl
dNTP	1	1	1	1	1	200 µM each
5'*AOX1*	0.5	0.5	0.5	0.5	0.5 [F]	50 pmol/µl
3'*AOX1*	0.5	0.5	0.5	0.5	0.5 [R1]	50 pmol/µl
DNA	5	5	0.46	0.14	0.3	variable
Total Vol (µl)	25	25	25	25	25	-

Master Mix 2 Components	**Volume added (µl)**	**Final Concentration**
$dddH_2O$	234.96	up to final vol of 300 µl
10 x buffer with 15 mM $MgCl_2$	60	1x
Pfu (3U/µl)	0.42 x 12 = 5.04	1.25U/ 50µl reaction
Total Volume (µl)	300 / 12= 25	-

Table 14. Master mix components used in the PCR of the 1436 and 1581 bp genes from *Pichia* transformants

Master Mix1 Components	3x pPIC9/ KSHV ORF 4 (1436) *Pichia*	pPIC9+ 1436bp gene	KSHV DNA	3x pPIC9/ KSHV ORF 4 (1581) *Pichia*	pPIC9+ 1581bp gene	KSHV DNA	GS115/ pPIC9 (BC)	pPIC9 vector	**Final Conc"**
$dddH_2O$	18	22.66	22.7	18	22.45	22.7	18	22.86	Up to final vol of 25 µl
dNTP mix	1	1	1	1	1	1	1	1	200 µM each
5'*AOX1*	0.5	0.5	0.5 [F]	0.5	0.5	0.5	0.5	0.5 [F]	50 pmol/µl
3'*AOX1*	0.5	0.5	0.5 [R2]	0.5	0.5	0.5	0.5	0.5 [R3]	50 pmol/µl
DNA	5	0.35	0.3	5	0.55	0.3	5	0.14	variable
Total Vol (µl)	25	25	25	25	25	25	25	25	-

Master Mix 2 Components	**Volume added (µl)**	**Final Concentration**
$dddH_2O$	234.96	Up to final vol of 300 µl
10 x buffer with 15 mM $MgCl_2$	60	1x
Pfu (3U/µl)	0.42 x 12 = 5.04	1.25U/ 50µl reaction
Total Volume (µl)	300 / 12= 25	-

The master mixes were thoroughly mixed on ice and centrifuged briefly to collect the samples at the bottom of each tube. Master mix 2 [25µl] was added to each one of the above master mix 1 [25µl] on ice and mixed thoroughly in order to produce a homogenous reaction. The samples were then placed in a thermocycler (ThermoHybaid cycler) and thermocycling was performed using the parameters described in Table 15. Each PCR sample [10 µl] was analysed on a 1 x TBE, 0.8% agarose gel as described per section 2.1.11.

This is a very useful analysis as it confirms whether or not the gene of interest is integrated into the *Pichia* genome. This experiment does not however provide information on the site of integration. Nevertheless, if screening Mut^+ integrants, two bands should be visualised as one corresponds to the gene of interest and the other to the intact *AOX*1 gene, which is approximately 2.2 kbp. On the other hand, if screening

Mut^S integrants only the band corresponding to the gene of interest should be visualised as the *AOX*1 gene is replaced and therefore lost during the integration event.

Table 15. Thermocycling Parameters used in the PCR of the *Pichia* His^+ Transformants

Step	Temperature (°C)	Time	Number of Cycles
Hot Start	94	2 min	1x
Denaturation	94	30 s	30x
Annealing	55	1 min	
Extension	72	4 min	
Final Extension	72	5 min	1x

2.3 Expression of the rKCPs in *P. pastoris*

The methylotrophic yeast *P. pastoris* strain of choice, GS115 (his4) (Invitrogen) was used for the heterologous production of the recombinant KSHV complement regulatory proteins.

2.3.1 Small & medium-scale expression of recombinant *Pichia* strains

Small-scale expression experiments were carried out to test whether the transformed *P. pastoris* recombinant colonies were suitable for KSHV ORF 4 protein expression. Post-PCR analysis of the *Pichia* integrants as described in section 2.2.7, the transformants containing the insert of interest were selected and screened for expression levels first in small-scale according to their Mut^S and Mut^+ phenotype. The wild-type *AOX*1 gene was shown to be present in all of the pPIC9/KSHV ORF 4 (735bp) and pPIC9/KSHV ORF 4 (1436bp)-recombinant *Pichia* strains analysed by PCR (Figure 25, 26) making these transformants more likely to be Mut^+. Therefore, for Mut^+ secreted expression, 5 ml BMGY were inoculated with each respective verified recombinant clone in a 250 ml conical flask. The yeast cultures were incubated overnight at 30°C in a shaking incubator (250 rpm) and growth was allowed to continue until the cells reached the logarithmic phase of A_{600} 2-6 as

determined by spectroscopic measurement of the absorbance at 600 nm. The cells were then harvested (3000 x g, 5 min, RT) and the supernatant discarded. The cell pellet was resuspended to an OD_{600} of 1.0 in buffered methanol-complex medium [(BMMY) 0.1% yeast extract, 0.2% peptone, 100 mM potassium phosphate buffer, pH 6.0, 1.34% YNB, 4 x 10^{-5} biotin, 1% methanol]. In order to maintain induction, 100% methanol was added to the cultures every 24 h to a final concentration of 2%. On the other hand, PCR analysis of the pPIC9/KSHV ORF 4 (1581bp)-recombinant *Pichia* strains showed the absence of the wild-type *AOX*1 gene (Figure 27) making these transformants more likely to be Mut^S. Therefore, for Mut^S secreted expression, 25 ml BMGY were inoculated with each respective verified recombinant clone in a 250 ml conical flask. The yeast cultures were incubated as described above and in order to induce expression, the cell pellets were resuspended in 1/5 BMMY of the original culture volume. Similarly, in order to maintain induction, 100% methanol was added to the cultures every 24 h to a final concentration of 1%.

Colonies from the small-scale experiments were selected for medium-scale [100 ml] production of the KSHV complement regulatory proteins. After 5 days (96-h post-induction) the cultures were centrifuged at 3000 x g for 5 min and the supernatant obtained was further centrifuged at 10 000 rpm for 45 min-1 h.

2.3.2 Optimisation of methanol-induced production of the recombinant proteins

A sample of the cell culture was taken before cell induction by resuspension of the harvested cells in BMMY (1 % methanol) followed by the collection of samples [1 ml] taken every 24 h over a period of 4-5 days. These samples were centrifuged at maximum speed for 5 min at room temperature and both the supernatant and the cell pellets were quickly frozen in liquid nitrogen and stored at -80°C until ready for further analysis. These samples were used to analyse expression levels and determine the optimal time post-induction to harvest the cells. Sodium dodecyl polyacrylamide gel electrophoresis (SDS PAGE) 5 x gel loading buffer [4 µl] (62.5 mM Tris-HCl pH 6.8, 10% (v/v) glycerol, 2% (w/v) SDS, 5% (v/v) β- mercaptoethanol, 0.05% (w/v) bromophenol blue) was added to the supernatants [20 µl], which were in turn heated at 95°C for 5 min and analysed by SDS PAGE electrophoresis.

2.3.3 Concentration of the Media containing the Secreted KSHV ORF 4 Proteins

The supernatant obtained was concentrated approximately three times by ultrafiltration through Pellicon®XL filtration unit (Millipore) (Figure. 10) with a molecular weight exclusion limit of 10 kDa. The device was used according to the operating instructions. The concentrated supernatant was clarified by passing through 0.22 μm filter to remove contaminating particles.

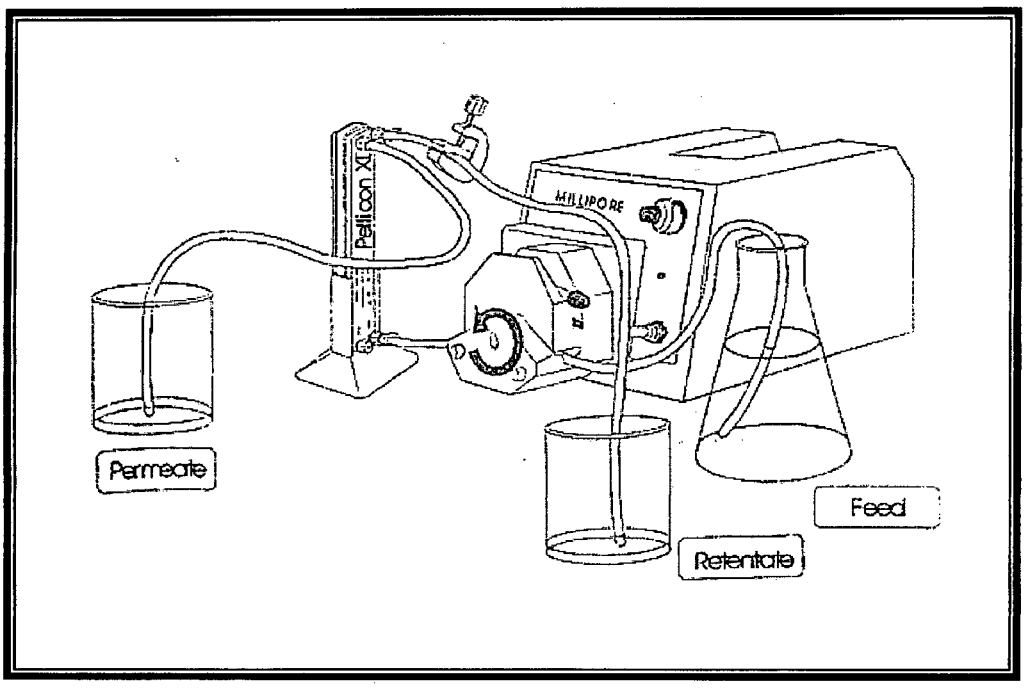

Figure 10. Illustration of the Pellicon XL-device

The supernatant (feed) was concentrated 3-fold under low pressure and the concentrated sample was collected through the retentate while the fraction below 10 kDa was excluded through the permeate.

2.3.4 Small-Scale Ammonium Sulphate Protein Precipitation

In order to determine the optimum precipitation conditions, ammonium sulphate powder was added to the supernatant in a small-scale [500- 1000 μl] at 4°C with shaking for 1 h to final saturations of 20, 30, 40, 50, 60, 70, 80 and 90%. The samples were then microcentrifuged at 3000-x g for about 40 min and the supernatant discarded while the pellet was resuspended in 50 μl of sterile saline.

2.3.5 Estimation of Protein Concentration

Intensities of SDS-PAGE bands were scanned with a densitometer (ChemiImager™ 5500) and the concentration of the *P. pastoris*-expressed KCP protein was quantitively estimated by comparison with a standard curve obtained with known amounts of protein.

2.4 Synthesis of a Polyclonal Anti-KCP Peptide Antibody

2.4.1 Peptide Selection for the Synthesis of the Polyclonal Antibody

The first step in the design of a suitable peptide antibody directed against the protein under investigation was the selection of an appropriate peptide sequence. When examining the protein sequence for potential antigenic epitopes, sequences which are hydrophilic, surface-orientated and random coil were taken into consideration. Therefore, algorithms were used to predict protein characteristics in terms of hydrophilicity/hydrophobicity and secondary structure regions such as α- helix, β-sheets and turns (Figure 11). GeneRunner and DNASTar™ software, which contains all the necessary algorithms including hydrophilicity and surface probability plots, as well as antigenic index, were used to select a potentially exposed immunogenic internal sequence for the generation of the peptide antibody.

After the identification of the protein region of interest, the length of the peptide was also considered and an 11-residue peptide, CHRPKIKNGDY, was chosen because it falls within the typical 10-20 residue peptide range. Shorter peptides are also easier to synthesise and are reasonably soluble in aqueous solutions and finally they may still possess some degree of secondary structure.

The chosen amino acid sequence was chemically synthesised in a Brazilian laboratory and it was then sent to Washington Biotechnology (USA) where it was used to generate an immunogen conjugated with the carrier protein, keyhole limpet hemocyanin (KLH), which is a large but non-immunogenic protein. This immunogen was in turn used to produce a rabbit polyclonal peptide-antibody for Immunoenzyme-histochemical assays, Immunodetection and Western blot analysis of the KSHV complement regulatory protein, KCP.

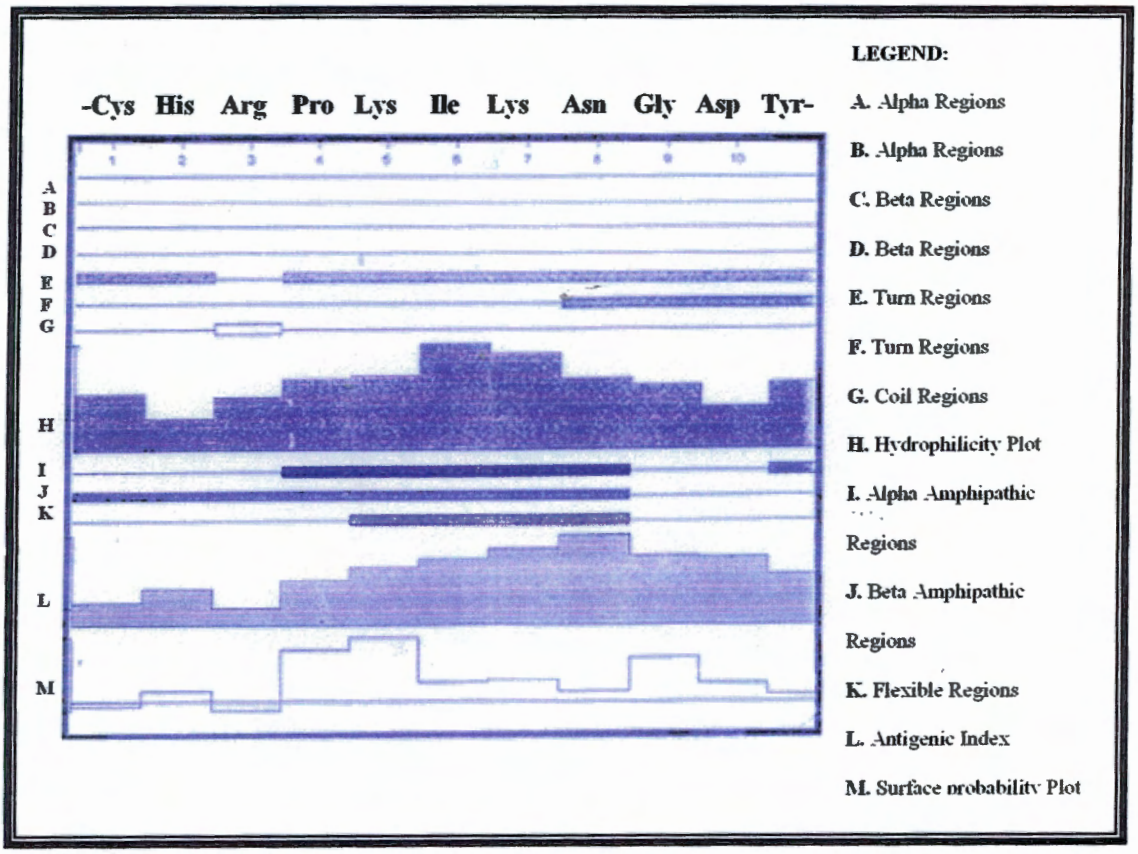

Figure 11. Criteria for the selection of a suitable KCP peptide

Figure 11 represents the algorithms that were used in order to select a suitable peptide for the synthesis of the rabbit anti-KCP peptide polyclonal antibody. High probability of surface exposure was analysed by algorithms A-G, which shows the structural components of the peptide, in other words, the potential to form turns or loops. These structures have a higher probability of surface exposure, whereas the more "rigid" structures such as the α-helices and β-strands are more likely to form the internal core of a protein. Positive peaks of hydrophilicity are represented by algorithm H that shows that this selected peptide is composed mainly of polar hydrophilic regions, which coincides with the lack of helix and β-strand structures depicted above. Also important is the immunogenecity of the peptide, which is measured by algorithm L, the antigenic index, showing that the selected sequence is composed of a larger number of highly immunogeneic residues such as, His, Lys, Leu, Asp, Arg and Tyr.

2.4.2 HiTrap Protein A Purification of the Polyclonal Anti-KCP Peptide Antibody

The anti-KCP peptide polyclonal IgG was purified from 5 ml of rabbit serum with a protein A HP column (Amersham) that has a very great affinity for binding IgGs especially produced in rabbits. A 5 ml syringe was filled with binding buffer (20 mM Sodium phosphate, pH 7.0) and after removing the stopper, the column was connected to the syringe with the provided adaptor. The twist-off end of the column was

removed and the 1 ml column was washed with 10 column volumes of binding buffer at approximately 1 ml/min flow rate. The serum sample was applied to the column using the syringe fitted to the luer adaptor. After application of the sample, the column was washed with 6 column volumes of binding buffer and 1 ml wash samples were collected for later analysis. The IgG antibodies was eluted with 3 column volumes of elution buffer (0.1 M Citric acid, pH 3.0) and 200 µl of purified fractions were collected in tubes containing 40 µl of neutralising buffer (1 M Tris-HCL, pH 9.0) and stored at 4°C until further SDS-PAGE analysis and estimation of antibody concentration. Before storage, the column was washed with 5 column volumes of 20% ethanol and it was stored at 4°C in 20% ethanol to prevent microbial growth.

2.4.3 Bio-Rad Protein Microassay for Antibody Quantification

The concentration of the purified IgG was determined by the Bio-Rad protein assay, which is based on the standard method of Bradford assay (Bradford, 1976). The assay was carried by making up a series of bovine serum albumin (BSA) dilutions between 125 µg/ml and 2000 µg/ml final BSA concentration using a microtiter plate (wells 2-8). Brilliant blue G based Bradford dye reagent [200 µl] was added to all the standards and to each purified fraction of unknown antibody concentration. The solutions were mixed by pipetting and the colour reaction was allowed to develop for at least 5 min at RT. The colour intensity of the samples was measured with a plate reader (Anthos 2010) at 595 nm. The A_{595} readings of the standards were plotted against the known BSA concentrations and a standard curve was generated (Figure 32). The unknown antibody concentrations of the purified fractions were directly determined from this standard curve. The fractions containing the purified antibody were aliquoted and stored at -20°C.

2.5 Immunological Detection, SDS-PAGE and Western blot Analysis

2.5.1 Immunological detection of KSHV ORF 4 proteins

The production of the proteins of interest in the supernatant of the yeast culture medium was analysed by slot-blot using the manifold II slot-blot system (Schleicher & Schuell).

Aliquots [100 µl] of supernatants were vacuum-blotted onto nitrocellulose Hybond-ECL membranes (Amersham), which were in turn incubated overnight at 4°C in blocking solution [5% (w/v) not-fat milk powder in Tris-buffered saline (TBS)]. After blocking, the membranes were incubated with the rabbit anti-KCP peptide polyclonal antisera at 1:1000 in Tris-buffered saline/Tween 20 (TBST). After two washes in TBST followed by two washes with blocking solution (10 min each), the membranes were incubated for 30 min with horseradish peroxidase-conjugated anti-rabbit IgG (Roche) at 1:12 000 in blocking solution. The membranes were rinsed thoroughly four times with TBST for 15 min each and bound antibodies were detected using the Chemiluminescence Western Blotting Kit (Mouse/Rabbit) system (Roche).

2.5.2 SDS PAGE Electrophoresis

Prepared protein samples were resolved by discontinuous [0.1% (w/v)] SDS and [12% (w/v)] PAGE according to the method of Laemmli (Laemmli, 1970) and O'Farrel (O' Farrel, 1975), using a Biorad electrophoresis set. The resolving gel was cast and layered with water to prevent oxidation of the gel, and it was allowed to polymerise for 25-30 min at room temperature. Immediately after casting the stacking gel (5 %), the comb was inserted and the gel polymerised as described above. The resolving and stacking gels were prepared by the mixing of the following components:

Table 16. Components used in the preparation of SDS- PAGE gels

Solution components	Resolving (12%) gel	Resolving (10%) gel	Stacking (5%) gel
dH_2O	4.9 ml	5.9 ml	3.4 ml
30% acrylamide solution	6.0 ml	5.0 ml	0.83 ml
1.5 M Tris pH 8.8	3.8 ml	3.8 ml	-
1.0 M Tris pH6.8	-	-	0.63 ml
10% SDS	0.15 ml	0.15 ml	0.05 ml
10% Ammonium persulphate	0.15 ml	0.15 ml	0.05 ml
TEMED	0.006 ml	0.006 ml	0.005 ml

The protein samples were resolved in running SDS-PAGE buffer (0.025 M Tris base, 0.0192 M glycine, 1% (w/v) SDS) at 150 V until the dye front migrated to the end of the gel.

After electrophoresis, the gel was removed and stained in Coomassie blue stain [0.1% (w/v) Coomassie brilliant blue R250, 40% (v/v) methanol, 10% (v/ v) glacial acetic acid] for 2 h with gentle agitation. The gel was then incubated in high-methanol distain [40% (v/v) methanol, 10% (v/v) glacial acetic acid] for approximately 3 h or low-methanol distain for 24 h.

2.5.3 Western Analysis of the expressed KSHV ORF 4 proteins

The KSHV ORF 4 proteins were analysed by [0.1% (w/v)] SDS and [10% (w/v)] PAGE gel electrophoresis according to standard methods. Proteins resolved by discontinuous SDS-PAGE were transferred to a nitrocellulose Hybond-ECL membrane using the Mini Trans-Blot Protean II cell apparatus set (Bio-Rad). During electrophoresis, the nitrocellulose membrane, the sheets of 3MM Whatman filter paper (cut to size) and the fibre pads were pre-equilibrated in ice-cold transfer buffer [192 mM Glycine, 25 mM Tris base and 20% (v/v) methanol]. Following electrophoresis, the gel was also equilibrated in ice-cold transfer buffer. Three sheets of 3MM Whatman filter paper were mounted on a fibre pad, which was in turn mounted on the black panel. The equilibrated polyacrylamide gel was placed on the filter paper and overlaid with the nitrocellulose membrane. The membrane was in turn, overlaid with another three sheets of 3MM Whatman filter paper followed by a fibre pad. This transfer cassette was arranged in transfer buffer such that no air bubbles were trapped between the gel and membrane. The Western transfer was allowed to occur for 1 h at 100 V in the presence of a magnetic stirrer and a heat trap unit. In order to determine whether the transfer was successful, the nitrocellulose membrane was stained with Ponceau S mix [0.5% (w/v) Ponceau S, 1% (v/v) glacial acetic acid] for 5-10 min, followed by rinsing with ddH_2O. The membranes were scanned and washed twice in TBS before subject to immunodetection.

2.5.4 Chemiluminescence-based Immunodetection of the rKCPs

The immunodetection of KSHV ORF 4 proteins on nitrocellulose membranes was performed using the BM Chemiluminescence Western Blotting Kit (Mouse/Rabbit) (Roche). The membrane was incubated overnight at 4°C in blocking solution [5% (w/v) not-fat milk powder in TBS] in order to prevent non-specific binding of antibody to the nitrocellulose membrane. The polyclonal rabbit anti-KCP peptide

primary antibody was appropriately diluted 1:500 in TBST [0.1% (v/v) Tween-20 in TBS]. The proteins of interest were detected by incubating the membranes with the primary antibody dilution for 1 h and 30 min at RT with gentle shaking. After incubation, the primary antibody dilution was removed and stored at 4°C for repeated use if necessary. The membranes were washed twice in TBST and twice in blocking solution at RT with shaking for 10 min each. The membrane was then incubated for 30 min with the horseradish peroxidase (POD)-conjugated secondary antibody (anti-mouse/rabbit IgG) diluted 1:12 000 in 0.5% (w/v) TBS blocking solution. Following incubation with the secondary antibody, the membranes were washed four times in large volumes of TBST with shaking for 15 min each. For the chemiluminescent detection, the BM Chemiluminescence Western Blotting Kit starting solution B was added to substrate solution A in a 1:100 ratio and the mixture was incubated at RT for at least 30 min. In the dark room with the red safety light on, the membrane was covered in detection solution for approximately 1 minute. After draining of the excess fluid, the membranes were placed in a specialized developing cassette, followed by exposure of the membranes to X-ray film for different time intervals (1 minute-10 min) depending on the strength of the signal obtained. The X-ray film was developed in developer solution (Agfa reagents) for 1-2 min, rinsed in stop solution (2% glacial acetic acid), fixed in fixer solution (Agfa reagents) and rinsed in water before drying.

2.6 Functional and Structural Analysis of the Expressed KSHV ORF 4 recombinant proteins

2.6.1 Biological Activity Test of the Secreted Proteins

The activity of the three different sized secreted rKCPs was tested by means of a hemolysis assay, which measured their ability to inhibit complement-mediated lysis of sensitized sheep red blood cells (ssRBCs) (Kotwal *et al*, 1990). The first step was to carry out a serum assay whereby a 50 µl aliquot of human serum, which was stored at -80°C, was gently thawed and diluted at 1:30, 1:60 and 1:90. Four reactions were set up as the follows: 3 x 75 µl ssRBC, 10 µl $DGVB^{2+}$ [2.5 mM veronal buffer, (pH 7.3) 72 mM NaCl, 140 mM Glucose, 0.1% gelatine, 1 mM $MgCl_2$, and 0.15 mM $CaCl_2$] and 15 µl of each pre-diluted serum respectively and 1 negative control,

whereby the serum was replaced with $DGVB^{2+}$ buffer. The reaction samples were incubated for 1 h at 37°C and centrifuged at 7000 rpm for 30 seconds. After centrifugation the positive samples were analysed with respect to the negative control which showed no cell lysis, in order to determine the dilution of serum known to disrupt ~95% of ssRBCs. The components of the hemolysis assay reactions were then added in the following order:

Table 17. Components used in the set up of the Hemolyis Assay reactions

Sample	ssRBC (µl)	Buffer (µl)	Sample (µl)	Serum (1:60) (µl)
Negative Control	75	25	_	_
Positive Control	75	10	_	15
BC	75	6	4	15
KCP-S	75	6	4	15
KCP-S	75	8	2	15
KCP-S	75	9	1	15
KCP-M	75	6	4	15
KCP-M	75	8	2	15
KCP-M	75	9	1	15
KCP-F	75	6	4	15
KCP-F	75	8	2	15
KCP-F	75	9	1	15

The test samples (KCP-S, KCP-M and KCP-F) were carried out in duplicate and upon 1 h incubation of the reaction samples at 37° and centrifugation at 7000 rpm for 30 seconds, 70 µl of the supernatants were transferred to a 96 well plate. The amount of hemoglobulin from the lysed cells was determined by measuring the absorbance at 405 nm using a microplate reader (Anthos 2010). In order to determine percentage hemolysis inhibition, the OD_{405} reading of each sample was divided by the OD_{405} reading of the positive control:

Sample OD_{405} / Positive control OD_{405} = X_1 x 100 = X_2 – 100 = % Inhibition

A bar graph was drawn to show percentage hemolysis inhibition (Y-axis) versus the different volumes/amounts of the rKCPs (X-axis) (Figure 36).

2.6.2 *N*-Deglycosylation Analysis of the Truncated KCP

The supernatant [60-90 µl] from cultures of recombinant strains containing approximately 30 µg of protein of interest was made up to 100 µl with 50 mM sodium phosphate solution pH 7.5. The protein sample was concentrated using a Speed Vac apparatus. The concentrated protein was then resuspended in 25 µl of 50 mM sodium phosphate solution, pH 7.5, after which 2.5 µl of denaturation buffer (0.2% SDS with 100 mM β-mercaptoethanol) was added. The reaction mixture was denatured by heating at 100°C for 10 min followed by incubation with 3 µl of peptide-*N*-glycosidase F (PNGase F) (Figure 12) enzyme solution (500 units/ml) for 3 –18 h at 37°C to allow de-glycosylation to occur, and then stopped by heating to 100 °C for 5 min. The samples were then assessed by SDS-PAGE. The glycoprotein, gp120 was run with the deglycosylation experiment as a positive control substrate since the composition of the reaction buffer may interfere with the deglycosylation of a glycoprotein. Similarly, purified VCP (from the WR strain) which does not contain any *N*-linked carbohydrate sites was used as a negative control to show that any shift in molecular weight was not due to contaminating proteases but as a result of PNGase F activity.

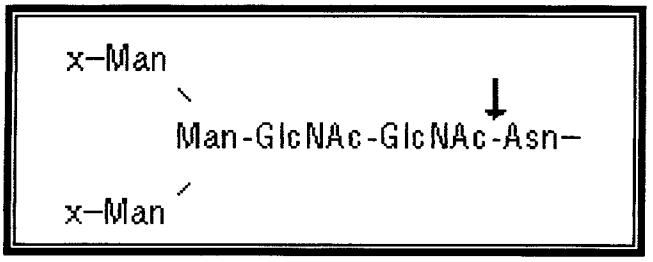

Figure 12. Schematic diagram of PGNase F *N*-deglycosylation

PNGase F is an amidase that cleaves between the innermost GlcNAc and asparagine residues of high mannose, hybrid, and complex oligosaccharides from *N*-linked glycoproteins. In other words, it hydrolyses nearly all types of *N*-glycan chains from glycopeptides/proteins [X= H or sugar (s)] (Maley *et al*, 1989).

2.7 Immunohistochemical Detection of the KCP in Kaposi's sarcoma

Coded human tissue samples from the pathological archives were kindly provided by Prof. D. Govender from the division of anatomical pathology, University of Cape Town. Furthermore, the specimens used in this study were completely anonymous therefore there was no knowledge of the patient identification.

All of the 12 KS cases under investigation were first subjected to Hematoxylin and Eosin (H & E) immunostaining which is a histological staining system commonly used for visualization of the cellular morphology of the tissue sections. This stain system is known to carry a positive charge because of a dye lake of hematein, which is an oxidation product of Hematoxylin, functioning as a basic dye. Therefore cell nuclei which are basophilic are stained blue. On the other hand, Eosin acts as a counter stain staining all the remaining tissue sections in different shades of red.

2.7.1 Coating of Slides with 3-aminopropyltriethoxyethylsilane

Tissue samples tend to float off the slides when subjected to wet heat and high temperature antigen retrieval methods, therefore in order to prevent this from happening, slides were coated with 3-aminopropyltri-ethoxyethylsilane [APES (98%)]. An approximately 3.3% solution of APES was prepared by adding 10 mls APES and 300 mls acetone together. The slides were packed into metal racks and washed in 1% aqueous detergent solution by soaking and some agitation, followed by a thorough wash in running tap water for about 60 min. The slides were then dried overnight at 37°C (or at 60°C for 4 h). Suitably sized dishes containing APES solution, acetone, and water were placed next to each other and the slide rack was dipped into each of the solutions as follows: APES 10 dips, acetone 3 dips, acetone 3 dips and water 3 dips. Finally, the slides were allowed to dry overnight at 37°C.

2.7.2 Immunohistochemistry of KS Tissue Samples with anti-KCP

Paraffin-embedded sections were cut at 2-4 μm, mounted on APES-coated slides and heat fixed on a hot-plate at approximately 75°C for 30 min. Heat-induced epitope retrieval (HIER) was carried in 1mM EDTA (pH 8.0) using a pressure cooker. Upon boiling of the buffer, the slides in a metal rack were immersed in the buffer and the

pressure cooker was sealed. Once at full pressure, a timer was set for 2 min followed by release of the pressure with running cold water. The slides were then washed in running tap water until the next step. After blocking of endogenous peroxidase activity with aqueous 1% H_2O_2 for 15 min, the sections were washed in phosphate-buffered saline containing 0.05% Tween-20 (PBS-T), and non-specific binding of secondary antibody was blocked with 5% normal goat serum for 15 min. The normal goat serum was drained off and the sections were incubated for 60 min at room temperature with a rabbit polyclonal antibody directed against a selected N-terminus peptide of the KCP (section 2.4.1) at 1:10 000 dilution, which was found to be optimal after a series of dilutions of the primary antibody ranging from 1: 250-1: 100 000 were tested. The primary antibody was substituted with PBS in sections used as negative controls and with anti-CD34 (1:50) (Novocastra), anti-CD31 (1:40) (DakoCytomation), anti-cyclin D1 (1:100) (NeoMarkers) and anti-LANA (1:25) (Novocastra) in sections used as positive controls. The sections were well rinsed with PBS-T and incubated for 30 min at room temperature with goat anti-rabbit secondary antibody-conjugated to peroxidase (EnVision). The slides were then rinsed with PBS followed by 5 min incubation with liquid 3, 3'-diaminobenzidine (DAB) substrate chromogen that was diluted according to instructions. The slides were rinsed in running tap water, counterstained with haematoxylin, dehydrated and mounted in Entellan.

CHAPTER THREE

RESULTS

3.1 Preparation of the KSHV ORF 4 DNA Constructs

3.1.1 Preparation of the pGEMT/KSHV ORF4 Gene Constructs

Background Information

The chosen vector for easy and convenient cloning of the genes of interest was the pGEM®-T easy system. The KSHV ORF4 PCR products were ligated into this expression vector to generate three recombinant plasmids, pGEMT/KSHV ORF 4 (735), pGEMT/KSHV ORF 4 (1436) and pGEMT/KSHV ORF 4 (1581) (Figure 13, B-D). The pGEM®-T easy vector contains multiple restriction sites within the multiple cloning region, which allow for the release of the insert by digestion with a single restriction enzyme (Figure 13, A). However, two different restriction enzymes from the multiple cloning region (*Eco* RI and *Not* I) were selected and used in the creation of the pGEMT/KSHV ORF 4 constructs and therefore, a double-digestion was carried out to release the inserts from the vector. If desired, insertional inactivation of the α-peptide could have been used as a tool for color screening of the recombinant clones on indicator plates containing the β-galactosidase substrate 5-bromo-4-chloro-3-indolyl-β-D-galactopyianoside (BCIG; X-gal).

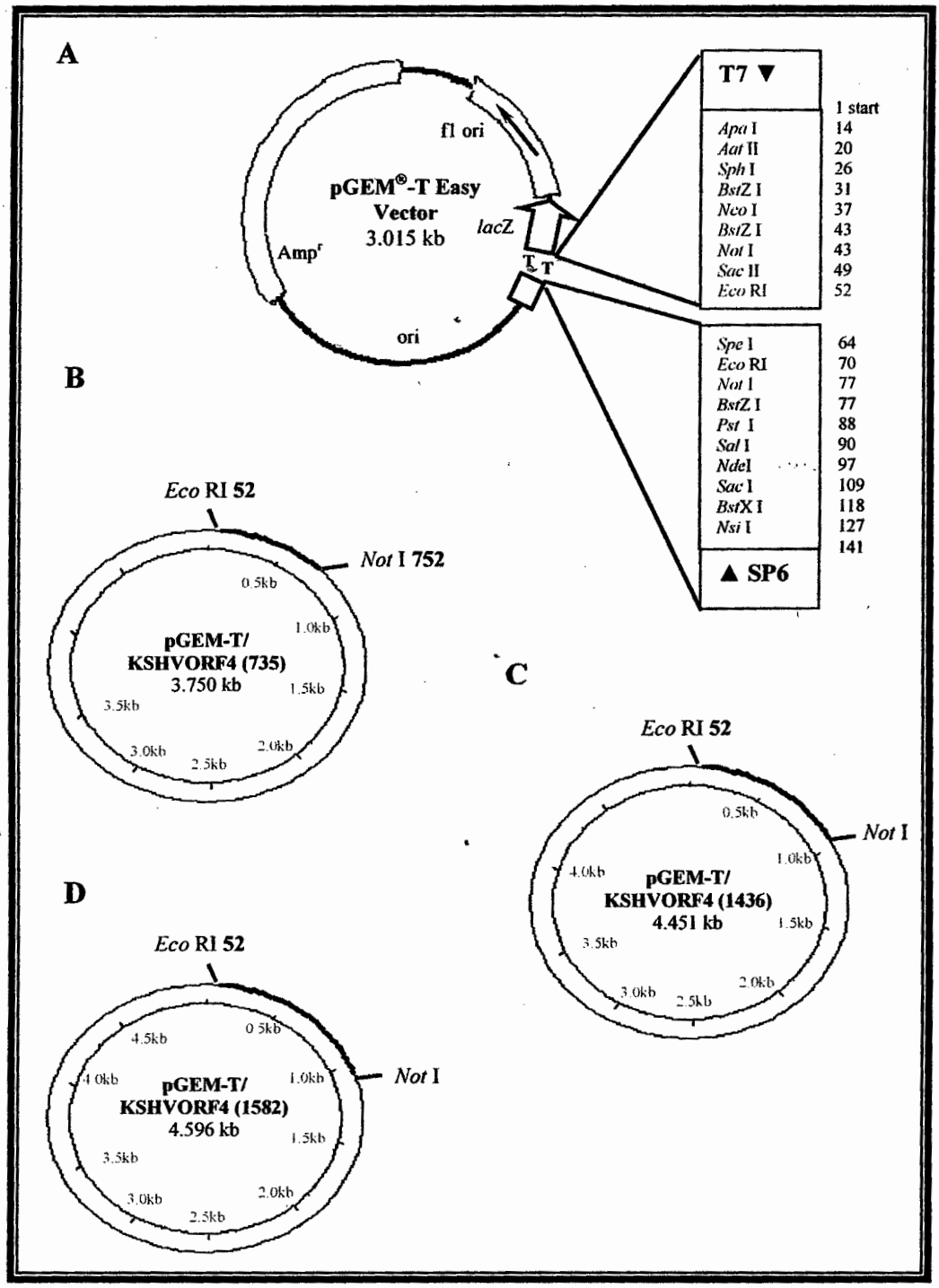

Figure 13. Restriction Plasmids Maps of the pGEMT-easy vector and constructs

A: pGEMT easy vector circle map showing the most important sequence reference points such as the T7 and SP6 RNA polymerase transcription sites, and a double multiple cloning region for easy and convenient ligation of the genes of interest to the vector. **B:** Double-restriction endonuclease digestion of the 3750 bp pGEMT/KSHV ORF 4 (735) construct with the REs *Eco* RI and *Not* I produces 4 fragments of sizes 2981 bp, 735 bp, 9 bp and 7 bp. **C:** Double-restriction endonuclease digestion of the 4491 bp pGEMT/KSHV ORF 4 (1436) construct with the REs *Eco* RI and *Not* I produces 4 fragments of sizes 2981 bp, 1436 bp, 9 bp and 7 bp. **D:** Double-restriction endonuclease digestion of the 4596 bp pGEMT/KSHV ORF 4 (1581) construct with the REs *Eco* RI and *Not* I produces 4 fragments of sizes 2981 bp, 1436 bp, 9 bp and 7 bp.

3.1.2 PCR amplification of KSHV ORF 4 gene from KSHV DNA

Three DNA-sections of the KSHV ORF4 encompassing SCRs 1 to 4 (Figure 8) were amplified from a KSHV DNA template by PCR using a KSHV ORF4-specific forward primer and three consecutive KSHV ORF4-specific reverse primers. The PCR products (10µl) were resolved by gel electrophoresis on 1% (w/v) agarose gel (Figure 14).

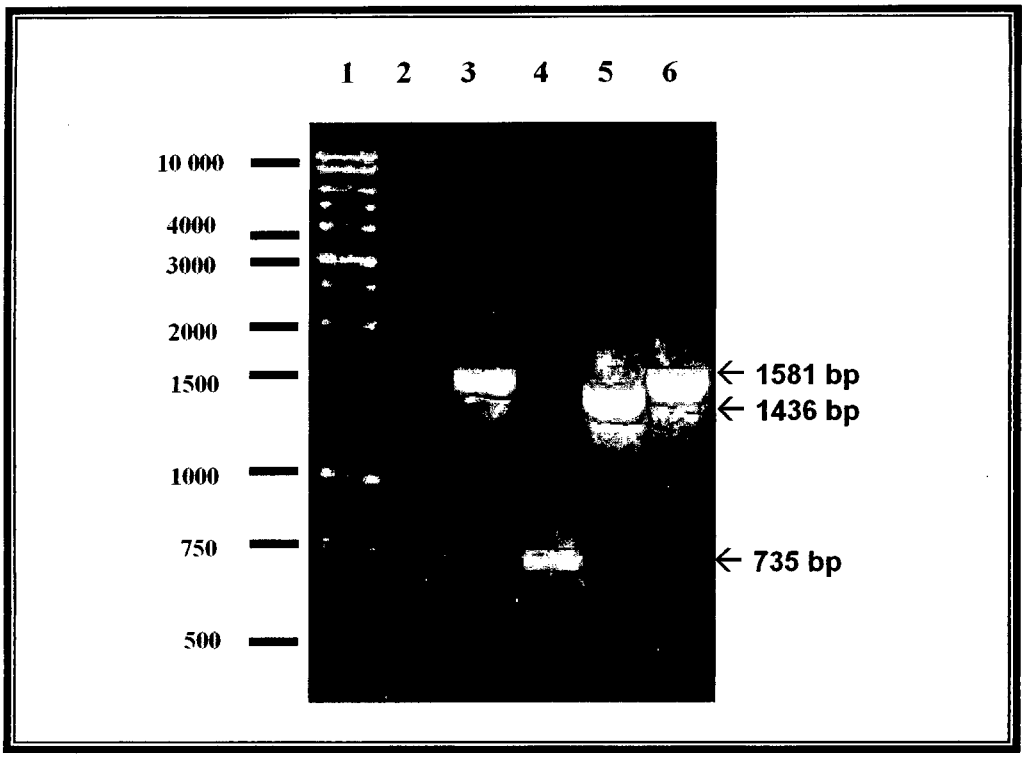

Figure 14. Agarose gel Analysis of the KSHV ORF 4 PCR products

Ethidium bromide stain of electrophoretically resolved [1% (w/v) agarose gel] PCR products; **Lane 1:** 1kb DNA ladder molecular weight marker (Promega); **Lane 2:** VCP amplified from Vaccinia virus DNA with the VCP-specific forward and reverse primers, used as a PCR positive control. A faint band of expected fragment size, 700 bp can be visualised; **Lane 3:** KSHV ORF 4-specific 1597 bp PCR product amplified from KSHV DNA template with the forward primer 03-1420 and the reverse primer 03-1421; **Lane 4:** KSHV ORF 4-specific 735 bp PCR product amplified from KSHV DNA template with the forward primer 03-0668 and the reverse primer 03-0669; **Lane 5:** KSHV ORF 4-specific 1436 bp PCR product amplified from KSHV DNA template with the forward primer 03-0668 and the reverse primer 03-0670; **Lane 6:** KSHV ORF 4-specific 1581 bp PCR product amplified from KSHV DNA template with the forward primer 03-0668 and the reverse primer 03-0671.

3.1.3 Small-scale preparation of plasmid DNA

Uncut double stranded plasmid DNA template, pGEMT/KSHV ORF 4 (735), pGEMT/KSHV ORF 4 (1436) and pGEMT/KSHV ORF 4 (1581) (labelled A1-4, B1-4 and C1-4 respectively) isolated from *E. coli* transformants using a modified alkaline lysis procedure [(QIAprep miniprep plasmid isolation kit (Qiagen)], was analysed by agarose gel electrophoresis (Figure 15). As expected a number of different bands of low electrophoretic mobility were obtained corresponding to the various conformations of DNA, namely the relaxed circular/nicked open circular or linear form and the supercoiled/covalently closed circular (CCC) form.

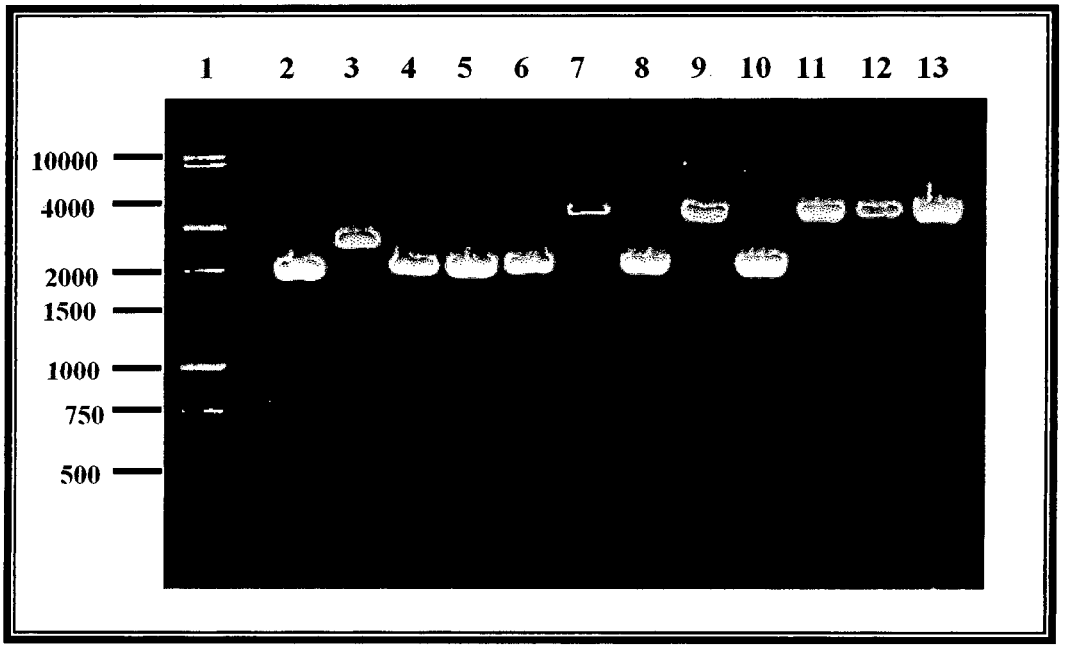

Figure 15. Agarose gel analysis of the isolated pGEMT plasmid DNA

Ethidium bromide stain of electrophoretically resolved [1% (w/v) agarose gel] isolated pGEMT-easy DNA using the QiaPrep small scale plasmid purification kit; **Lane 1:** 1kb DNA ladder molecular weight marker; **Lanes 2-5:** Uncut pGEMT/KSHV ORF 4 (735) (sample A1-A4); **Lanes 6-9:** Uncut pGEMT/KSHV ORF 4 (1436) (sample B1-B4); **Lanes 10-13:** Uncut pGEMT/KSHV ORF 4 (1581) (sample C1-C4). All lanes (2-13) show the different possible conformations of DNA, namely the nicked open circular (top band) and supercoiled (bottom band).

3.1.4 RE Digestion Analysis of the pGEMT-easy DNA Constructs

Double stranded plasmid DNA template, pGEMT/KSHV ORF 4 (735), pGEMT/KSHV ORF 4 (1436) and pGEMT/KSHV ORF 4 (1581), labelled A1-4, B1-4 and C1-4 respectively, isolated from *E. coli* transformants was subjected to

restriction endonuclease digestion and the DNA fragments were analysed by agarose gel electrophoresis (Figure 16)

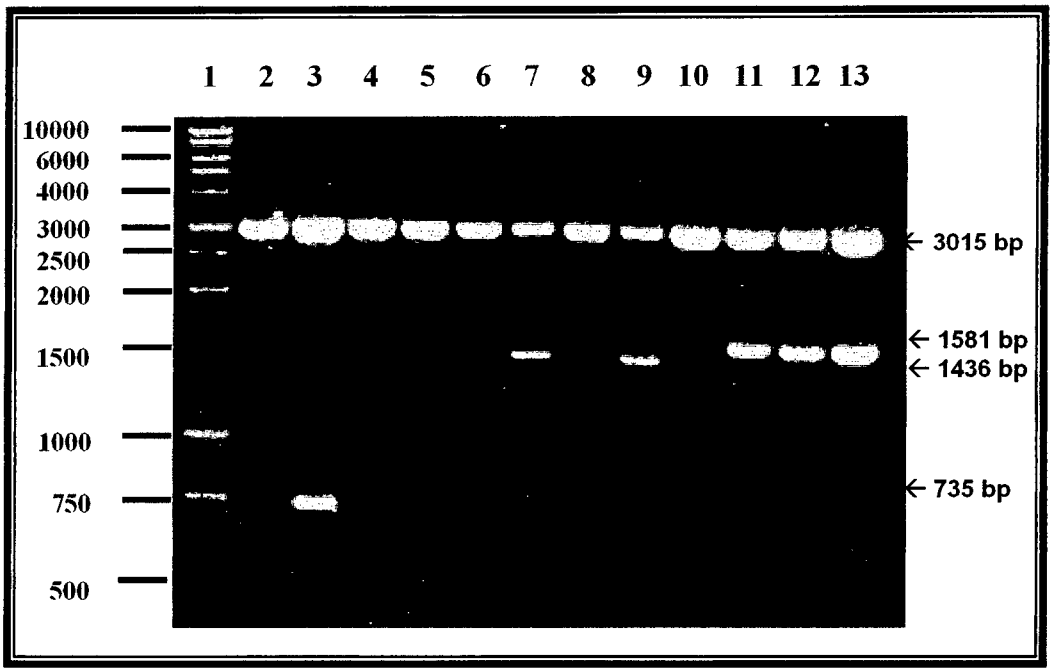

Figure 16. Agarose gel of the pGEMT/KSHV ORF 4 constructs RE analysis

Ethidium bromide stain of electrophoretically resolved [1% (w/v) agarose gel] *Eco* RI and *Not* I digested pGEMT/KSHV ORF4 DNA constructs; **Lane 1:** 1kb DNA ladder molecular weight marker; **Lanes 2, 4 and 5:** *Eco* RI and *Not* I digested pGEMT/KSHV ORF 4 (735) into which the KSHV ORF4-specific 735 bp PCR product was not ligated; **Lanes 3:** *Eco* RI and *Not* I digested pGEMT/KSHV ORF 4 (735) into which the KSHV ORF4-specific 735 bp PCR product was successfully ligated; **Lane 6 and 8:** *Eco* RI and *Not* I digested pGEMT/KSHV ORF 4 (1436) into which the KSHV ORF4-specific 1436 bp PCR product was not ligated; **Lane 7 and 9:** *Eco* RI and *Not* I digested pGEMT/KSHV ORF 4 (1436) into which the KSHV ORF4- specific 1436 bp PCR product was successfully ligated; **Lane 10:** *Eco* RI and *Not* I digested pGEMT/KSHV ORF 4 (1581) into which the KSHV ORF4- specific 1581 bp PCR product was not ligated; **Lanes 11-13:** *Eco* RI and *Not* I digested pGEMT/KSHV ORF 4 (1581) into which the KSHV ORF4-specific 1581 bp PCR product was successfully ligated.

The *Eco* RI- and *Not* I- cut pGEMT/KSHV ORF 4 (735) (Figure 16, lane 3) resolved into two visible bands corresponding to the expected 2981 bp and 735 bp DNA fragments while that of the *Eco* RI- and *Not* I- cut pGEMT/KSHV ORF 4 (735) (Figure 16, lane 2, 4 and 5) resolved into only one visible band corresponding to 2981 bp DNA fragment showing that only one out of the four constructs contained the 735 bp insert of interest.

Similarly, the *Eco* RI- and *Not* I- cut pGEMT/KSHV ORF 4 (1436) (Figure 16, lanes 7 and 9) resolved into two visible bands corresponding to the expected 2981 bp and 1436 bp DNA fragments while that of the *Eco* RI- and *Not* I- cut pGEMT/KSHV ORF 4 (1436) (Figure 16, lane 6,9) resolved into only one visible band corresponding to 2981 bp DNA fragment showing that two out of the four constructs contained the 1436 bp insert of interest.

Furthermore, the *Eco* RI- and *Not* I-cut pGEMT/KSHV ORF 4 (1581) (Figure 16, lanes 11-13) resolved into two visible bands corresponding to the expected 2981 bp and 1581 bp DNA fragments while that of the *Eco* RI- and *Not* I- cut pGEMT/KSHV ORF 4 (1581) (Figure 16, lane 10) resolved into only one visible band corresponding to 2981 bp DNA fragment showing that three out of the four constructs contained the 1581 bp insert of interest.

3.1.5 Directional Analysis of the Cloned Genes by RE Digestion

All of the pGEMT/KSHV ORF4 constructs digested with *Bam* HI resulted in the expected linear fragments of 3750bp, 4450 bp and 4596 bp corresponding to the pGEMT-easy constructs containing the 735bp, 1436 bp and 1581bp genes respectively. The restriction enzyme *Bam* HI does not cut the pGEMT-easy vector but it cuts all three inserts at position 643 bp as determined by GeneRunner software. The fact that this RE linearised all the constructs under investigation shows that the inserts were ligated in the correct orientation, in other words, the top strand of the insert goes from 5' → 3' and therefore the restriction enzyme is capable of recognising its respective restriction site (Figure 9).

The RE chosen as a linearization positive control, *Eco* RV, capable of cutting the vector once but not the insert was not a good choice because in the preparation of the pGEMT-easy vector, the vector was linearised at base 60 with *Eco* RV and a T added to both 3'-ends as previously described in section 2.1.6. This site is not recovered upon ligation of the vector with the insert and as a result, digestion of the constructs with *Eco* RV did not yield any linear product as seen in Figure 17.

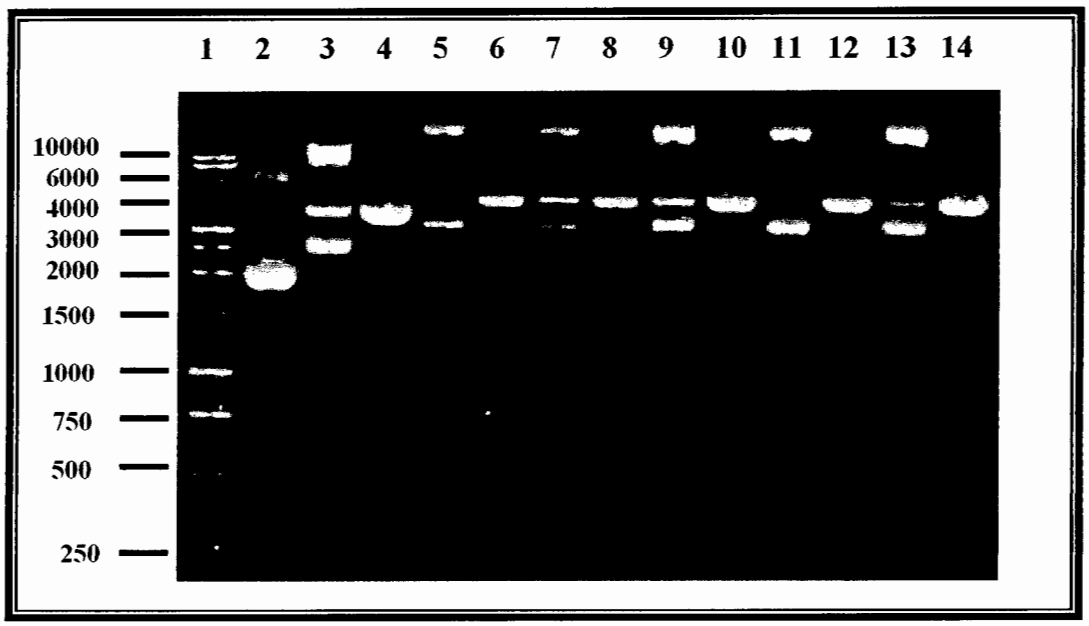

Figure 17. Agarose gel of the directional analysis of the inserts by RE digestion

Ethidium bromide stain of electrophoretically resolved [1% (w/v) agarose gel] *Eco* RI and *Not* I digested pGEMT/KSHV ORF4 DNA constructs; **Lane 1:** 1kb DNA ladder molecular weight marker; **Lane 2:** Uncut pGEMT/KSHV ORF 4 (735 bp) (negative control showing the different possible conformations of DNA); **Lane 3:** *Eco* RV cut pGEMT/KSHV ORF 4 (735 bp) (Unsuccessful positive control as *Eco* RV does not linearise the contruct); **Lane 4:** *Bam* HI linearised pGEMT/KSHV ORF 4 (735 bp) (expected fragment obtained of size 3750 bp); **Lane 5 and 7:** *Eco* RV cut pGEMT/KSHV ORF 4 (1436 bp) (Unsuccessful positive control as *Eco* RV does not linearise the contruct); **Lane 6 and 8:** *Bam* HI linearised pGEMT/KSHV ORF 4 (1436 bp) (expected fragment obtained of size 4450 bp); **Lane 9, 11 and 13:** *Eco* RV cut pGEMT/KSHV ORF 4 (1581 bp) (Unsuccessful positive control as *Eco* RV does not linearise the contruct); **Lane 10, 12 and 14:** *Bam* HI linearised pGEMT/KSHV ORF 4 (1581 bp) (expected fragment obtained of size 4596 bp).

3.1.6 DNA Sequencing Results

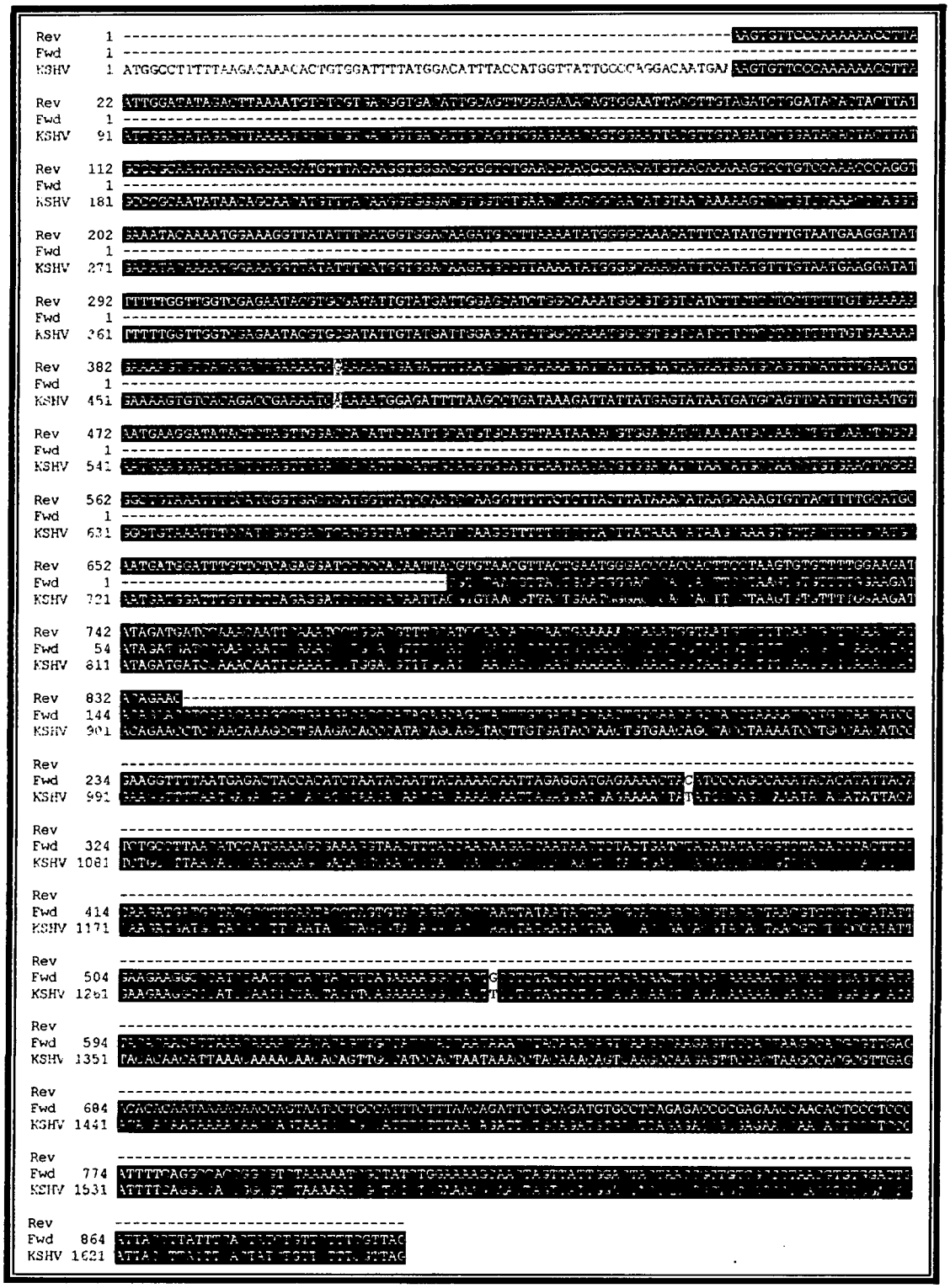

Figure 18. Multiple Sequence Alignment of the Cloned KCP Gene with the pGEMT primers DNA Sequencing Results

The sequences of the cloned gene obtained from amplification with the pGEMT forward and reverse primers shown in blue and red respectively was compared to the KSHV ORF 4 sequence from the database (green) using Clustal W (Higgins *et al*, 1994). The results are represented in box shade format.

pGEMT/KSHV ORF 4 (1581 bp) plasmid DNA was isolated from several colonies of *E. coli* cells and sequencing was done from both ends of the inserted full length KCP gene using pGEMT-easy specific forward and reverse primers. Similarly, pPIC9/KSHV ORF 4 (1581 bp) plasmid DNA was also subject to DNA sequencing using the standard 5' and 3' *AOX1* primers. The DNA sequencing results obtained were fairly precise for the exception of three sequence-specific base mutations at positions 575 (grey), 1055 and 1305 (white) as shown in Figure 18.

To investigate these mutations at the protein level, Clustal W was also used to compare the protein sequence of the cloned KSHV ORF4 as obtained from the DNA sequencing results, with that of the database (Figure 19). The protein multiple sequence alignment shows that the base mutations present at the DNA level caused non-conservative amino acid changes as denoted by the red text in Figure 19.

```
 KCP      1 MAFLRQTLWILWTFTMVIGQDNEKCSQKTLIGYRLKMSRDGDIAVGETVELRCRSGYTTY
rKCP      1 MAFLRQTLWILWTFTMVIGQDNEKCSQKTLIGYRLKMSRDGDIAVGETVELRCRSGYTTY
            ************************************************************

 KCP     61 ARNITATCLQGGTWSEPTATCNKKSCPNPGEIQNGKVIFHGGQDALKYGANISYVCNEGY
rKCP     61 ARNITATCLQGGTWSEPTATCNKKSCPNPGEIQNGKVIFHGGQDALKYGANISYVCNEGY
            ************************************************************

 KCP    121 FLVGREYVRYCMIGASGQMAWSSSPPFCEKEKCHRPKIKNGDFKPDKDYYEYNDAVHFEC
rKCP    121 FLVGREYVRYCMIGASGQMAWSSSPPFCEKEKCHRPKIENGDFKPDKDYYEYNDAVHFEC
            ************************************ ***********************

 KCP    181 NEGYTLVGPHSIACAVNNTWTSNMPTCELAGCKFPSVTHGYPIQGFSLTYKHKQSVTFAC
rKCP    181 NEGYTLVGPHSIACAVNNTWTSNMPTCELAGCKFPSVTHGYPIQGFSLTYKHKQSVTFAC
            ************************************************************

 KCP    241 NDGFVLRGSPTITCNVTEWDPPLPKCVLEDIDDPNNSNPGRLHPTPNEKPNGNVFQRSNY
rKCP    241 NDGFVLRGSPTITCNVTEWDPPLPKCVLEDIDDPNNSNPGRLHPTPNEKPNGNVFQRSNY
            ************************************************************

 KCP    301 TEPPTKPEDTHTAATCDTNCEQPPKILPTSEGFNETTTSNTITKQLEDEKTISQPNTHIT
rKCP    301 TEPPTKPEDTHTAATCDTNCEQPPKILPTSEGFNETTTSNTITKQLEDEKTTSQPNTHIT
            ************************************************** ********

 KCP    361 SALTSMKAKGNFTNKTNNSTDLHIASTPTSQDDATPSIPSVQTPNYNTNAPTRTLTSLHI
rKCP    361 SALTSMKAKGNFTNKTNNSTDLHIASTPTSQDDATPSIPSVQTPNYNTNAPTRTLTSLHI
            ************************************************************

 KCP    421 EEGPSNSTTSEKATSSTLSHNSHKNDTGGIYTTLNKTTQLPSTNKPTNSQAKSSTKPRVE
rKCP    421 EEGPSNSTTSEKATASTLSHNSHKNDTGGIYTTLNKTTQLPSTNKPTNSQAKSSTKPRVE
            ************** ********************************************

 KCP    481 THNKTTSNPAISLTDSADVPQRPREPTLPPIFRPPASKNRYLEKQLVIGLLTAVALTCGL
rKCP    481 THNKTTSNPAISLTDSADVPQRPREPTLPPIFRPPASKNRYLEKQLVIGLLTAVALTCGL
            ************************************************************

 KCP    541 ITLFHYLFFR
rKCP    541 ITLFHYLFFR
            **********
```

Figure 19. Recombinant and Wild-type KCP Multiple Sequence Alignment using Clustal W

Figure 19 shows 99.5% identity in the 550 residues overlap between the recombinant and the wild-type KSHV ORF 4 protein sequence. The remaining 0.5% accounts for the three amino acid changes, Lysine to Glutamic acid at position 159, Isoleucine to Threonine at position 352 and finally Serine to Alanine at position 435.

3.1.7 Preparation of the pPIC9/KSHV ORF4 Gene Constructs

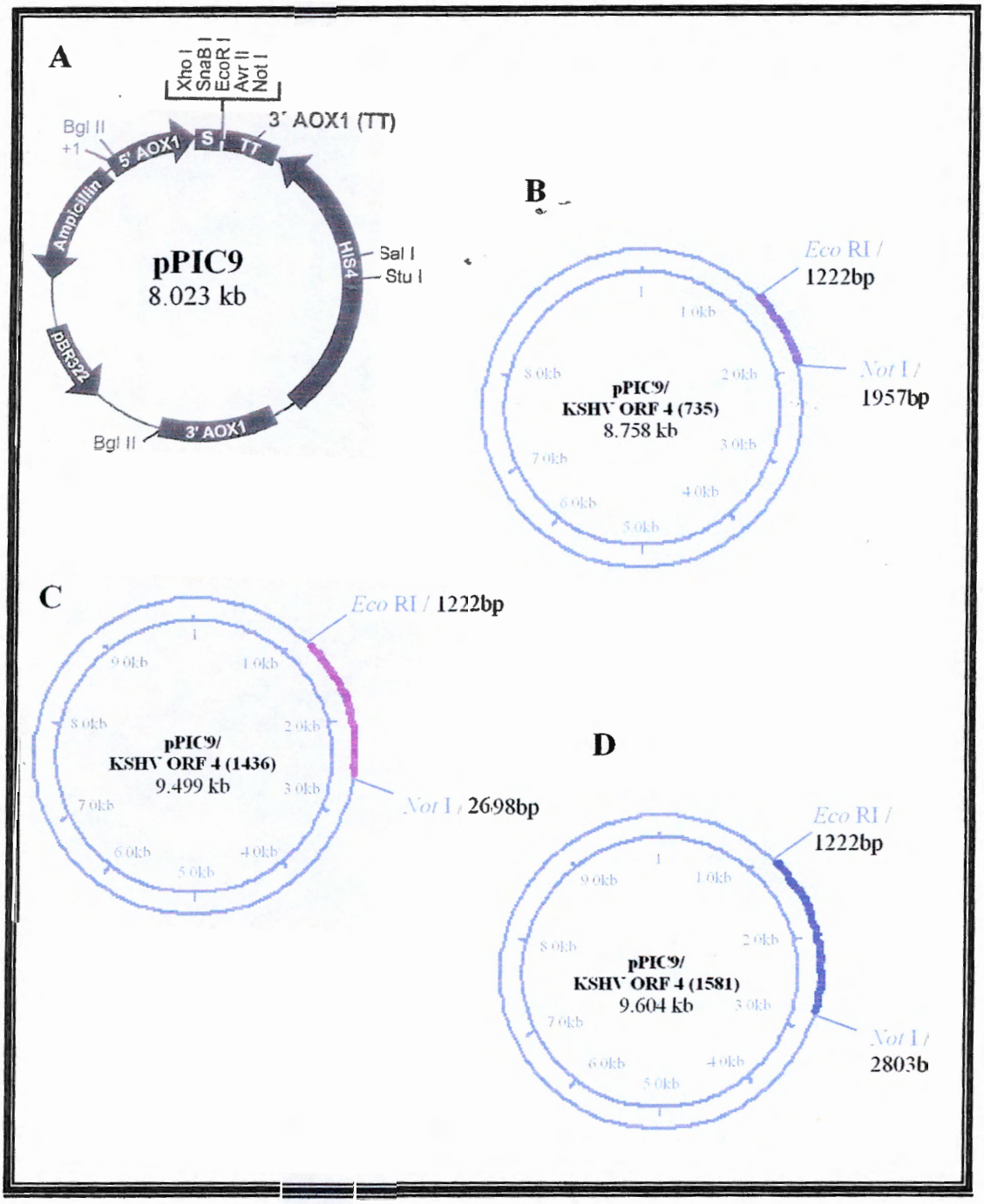

Figure 20. Restriction Plasmids Maps of the pPIC9 vector and constructs

A: Vector circle map showing the location and size of each feature of pPIC9, including a multiple cloning site for easy ligation of the genes of interest to the vector. **B:** Double-restriction endonuclease digestion of the 8758 bp pPIC9/KSHV ORF 4 (735) construct with the REs *Eco* RI and *Not* I produces 2 fragments of sizes 8023 and 735 bp. **C:** Double-restriction endonuclease digestion of the 9499 bp pPIC9/KSHV ORF 4 (1436) construct with the REs *Eco* RI and *Not* I produces 2 fragments of sizes 8023 bp and 1436 bp. **D:** Double-restriction endonuclease digestion of the 9604 bp pPIC9/KSHV ORF 4 (1581) construct with the REs *Eco* RI and *Not* I produces 2 fragments of sizes 8023 bp and 1581 bp.

3.1.8 Small-scale Isolation and RE Analysis of pPIC9 Plasmid DNA

Double stranded plasmid DNA template, pPIC9 isolated from *E. coli* transformants using the QIAprep miniprep plasmid isolation kit, was subject to *Hind* III and *Pst* I RE digestion and the DNA fragments were analysed by agarose gel electrophoresis (Figure 21). Uncut pPIC9 DNA was used as a negative control and as expected, a number of different bands of low electrophoretic mobility were obtained (Figure 21, lanes 1 and 5).

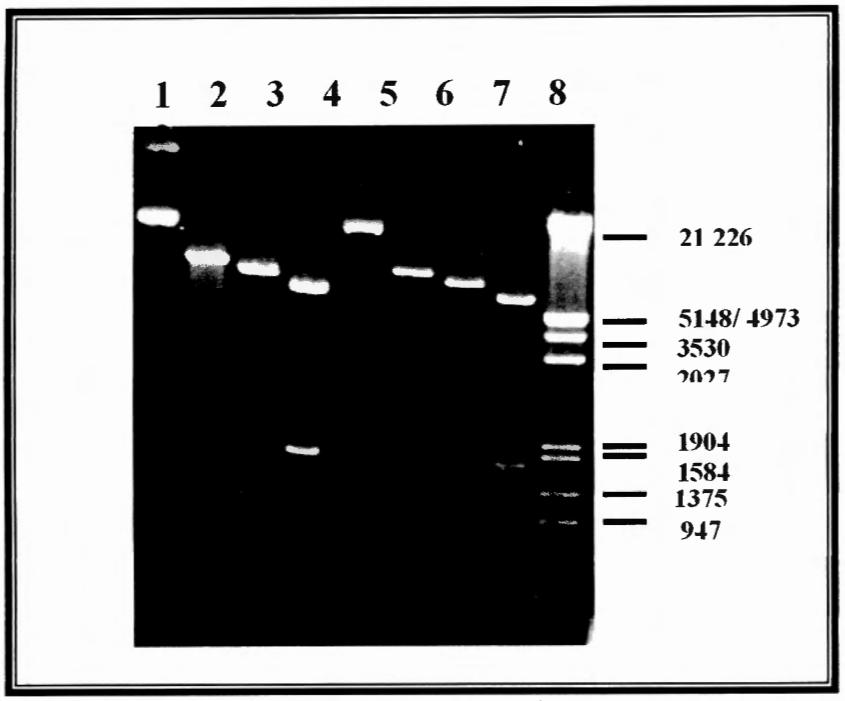

Figure 21. Agarose gel of the pPIC9 Restriction endonuclease analysis

Agarose gel [0.8 % (w/v)] electrophoresis was used to analyse the restriction enzyme digestion products of the pPIC9 plasmid DNA; **Lanes 1 and 5:** Uncut pPIC9, negative control showing the different possible conformations of DNA; **Lanes 2 and 6:** *Sac* I linearised pPIC9, expected fragment obtained of size 8023 bp; **Lanes 3 and 7:** pPIC9 cut with *Hind* III, only one of the four expected fragments is visible of size 7302 bp; **Lanes 4 ad 8:** *Pst* I-cut pPIC9, expected fragments obtained of sizes 6361 bp and 1662 bp; **Lane 9:** λ DNA/*Eco* RI and *Hind* III molecular weight marker (Promega).

The pPIC9 plasmid DNA was linearised when digested with *Sac* I and therefore resolved into a single band of expected molecular size 8.023 kbp (Figure 21, lanes 2 and 6). The *Hind* III-cut pPIC9 (Figure 21, lanes 3 and 7) should resolve into 4 fragments (7302, 370, 339 and 12 bp) but only the DNA fragment corresponding to size 7.302 kbp is visible in Figure 21 as the other three fragments are too small. On

the other hand, the *Pst* I-cut pPIC9 (Figure 21, lanes 4 and 8), resolved into two visible bands, corresponding to the expected 6.361 and 1.662 kbp DNA fragments.

3.1.9 DNA Isolation from Low-melt Gels

Successful pGEMT-easy clones containing the DNA fragments of interest were digested with *Eco* RI and *Not* I as described in section 2.1.10. The *Eco RI/Not I* KSHV ORF 4 DNA fragments were recovered from a low melting temperature agarose gel using the Wizard® SV system.

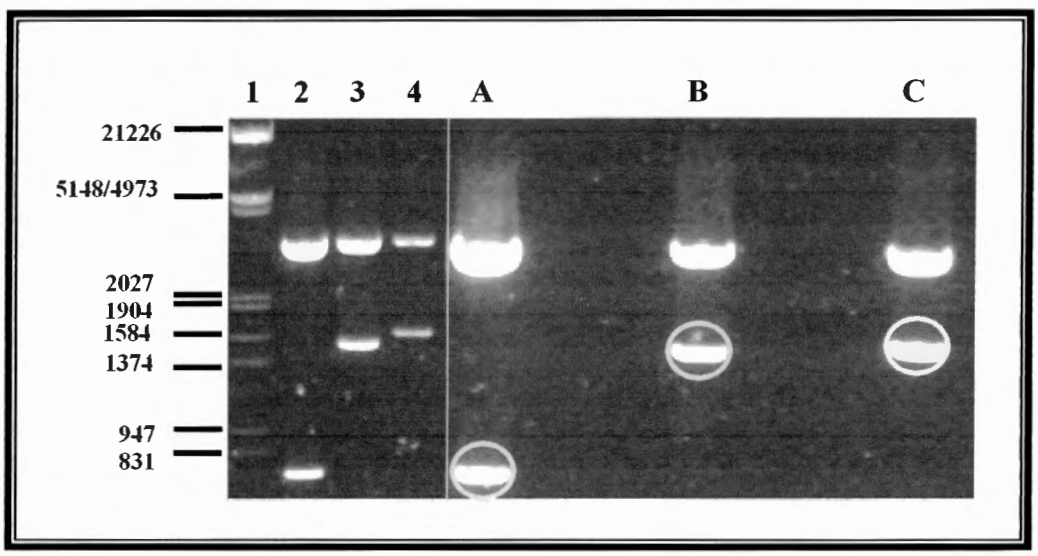

Figure 22. Agarose gel of the genes of interest recovered from low-melt gel

Ethidium bromide stain of electrophoretically resolved [1% (w/v) agarose gel] *Eco* RI and *Not* I digested pGEMT/KSHV ORF 4 DNA constructs; **Lane 1:** λ DNA/*Eco* RI and *Hind* III molecular weight marker; **Lane 2:** *Eco* RI and *Not* I digested pGEMT/KSHV ORF 4 (735) (expected fragments obtained of sizes 2981 bp and 735 bp); **Lane 3:** *Eco* RI and *Not* I digested pGEMT/KSHV ORF 4 (1436) (expected fragments obtained of sizes 2981 bp and 1436bp); **Lane 4:** *Eco* RI and *Not* I digested pGEMT/KSHV ORF 4 (1581) (expected fragments obtained of sizes 2981 and 1581 bp); **Lanes A-C:** Exactly as per lanes 2-4 respectively for the exception that a greater volume of DNA was loaded instead for extraction of the marked DNA fragments from the agarose gel.

3.1.10 RE Digestion Analysis of the pPIC9 DNA Constructs

Double stranded plasmid DNA template, pPIC9/KSHV ORF 4 (735), pPIC9/KSHV ORF 4 (1436) and pPIC9/KSHV ORF 4 (1581) (labelled A1-3, B1-3 and C1-3 respectively) isolated from *E. coli* transformants was subjected to restriction

endonuclease digestion and the DNA fragments were analysed by agarose gel electrophoresis (Figure 23).

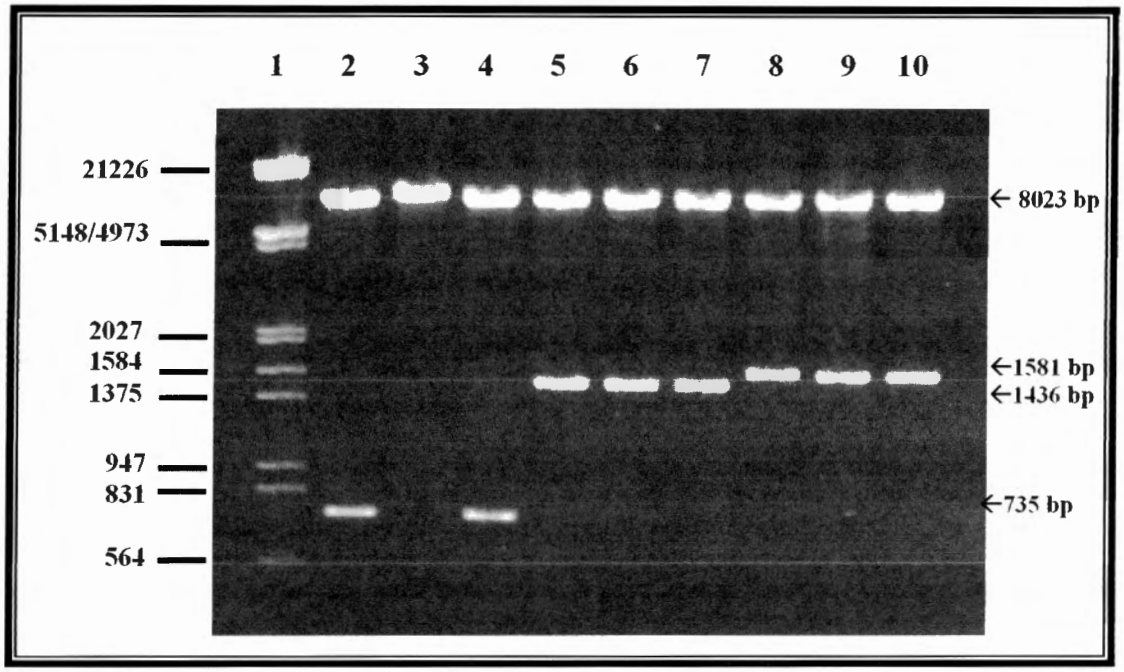

Figure 23. Agarose gel of the pPIC9/KSHV ORF4 constructs RE analysis

Ethidium bromide stain of electrophoretically resolved [1% (w/v) agarose gel] *Eco* RI and *Not* I digested pPIC9/KSHV ORF4 DNA constructs; **Lane 1:** λ DNA/*Eco* RI and *Hind* III molecular weight marker; **Lanes 2 and 4:** *Eco* RI and *Not* I digested pPIC9/KSHV ORF 4 (735) into which the KSHV ORF4 *Eco* RI/*Not* I 735 bp DNA fragment was successfully ligated; **Lanes 3:** *Eco* RI and *Not* I digested pPIC9/KSHV ORF 4 (735) into which the KSHV ORF4 *Eco* RI/*Not I* 735 bp DNA fragment was not ligated; **Lanes 5-7:** *Eco* RI and *Not* I digested pPIC9/KSHV ORF 4 (1436) into which the KSHV ORF4 *Eco* RI/*Not I* 1436 bp DNA fragment was successfully ligated; **Lanes 8-10:** *Eco* RI and *Not* I digested pPIC9/KSHV ORF 4 (1581) into which the KSHV ORF4 *Eco* RI/*Not I* 1581 bp DNA fragment was successfully ligated.

The *Eco* RI- and *Not* I-cut pPIC9/KSHV ORF 4 (735) (Figure 23, lane 2 and 4) resolved into two visible bands corresponding to the expected 8000 bp vector and the 735 bp DNA fragment while that of the *Eco* RI- and *Not* I-cut pPIC9/KSHV ORF 4 (735) (Figure 23, lane 3) resolved into only one visible band corresponding to 8000 bp vector DNA, showing that two out of the three constructs contained the 735 bp gene of interest. Furthermore, the *Eco* RI- and *Not* I-cut pPIC9/KSHV ORF 4 (1436) (Figure 23, lanes 5-7) resolved into two visible bands corresponding to the expected 8000 bp vector and the 1436 bp DNA fragment showing that all three recombinants under investigation were transformed with pPIC9 containing the 1436 bp insert of

interest. Similarly, the *Eco* RI- and *Not* I- cut pPIC9/KSHV ORF 4 (1581) (Figure 23, lanes 8-10) resolved into two visible bands corresponding to the expected size of the vector, 8000 bp and the 1581 bp DNA fragment showing again that the three picked *E. coli* recombinants were successfully transformed with pPIC9 containing the 1581 bp gene of interest.

3.2 Transformation and Selection for Positive Clones

Many transformants as selected by their ability to grow in the absence of histidine (His^+) were obtained in all of the transformation experiments carried out.

3.2.1 Screening for Mut^+ and Mut^S Transformants

After transformation of the chemically competent *Pichia* cells with pPIC9 DNA constructs containing the genes of interest, His^+ GS115 transformants were readily distinguished between Mut^+ (Methanol utilisation plus), which refers to the wild type ability of the cells to metabolize methanol as the sole carbon source, and Mut^S (Methanol utilisation slow) phenotype by patching selected colonies on MM versus MD plates.

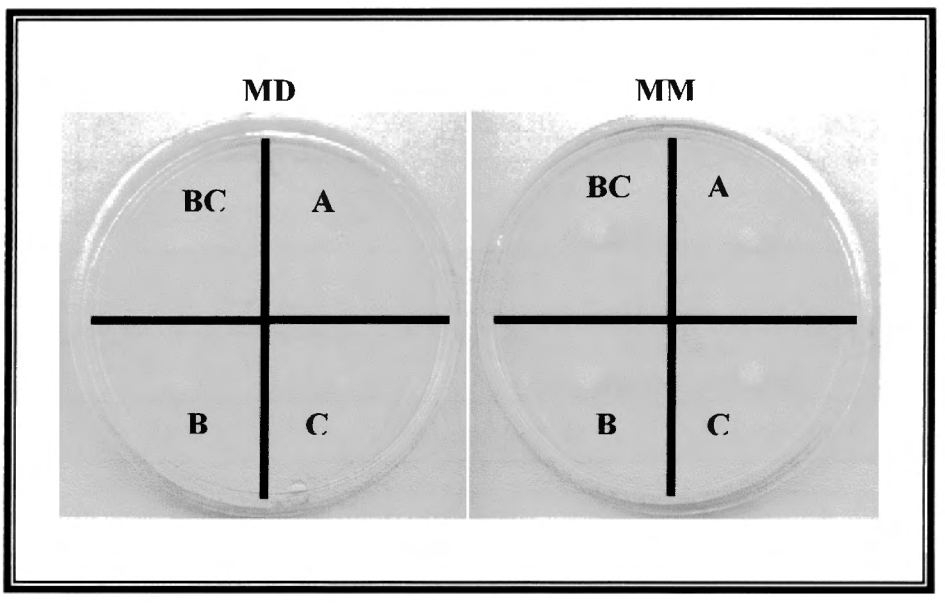

Figure 24. His^+ GS115 *P. pastoris* transformants are mostly Mut^s phenotype

His^+ transformants, **BC** (Background control: *Pichia* transformed with pPIC9 vector without the insert), **A** [pPIC9/KSHV ORF4 (735)], **B** [pPIC9/KSHV ORF4 (1436)], **C** [pPIC9/KSHV ORF4 (1581)], were screened for the Mut^+ and Mut^S phenotype by patching selected colonies first on a MM plate and then similarly on a MD plate.

The screening of His^+ transformants shows that transformation of the GS115 with *Sac* I-linearised pPIC9 (BC) and pPIC9 constructs (A-C) favoured recombination at the *AOX*1 gene. Most of the cell's alcohol oxidase activity is lost upon disruption of the *AOX*1 gene resulting in a strain that is phenotypically Mut^S. Consequently, these transformants cannot efficiently metabolise methanol as a carbon source and therefore grow poorly on MM medium (Figure 24).

3.2.2 PCR analysis of *Pichia* transformants

In order to confirm that the three different sized-KSHV ORF 4 gene had integrated into the *P. pastoris* genome, genomic DNA isolated from colonies transformed with empty pPIC9 or KCP-containing vectors was analysed by PCR with specific *AOX*1 primers.

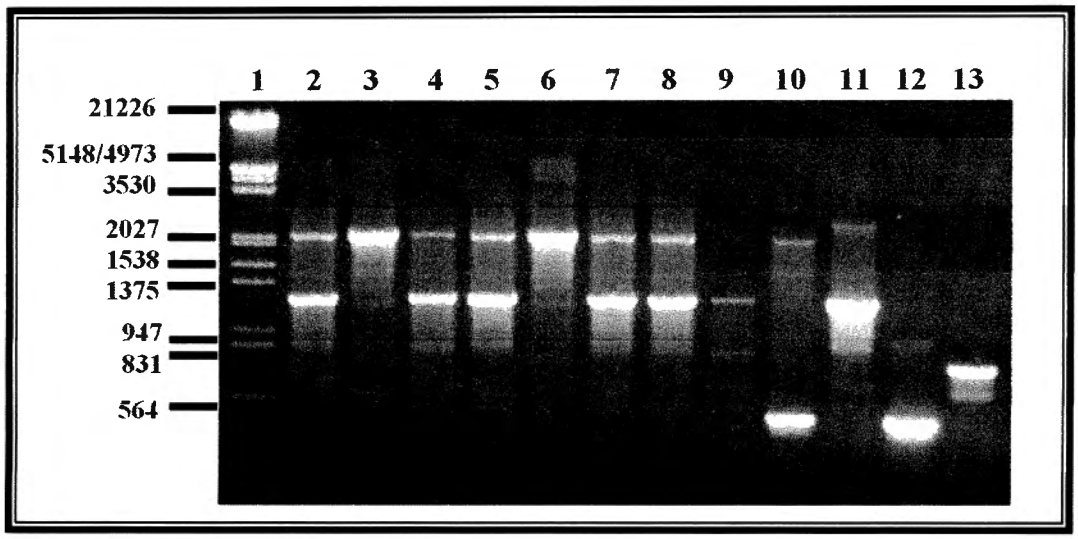

Figure 25. PCR analysis of the pPIC9/KSHV ORF 4 (735) *Pichia* transformants

Ethidium bromide stain of electrophoretically resolved [1% (w/v) agarose gel] of the isolated genomic DNA; **Lane 1:** λ DNA/*Eco* RI and *Hind* III molecular weight marker; **Lanes 2-9:** pPIC9/KSHV ORF 4 (735) *Pichia* recombinants. It can be seen that His^+ transformants in lanes 2, 4-5, 7-8 contain insert [735 bp (gene of interest) + 492 bp (from the vector) = 1227 bp DNA fragment] unlike the transformants in lanes 3 and 6. Furthermore, the recombinant in lane 9 may be a Mut^S as there is no wild-type *AOX*1 gene; **Lane 10:** GS115/pPIC9 (no insert), showing the 492 bp product and the wild-type *AOX*1 gene; **Lane 11:** pPIC9 with the gene of interest, showing the expected size of the gene of interest cloned into pPIC9 (735 bp +492 bp = 1227); **Lane 12:** pPIC9 alone, showing the 492 bp PCR product made from pPIC9 by priming with the 5' and 3' *AOX*1 primers; **Lane 13:** PCR positive control, showing the 735 bp PCR product made from the KSHV genomic DNA from PEL by priming with the 5' 03-0668 and the 3' 03-0669 primers.

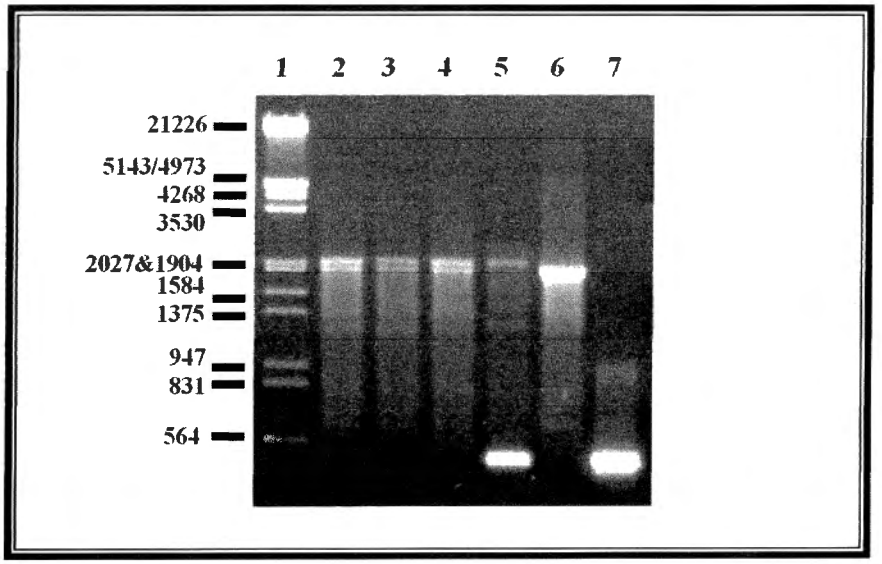

Figure 26. PCR analysis of the pPIC9/KSHV ORF 4 (1436) *Pichia* transformants

Ethidium bromide stain of electrophoretically resolved [1% (w/v) agarose gel] of the isolated genomic DNA; **Lane 1:** λ DNA/*Eco* RI and *Hind* III molecular weight marker; **Lanes 2-4:** pPIC9/KSHV ORF 4 (1436) *Pichia* recombinants, it can be seen that all the three His^+ transformants in lanes 2-4 contain insert [1436 bp (gene of interest) + 492 bp (from the vector) = 1928 bp DNA fragment] as well as the wild-type *AOX*1 gene making them Mut^+ ; **Lane 5:** GS115/pPIC9 (no insert), showing the 492 bp product and the wild-type *AOX*1 gene; **Lane 6:** pPIC9 with the gene of interest, showing the expected size of the gene of interest cloned into pPIC9 (1436 bp +492 bp = 1928); **Lane 7:** pPIC9 alone, showing the 492 bp PCR product made from pPIC9 by priming with the 5' and 3' *AOX*1 primers.

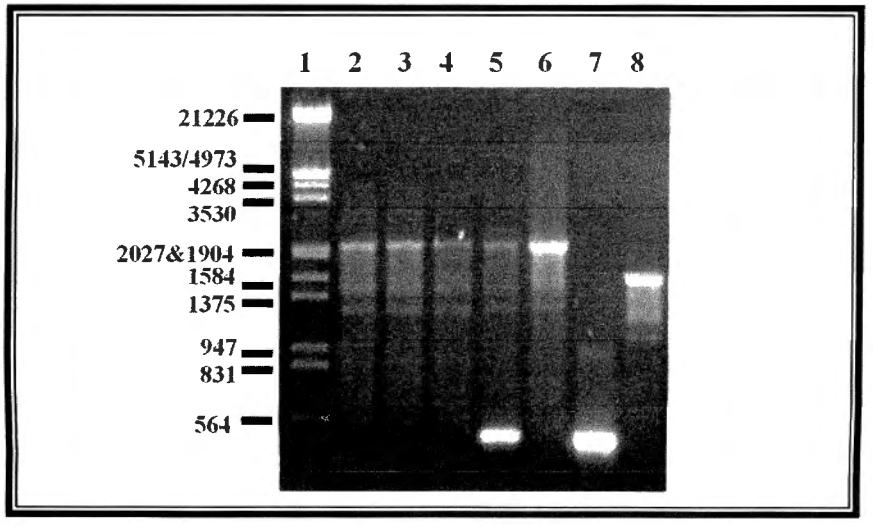

Figure 27. PCR analysis of the pPIC9/KSHV ORF 4 (1581) *Pichia* transformants

Ethidium bromide stain of electrophoretically resolved [1% (w/v) agarose gel] of the isolated genomic DNA; **Lane 1:** λ DNA/*Eco* RI and *Hind* III molecular weight marker; **Lanes 2-4:** pPIC9/KSHV ORF 4 (1581) *Pichia* recombinants. It can be seen that the His^+ transformants in lanes 2 and 3 contain insert [1581 bp (gene of interest) + 492 bp (from the vector) = 2073 bp DNA fragment] but may be Mut^S as there is no wild-type *AOX*1 gene; Lane 4, although from a His^+ transformant, does not contain the gene of interest; **Lane 5:** GS115/pPIC9 (no insert),

showing the 492 bp product and the wild-type *AOX*1 gene; **Lane 6:** pPIC9 with the gene of interest, showing the expected size of the gene of interest cloned into pPIC9 (1581 bp +492 bp = 2073 bp); **Lane 7:** pPIC9 alone, showing the 492 bp PCR product made from pPIC9 by priming with the 5' and 3' *AOX*1 primers; **Lane 8:** PCR positive control, showing the 1581 bp PCR product made from the KSHV genomic DNA from PEL by priming with the 5' 03-0668 and the 3' 03-0671 primers.

PCR products corresponding to fragments of the expected sizes of pPIC9/KSHV ORF4 (735), (1436), and (1581)-containing transformants were observed as 1227 bp, 1928 bp and 2073 bp DNA fragments as per Figures 25, 26 and 27 respectively.

3.3 Expression of Recombinant KCP in *Pichia pastoris*

Recombinant colonies with the KSHV ORF 4 gene integrated in their genomes were initially used for small-scale [5 ml] expression experiments in BMMY medium. Small-scale expression was followed by medium-scale [100 ml] production of KSHV ORF 4 proteins from recombinant *P. pastoris* colonies transformed with the three *Sac* I-digested pPIC9/KSHV ORF4 plasmid constructs. Culture media supernatants from colonies transformed with the pPIC9 empty vector digested with *Sac* I pre-and 96 h post-induction was included as a negative control in all of the protein expression experiments.

3.3.1 Optimisation of methanol-induced production of the rKCPs

The time-dependent induction of the heterologous production of the recombinant KCP proteins in *P. pastoris* [pPIC9/KSHV ORF4 (735)] (Figure 33 A), [(pPIC9/KSHV ORF4 (1436)] (Figure 34 B) and [pPIC9/KSHV ORF4 (1581)] (Figure 35 B) by addition of methanol was investigated over a period of 4 days. KSHV ORF4 proteins were first detected in the culture supernatant at 48 h post-induction and the amount of protein expressed increased after 72 and 96 h. However, the presence of these proteins at their maximal expression level was found to occur after 96 h post-induction the time at which the cells were harvested and the supernatants collected. The theoretical subunit molecular mass of the small, medium and full-length KSHV ORF 4 polypeptide as calculated from their primary amino acid sequence is 27163.5, 53901.4 and 57897.6 Da, respectively. However, the expressed proteins migrated as bands of double their theoretical molecular sizes. This higher molecular mass may be the result of posttranslational-modification of the protein by the yeast such as glycosylation of

the proteins since the primary sequence contains a number of potential *N*-linked carbohydrate sites with high probability of glycosylation (Figure 6).

3.3.2 Estimation of Protein Concentration in the Culture Media

Intensities of SDS-PAGE bands (Figure 28) were scanned with a densitometer (ChemiImager™ 5500) and the concentration of the *P. pastoris*-expressed KCP protein was qualifiedly estimated by comparison with a standard curve obtained with known amounts of protein.

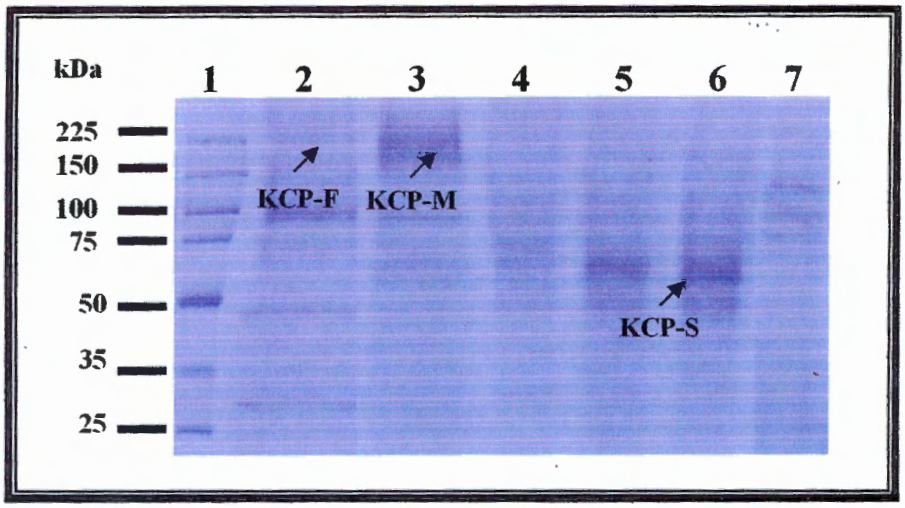

Figure 28. Coomassie-stained SDS-PAGE gel scanned with the Densiometer for estimation of protein concentration

Lane 1: Broad range protein molecular weight marker (Promega); **Lane 2:** Yeast culture supernatant showing KCP-F 96-h post-induction with methanol [30 µl loaded]; **Lane 3:** Yeast culture supernatant showing KCP-M 96-h post-induction [30 µl loaded]; **Lane 4:** Yeast culture supernatant showing KCP-S 96-h post-induction and prior to ultrafiltration; **Lanes 5 and 6:** Yeast culture supernatant showing KCP-S 96-h post-induction and post to ultrafiltration [30 µl loaded]; **Lane 7:** BC: Yeast culture supernatant of a recombinant colony transformed with pPIC9 empty vector 96-h post-induction.

Table 18. SDS-PAGE gel (Figure 29) Densiometer scan Autogrid Results

Protein Size / Name	Lane	Peak	Protein Band % Intensity	Protein Amt (ng)
150 kDa protein std	1	2	8.8	200 ng x 0.088= 17.6
225 kDa protein std	1	1	11.2	200 ng x 0.112 = 22.4
100 kDa protein std	1	3	11.4	200 ng x 0.114 = 22.8
75 kDa protein std	1	4	12.2	200 ng x 0.122 = 24.4
25 kDa protein std	1	7	13.0	200 ng x 0.130 = 26

35 kDa protein std	1	6	18.3	200 ng x 0.183 = 36.6
50 kDa protein std	1	5	25.2	600 ng x 0.252 = 151.2
KCP-S	8	3	75.5	X_1
KCP-M	5	1	96.0	X_2
KCP-F	2	1	26.4	X_3

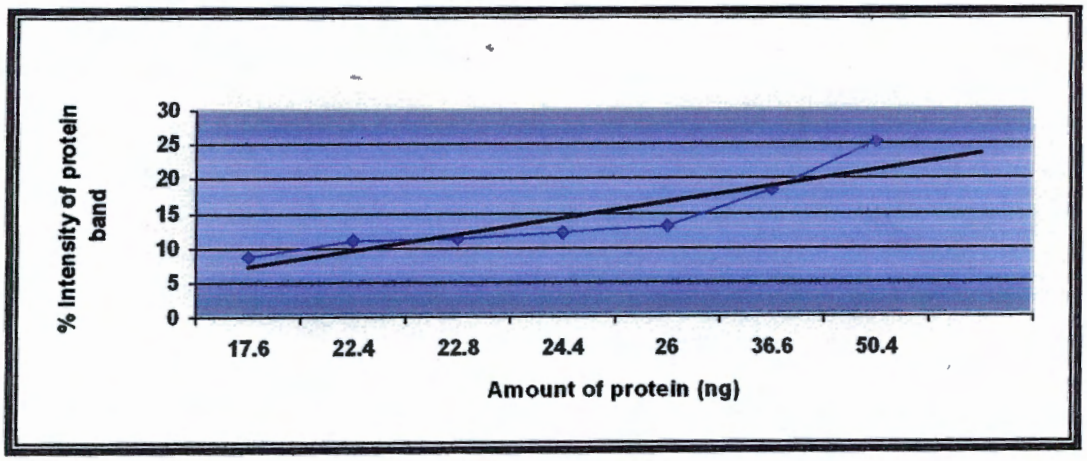

Figure 29. Standard Curve used to estimate the concentration of the expressed KCPs present in the culture media

The concentration of the *P. pastoris*-expressed KCP proteins was quantitively estimated by comparison with a standard curve obtained with known amounts of protein standards. The slope of the curve (m) was found to be 0.5.

The unknown protein concentrations were directly determined by use of the following equations:

$$\mathbf{m = Y_2 - Y_1 / X_2 - X_1} \quad \text{or} \quad \mathbf{Y = mX + c}$$

Where, $c = 0$

Therefore, [KCP-S]: $75.5\ \% = 0.5 \times X_1 + 0$ therefore, $X_1 = 151$ ng

$\therefore$ 151 ng in 30 µl → 5033 ng in 1000 µl $\therefore$ [KCP-S] = 5033 ng/ml = 5µg/ml

Similarly, under these calculations, the yield of *P. pastoris* expressed KCP-M (X_2) and KCP-F (X_3) was about 6.4 and 1.76 µg per millilitre of yeast culture medium respectively. This protein concentration estimation correlates with the fact that the first two recombinant proteins, KCP- S and M were obtained from medium-scale expression [100 ml] whereas the last one, KCP-F shown here and used throughout the project was obtained from a small-scale experiment [5 ml].

3.3.3 Small-scale Ammonium Sulphate Protein Precipitation

SDS-PAGE analysis revealed that the rKCP-S and -F recombinant proteins precipitated to some degree at all ammonium sulphate saturation levels, while the best rKCP precipitation yield was reached at 80-90% ammonium sulphate saturation level (Figure 30). The precipitated proteins from the media were redissolved in 50 µl of saline (0.9% NaCl) and were used in the hemolysis assay to determine whether the expressed proteins are biologically active.

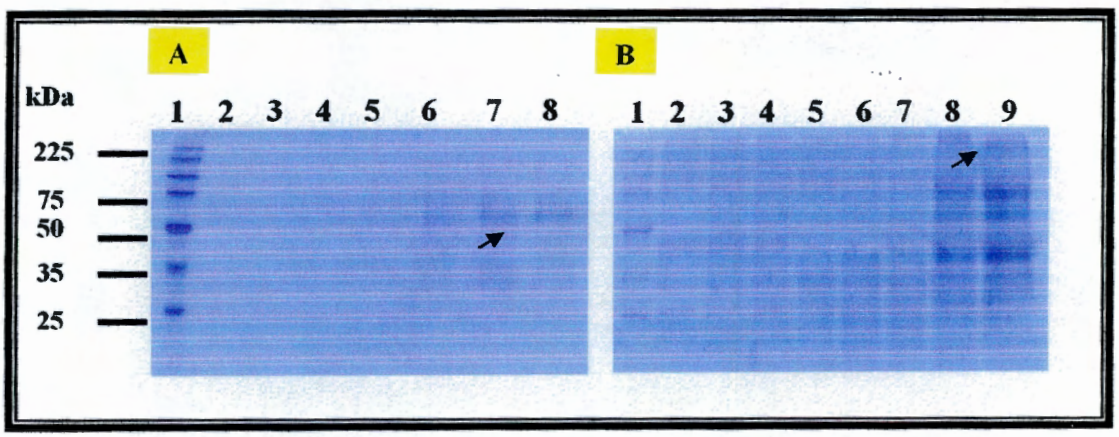

Figure 30. SDS-PAGE Analysis of rKCPs Precipitated from the Supernatant with Saturated Ammonium Sulphate

Figure 30A: Lane 1: Broad range protein molecular weight marker; **Lanes 2-8:** precipitates prepared from cultured supernatants [500 µl] of recombinant strain [pPIC9/KSHV ORF4 (735bp)] with 30, 40, 50, 60, 70, 80 and 90 % saturated ammonium sulphate, respectively. **Figure 30B: Lane 1:** Broad range protein molecular weight marker [225, 150, 100, 75, 50, 35 and 25 kDa (from top to bottom)]; **Lanes 2-9:** precipitates prepared from cultured supernatants [1 ml] of recombinant strain [pPIC9/KSHV ORF4 (1581bp)] with 20, 30, 40, 50, 60, 70, 80 and 90 % saturated ammonium sulphate, respectively. Arrows indicate maximal level of precipitated protein of interest.

3.4 Synthesis of a Polyclonal Anti-KCP Peptide Antibody

Upon selection of a suitable KCP peptide sequence common to all three different sized KCPs, the sequence was forwarded to a Brazillian research group, who kindly synthesised the peptide. Five milligrams of the chemically synthesised peptide was coupled to KLH and used to produce the polyclonal anti-KCP peptide antibody in rabbits.

3.4.1 HiTrap protein A purification of the anti-KCP Antibody

Protein A that is derived from a strain of *Staphylococcus aureus,* contains five regions that bind to the Fc region of IgG. As an affinity ligand, protein A is immobilized to sepharose so that these regions are free to bind. One molecule of immobilized protein A can bind at least two molecules of IgG. SDS-PAGE analysis revealed that the polyclonal anti-KCP peptide antibody and other IgGs were successfully purified from the serum sample (starting material) using a protein-A sepharose column. Under reducing conditions, the interchain disulfide bonds of an IgG molecule are split and if the sulfhydyl groups are blocked, two heavy chains (molecular weight 50 kDa each) and two light chains (25 kDa each) are formed as shown by the eluted fractions in Figure 31, lanes 5-9.

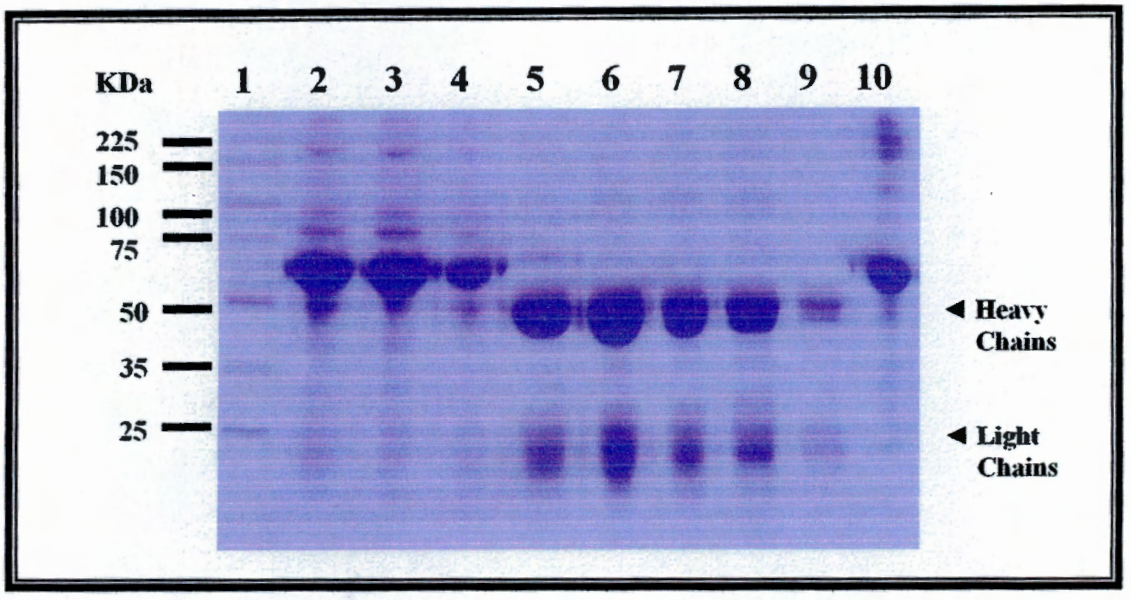

Figure 31. SDS-PAGE Analysis of the Anti-KCP Antibody Purification Stages

Lane 1: Broad range protein molecular weight marker [225, 150, 100, 75, 50, 35, 25 kDa (from top to bottom)]; **Lane 2:** Starting material: serum containing the antibody of interest prior binding to the column; **Lane 3:** Flow through: serum post binding and prior to purification; **Lane 4:** First [20 mM sodium phosphate buffer (pH 7.0)] wash out of 6 total washes; **Lanes 5-9:** Third-seventh [0.1 M citric acid (pH 3.0)] elutions respectively; **Lane 10:** BSA (2 mg/ml) used as a quantitive protein control.

3.4.2 Bio-Rad Antibody Quantification Microassay

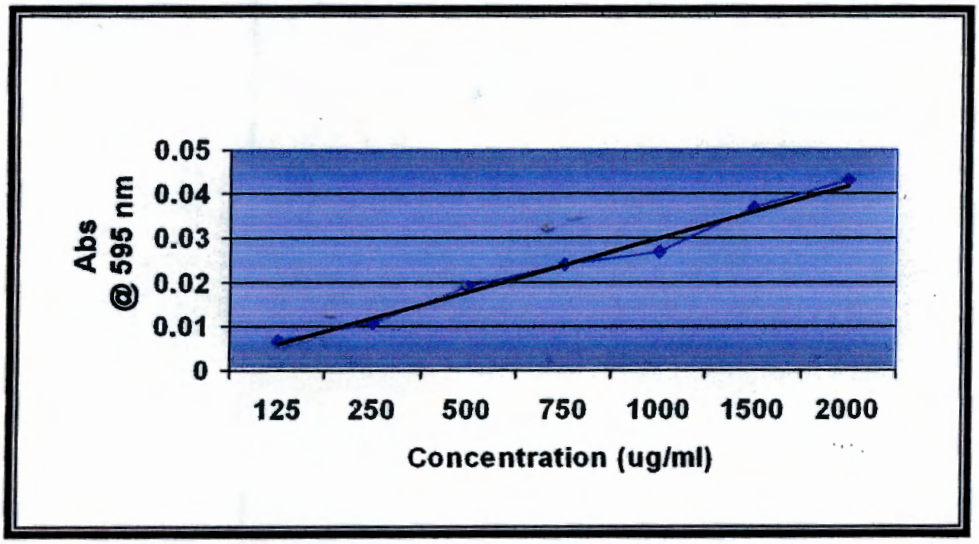

Figure 32. BSA Standard Curve used to Determine Anti-KCP Antibody Concentration

The A_{595} readings of the standards were plotted against the known BSA concentrations and a standard curve was generated. The microplate reader (Anthos 2010) evaluation results revealed that the standard curve was 98.7% accurate and that the slope of the curve (m) was 1.89×10^{-5}, which was used in the equation described below.

The unknown antibody concentrations of the purified fractions were directly determined by use of the following equation:

$$m = Y_2 - Y_1 / X_2 - X_1 \quad \text{or} \quad Y = mX + c$$

Where, c = 0.00744

The purified antibody concentration of elution fractions 3-6 (Figure 31, lanes 5-8) was 3303 µg/ml, 10484 µg/ml, 5468 µg/ml and 2934 µg/ml respectively.

3.5 Immunological Detection, SDS-PAGE and Western Blot Analysis of the rKCP proteins

Expression of the viral proteins was confirmed by slot-blot serological analysis after blotting 100 µl of culture media supernatant onto nitrocellulose Hybond-ECL membranes. Western blot analysis with the rabbit polyclonal antibody directed against a selected KSHV ORF 4 peptide (Figure 11) showed that the *P. pastoris*-heterologously expressed soluble-, medium- and full-length KCPs migrated

electrophoretically as higher bands which most likely is due to glycosylation of the proteins as in addition to the presence of potential *N*- and *O*-linked carbohydrate sites in the protein's primary sequence, diffused bands were obtained in all the westerns carried out, which is characteristic of glycoproteins. The time-course of expression of the KCP-S and KCP-M protein was also followed by Western blot analysis, which showed that the protein could be first detected at 48 h post-induction and the amount of protein built up after 72 and 96 h (Figure 33B and 34C).

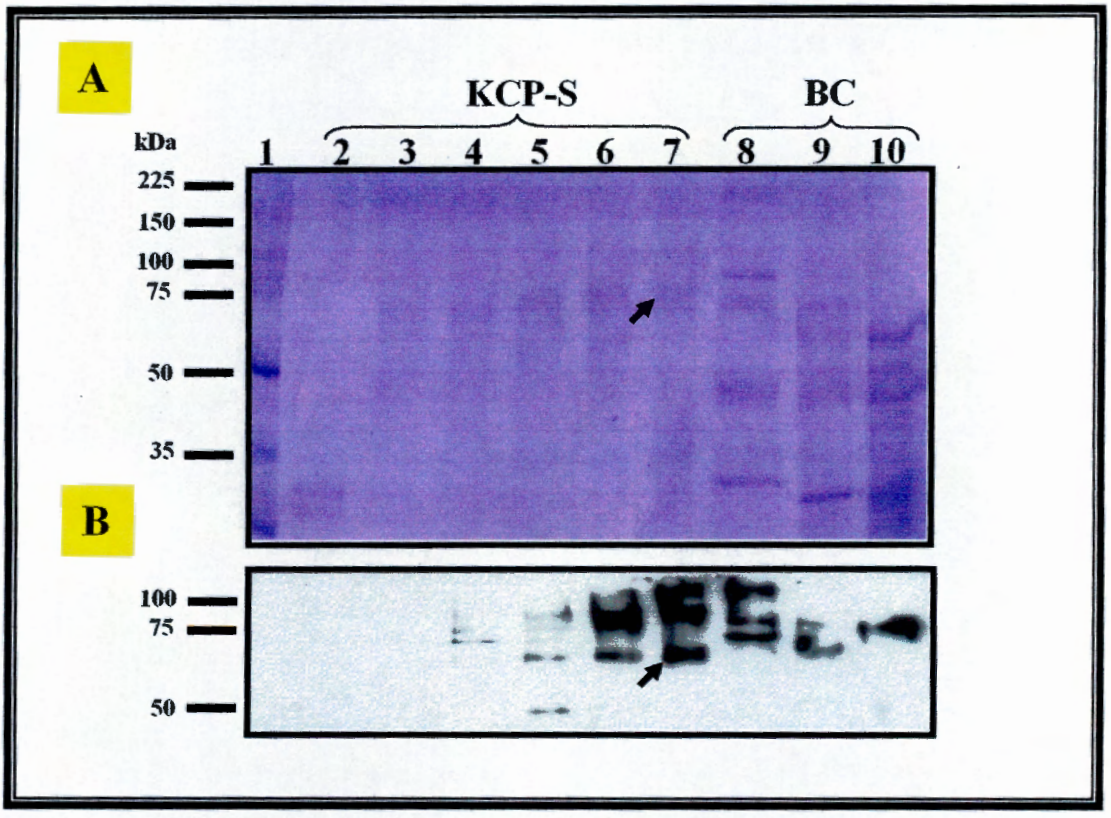

Figure 33. Expression and Detection of the Recombinant KCP – S protein

Figures 33A: Coomassie-stained SDS-PAGE gel of the induction profile of the KSHV ORF 4-S recombinant protein. **Lane 1:** Broad range protein molecular weight marker; **Lane 2:** supernatant before induction; **Lane 3:** 24 h post-induction; **Lane 4:** 48 h post-induction; **Lane 5:** 72 h post-induction; **Lane 6:** 96 h post-induction; **Lane 7:** 96 h post-induction concentrated supernatant using the pellicon XL device; **Lane 8:** BC pre-induction; **Lane 9:** BC 72 h post-induction; **Lane 10:** BC 96 h post-induction. **Figure 33B:** Western Blot detection of the expression profile using rabbit anti-KCP peptide polyclonal antibody. In addition to the protein of interest, the antibody recognised several larger and smaller bands that may represent multimer aggregates and degradation products respectively. The time-course expression of the protein was monitored every 24 h from 0 to 96 h (lanes 2-6) after induction, loading 30 µl of clarified supernatant per well. Arrows indicate maximal level of protein.

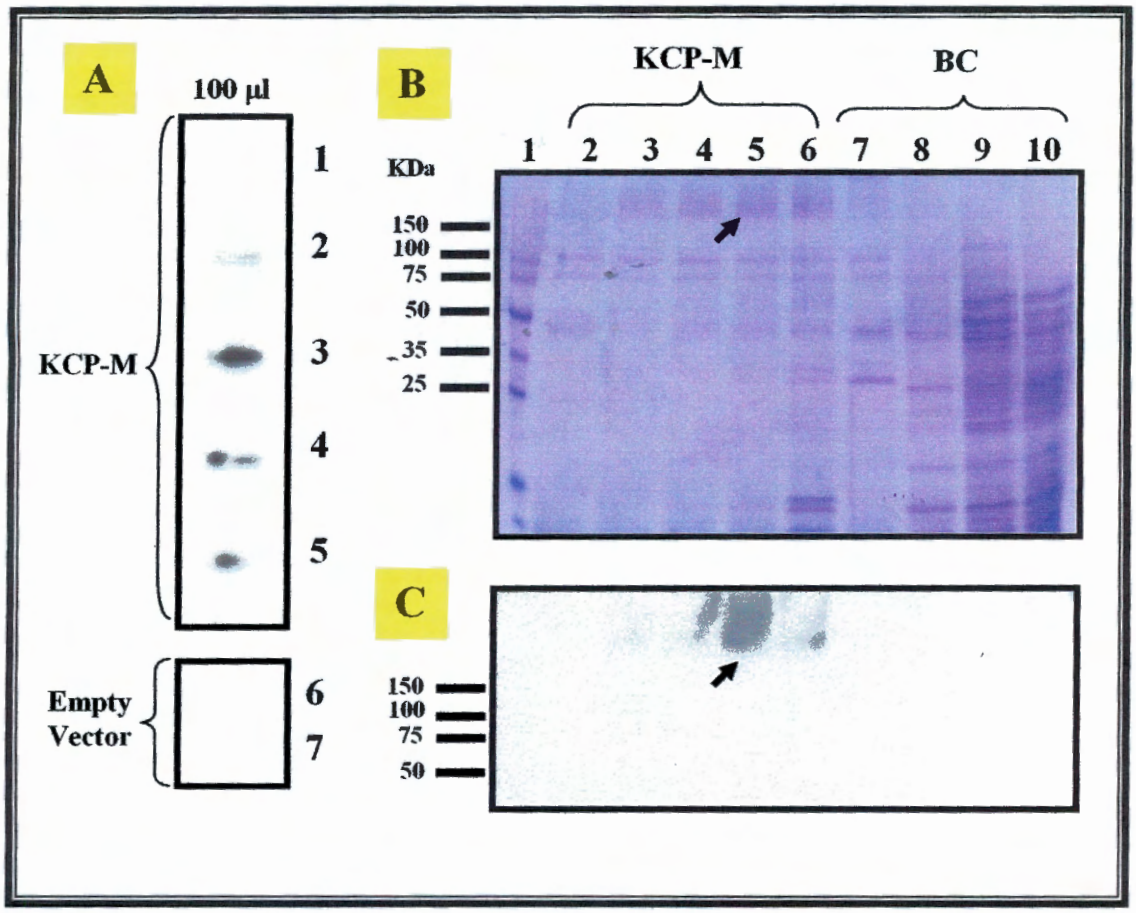

Figure 34. Expression and Detection of the Recombinant KCP – M protein

Figure 34A: Slot-blot incubated with rabbit anti-KCP peptide polyclonal antibody, after medium-scale KCP-M protein expression with a *P. pastoris* recombinant colony, obtained upon transformation with *Sac* I-digested pPIC9/KSHV ORF4 (1436 bp) DNA construct. 100 µl of supernatant from the pre-induction sample (row 1) and from the different time-points post-induction (rows 2-5) were blotted as indicated. Equal volumes of supernatant of a recombinant colony transformed with *Sac* I-digested pPIC9 empty vector (BC) pre-induction (row 6) and 96 h post-induction (row 7) samples were also included. **Figures 34B:** Coomassie-stained SDS-PAGE gel of the induction profile of the KCP-M recombinant protein. **Lane 1:** Broad range protein molecular weight marker; **Lane 2:** supernatant before induction; **Lane 3:** 24 h post-induction; **Lane 4:** 48 h post-induction; **Lane 5:** 72 h post-induction; **Lane 6:** 96 h post-induction; **Lane 7:** BC before induction; **Lane 8:** BC 48 h post-induction; **Lane 9:** BC 72 h post-induction; **Lane 10:** BC 96 h post-induction. **Figure 35C:** Western Blot detection of the expression profile using rabbit polyclonal anti-KCP peptide antibody. The time-course expression of the protein was monitored every 24 h from 0 to 96 h (lanes 2-6) after induction, loading 30 µl of clarified supernatant per well. Arrows indicate maximal level of protein.

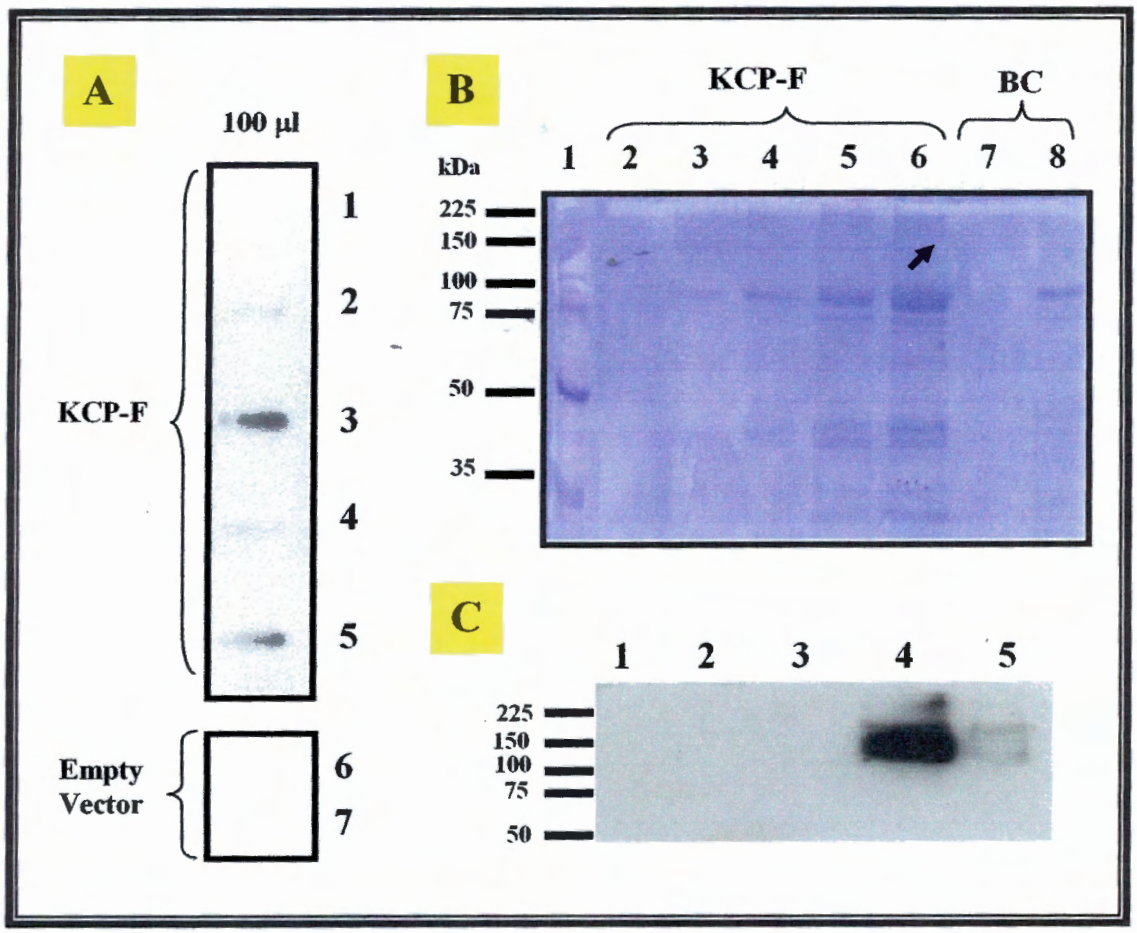

Figure 35. Expression and Detection of the Recombinant KCP – F protein

Figure 35A: Slot-blot incubated with anti-KCP peptide polyclonal antibody, after medium-scale KSHV ORF 4-F protein expression with a *P. pastoris* recombinant colony, obtained upon transformation with *Sac* I-digested pPIC9/KSHV ORF4 (1581 bp) DNA construct. 100 µl of supernatant from the pre-induction sample (row 1) and from the different time-points post-induction (rows 2-5) were blotted as indicated. Equal volumes of supernatant of a recombinant colony transformed with *Sac* I-digested pPIC9 empty vector (BC) pre-induction (row 6) and 96 h post-induction (row 7) samples were included. **Figures 35B:** Coomassie-stained SDS-PAGE gel of the KSHV ORF4-F recombinant protein induction profile. **Lane 1:** Broad range protein molecular weight marker; **Lane 2:** supernatant before induction; **Lane 3:** 24 h post-induction; **Lane 4:** 48 h post-induction; **Lane 5:** 72 h post-induction; **Lane 6:** 96 h post-induction; **Lane 7:** BC before induction; **Lane 8:** BC 96 h post-induction. **Figure 35C:** Western Blot detection of the KCP-F in a different media using anti-KCP peptide polyclonal antibody. **Lane 1:** Broad range molecular weight marker; **Lane 2:** supernatant before induction [20 µl]; **Lane 3:** 72 h post-induction [20 µl]; **Lane 4:** 72 h post-induction (100 µl concentrated with the speedvac); **Lane 5:** KCP-M 96 h post-induction supernatant used as a positive control for Western blot analysis.

3.6 Functional and Structural Analysis of the Expressed rKCPs

3.6.1 Recombinant KCP-S protein is Functional

All three recombinant KSHV ORF 4 proteins expressed in the yeast, *Pichia pastoris*, were tested for biological activity by determining their ability to inhibit complement-mediated lysis of ssRBCs (Figure 36). The results show that the ammonium-sulphate precipitated-supernatant from a *Pichia* culture transformed with pPIC9/KCP-S contained a functional regulator of human complement capable of binding complement proteins in a concentration-dependent fashion as 1 µl, 2 µl and 4 µl caused 12.3%, 36.85, and 82.5 % complement inhibition respectively as depicted in Figure 36.

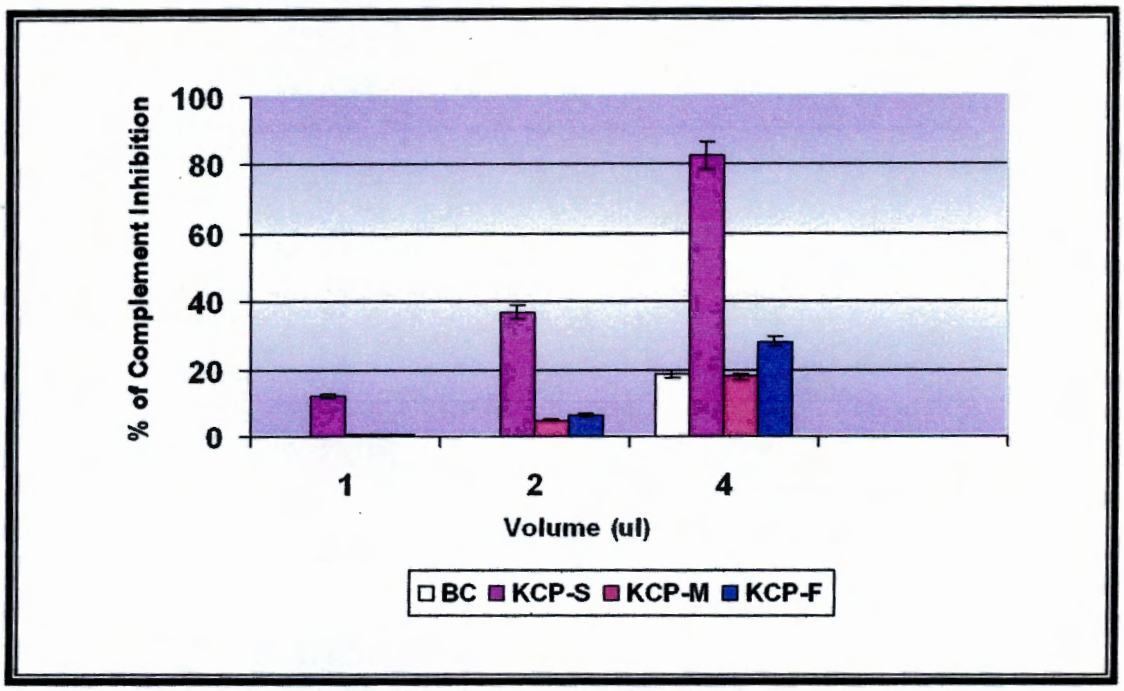

Figure 36. Inhibition of the classical pathway-mediated Lysis of ssRBC by rKCP

Supernatants from cultured recombinant (KCP-S, -M and –F) and control (BC) strains were tested for biological activity by determining their ability to inhibit complement classical pathway-mediated lysis of antibody-coated sheep erythrocytes.

3.6.2 Truncated KCP-S Protein is *N*-Glycosylated

Protein motif search engines were used to confirm the presence of 15 potential *N*-glycosylation sites in the conceptually translated primary sequence of the KSHV ORF 4 (Figure 6). To examine the recombinant KCP-S for *N*-linked glycosylation, the

enzyme that releases asparagine-linked oligosaccharides from glycoproteins (Figure 12). The results show a shift in molecular weight between treated and untreated KCP-S from 56 kDa to approximately 27 kDa, the protein's theoretical molecular weight (Figure 37), indicating the presence of functional *N*-glycosylation sites in this heterologously expressed truncated protein.

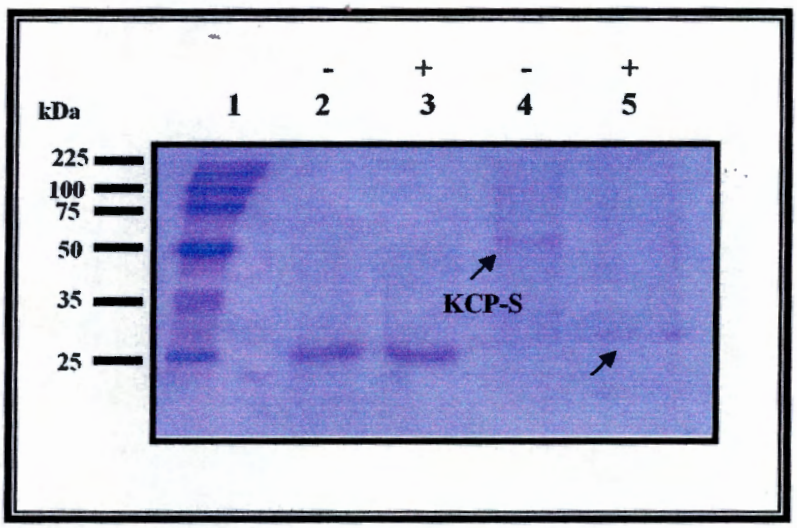

Figure 37. SDS-PAGE Analysis of Enzymatic Deglycosylation with PNGase F shows that truncated KCP is *N*-glycosylated

Coomassie-stained SDS-PAGE gel of the PNGase F enzyme digestion of the KCP-S. **Lane 1:** Broad range protein molecular weight marker; **Lane 2 and 3:** VCP from the WR strain which does not contain any *N*-linked carbohydrate sites was used as a PNGase F deglycosylation negative control; **Lane 4:** supernatant of culture from pPIC9/KSHV ORF 4 (735 bp) recombinant strain; **Lane 5:** supernatant of culture from pPIC9/KSHV ORF 4 (735bp) recombinant strain after incubation with PNGase F. Plus (+) and negative (-) symbols indicate with and without PNGase F treatment respectively.

3.7 Immunohistochemical Studies of KS Tissues with Polyclonal Anti-KCP Peptide Antibody

3.7.1 Pre-Immune and Antibody Controls of Immunostaining

The results acquired for the antibody control were successful as no specific immunostaining of the cells took place in the absence of both the primary and the secondary antibody (Figure 38).

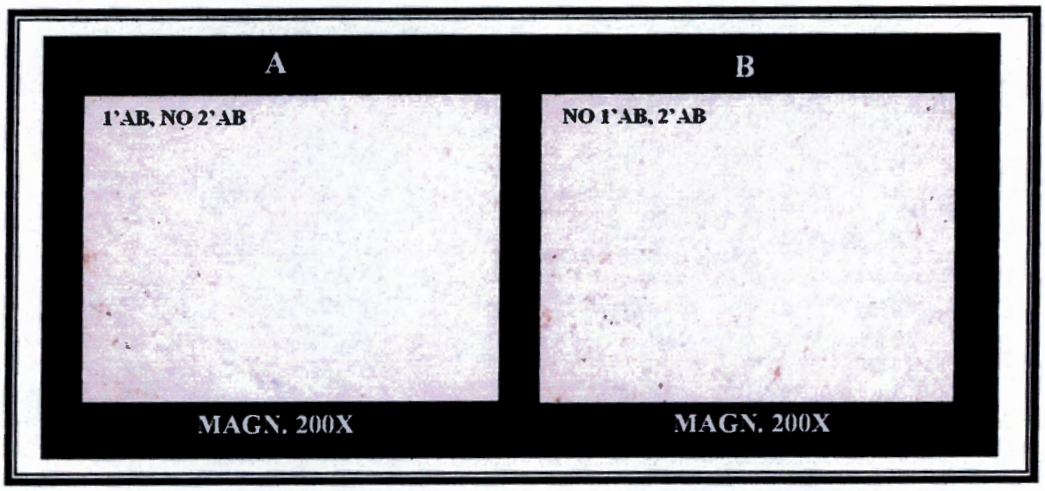

Figure 38. The Primary and Secondary Controls showed no specific staining
Paraffin-embedded nodular Kaposi's sarcoma tissue section (case no.6587/01 $A1^{SK}$) were cut at 2-4 μm, mounted on APES-coated slides and heat fixed on a hot-plate at approximately 75°C for 30 min. **Figure 38A:** Following tissue fixation, the section underwent immunostaining by incubation with anti-KCP primary antibody but no specific secondary antibody. **Figure 38B:** Same as for figure 38A for the exception that the section was incubated with secondary antibody only and no primary antibody. Tissue sections were counterstained with haematoxylin, dehydrated, mounted in Entellan and visualised using light microscopy techniques. 1' and 2' refers to primary and secondary antibodies respectively.

Likewise, the results obtained for the pre-immune control, which is the rabbit's serum before being exposed to the antigen of origin were also successful. The background immunostaining detected for the pre-immune staining was not as intense as that of the antibody immunostaining particularly post sepharose protein-A-clean up of the IgG used in this study as per section 2.4.2. In addition, the staining was rather ubiquitous as opposed to the more defined staining patterns observed with the antibody immunostaining (Figure 39).

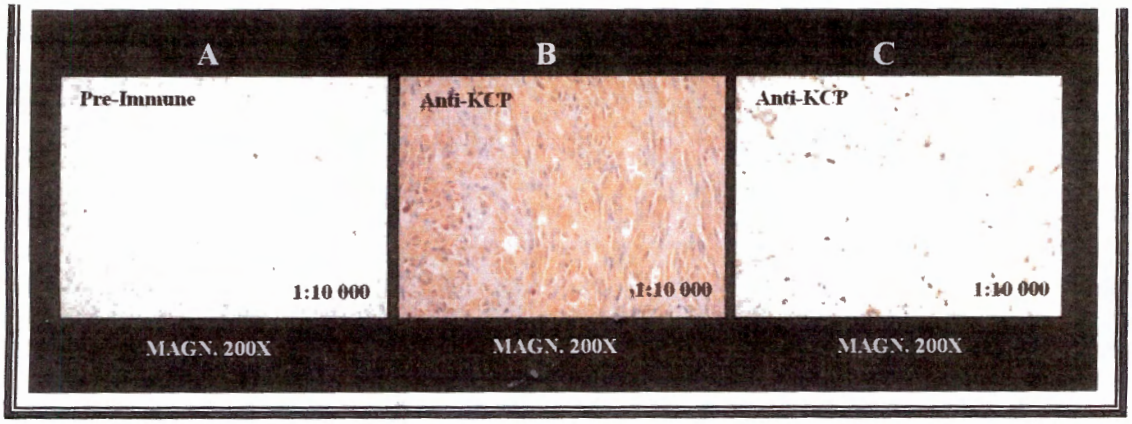

Figure 39. The pre-immune control indicates that the staining obtained with the anti-KCP primary antibody is more specific

Paraffin-embedded nodular Kaposi's sarcoma tissue section (case no.6587/01 $A1^{SK}$) were cut at 2-4 µm, mounted on APES-coated slides and heat fixed on a hot-plate at approximately 75°C for 30 min. **Figure 39A:** Following tissue fixation, the section underwent immunostaining by incubation with pre-immune serum followed by incubation with peroxidase-conjugated goat anti-rabbit secondary antibody. **Figure 39B:** Same as for Figure 39A, for the exception that the section was incubated with anti-KCP primary antibody before sepharose protein-A-clean up of the IgG. **Figure 39C:** Same as for Figure 39B for the exception that the section was incubated with anti-KCP primary antibody post to sepharose protein-A-clean up of the IgG.

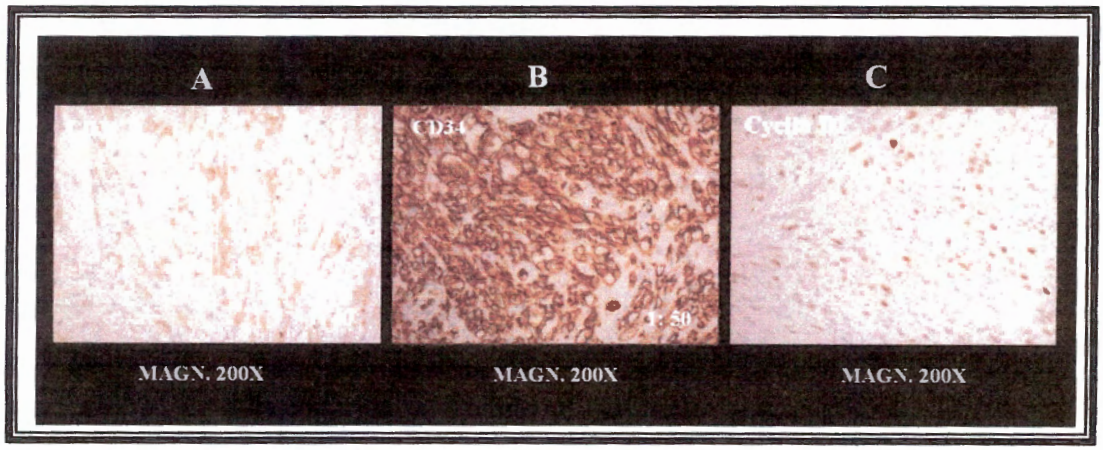

Figure 40. Positive Controls showing expected Immunostaining of the KS tissue

Paraffin-embedded nodular Kaposi's sarcoma tissue section (case no.6587/01 $A1^{SK}$) were cut at 2-4 µm, mounted on APES-coated slides and heat fixed on a hot-plate at approximately 75°C for 30 min. **Figure 40A:** Following tissue fixation, the section underwent immunostaining by incubation with monoclonal mouse anti-human CD31, an antibody which predominantly displays staining of the cell membrane, followed by incubation with peroxidase-conjugated goat anti-mouse secondary antibody.

mouse anti-CD34, which as anti-CD31, it is primarily used to label endothelial cells but unlike anti-CD31, it strongly stains the endothelial cell cytoplasm. **Figure 40C:** Same as for Figure 40A, for the exception that the section was incubated with anti-Cyclin D1 as a positive control for nuclear staining. Tissue sections were counterstained with haematoxylin, dehydrated, mounted in Entellan and visualised using light microscopy techniques.

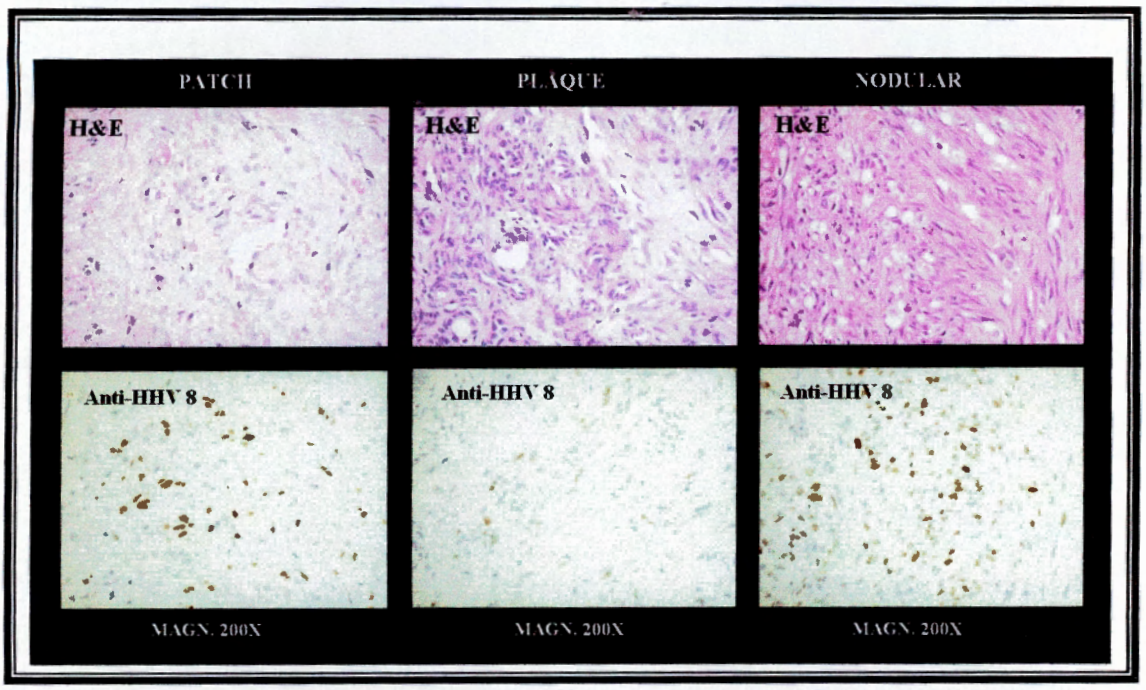

Figure 41. Different Stages of KS displaying HHV 8 Nuclear Positivity in the Lesional Spindle Cells

Paraffin-embedded patch (case no. 1418/03 B1), plaque (case no. 13132/99A1) and nodular (case no. 12362/02 A1) Kaposi's sarcoma tissue sections were cut at 2-4 μm, mounted on APES-coated slides and heat fixed on a hot-plate at approximately 75°C for 30 min. Following tissue fixation, the sections underwent immunostaining by incubation with mouse anti-LANA monoclonal antibody, followed by incubation with peroxidase-conjugated goat anti-mouse secondary antibody. Tissue sections were counterstained with haematoxylin, dehydrated, mounted in Entellan and visualised using light microscopy techniques.

3.7.2 Immunohistochemical Detection of Endogenous KCP Protein in Kaposi's sarcoma

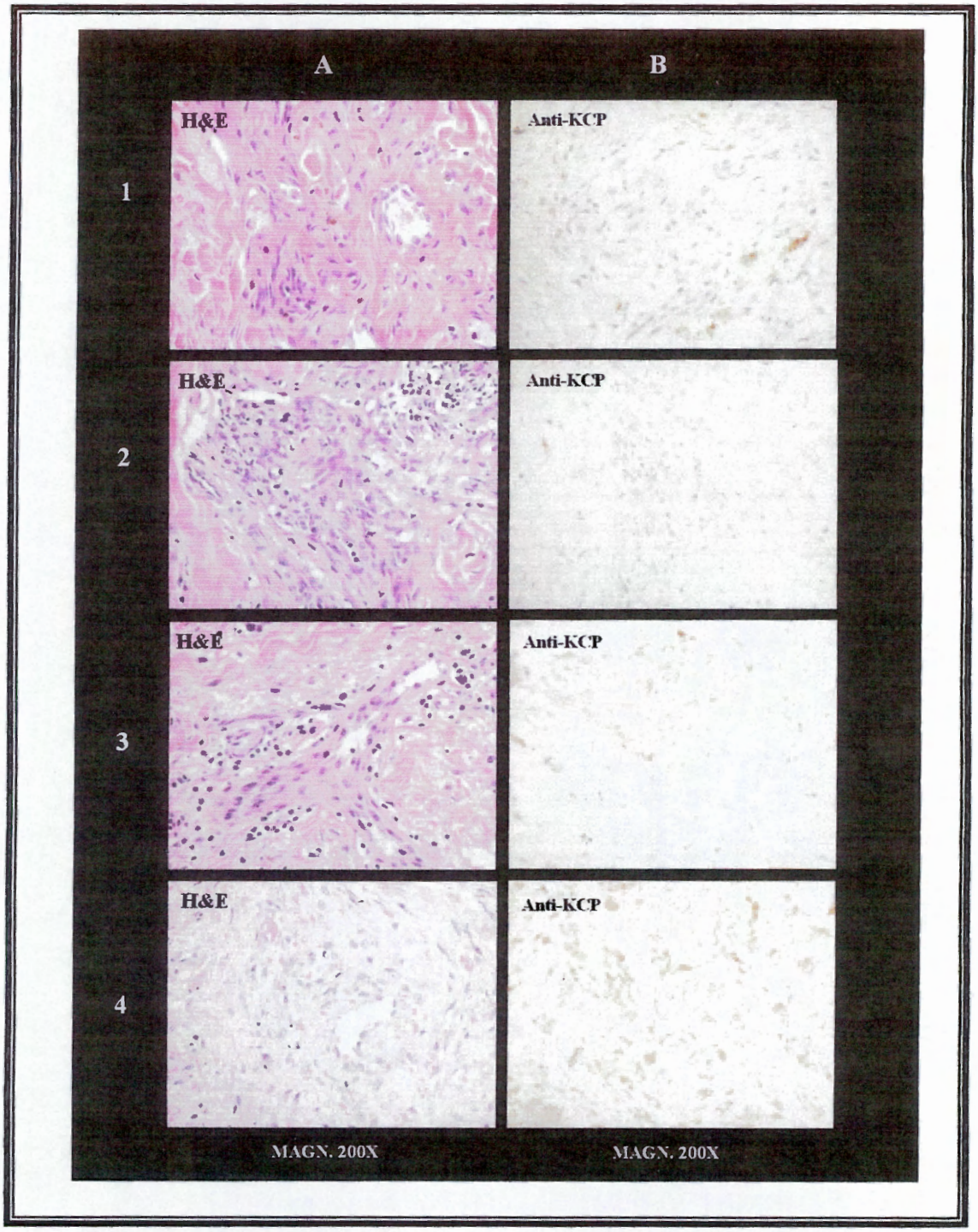

Figure 42. Immunohistochemical Analysis of Various Early Patch Stage KS with anti-KCP Peptide Primary Antibody (Immunoperoxidase, 200x)

Paraffin-embedded patch Kaposi's sarcoma tissue sections (**1:** case no. 13360/99A1; **2:** 8230/00; **3:** 1835/01A1; **4:** 1418/03B1) were cut at 2-4 μm, mounted on APES-coated slides and heat fixed on a hot-plate at approximately 75°C for 30 min. **Figure 42A:** Cellular morphology by H&E staining of the

early patch stage KS tissue sections showing jagged vascular channels, elongated spindle cells lining clear slit-like spaces and permeating through dermal collagen bundles, small degree of inflammation and red blood cells; **Figure 42B:** Post tissue fixation, these sections underwent immunostaining by incubation with polyclonal rabbit anti-KCP primary antibody, followed by incubation with peroxidase-conjugated goat anti-rabbit secondary antibody. Tissue sections were counterstained with haematoxylin, dehydrated, mounted in Entellan and visualised using light microscopy techniques.

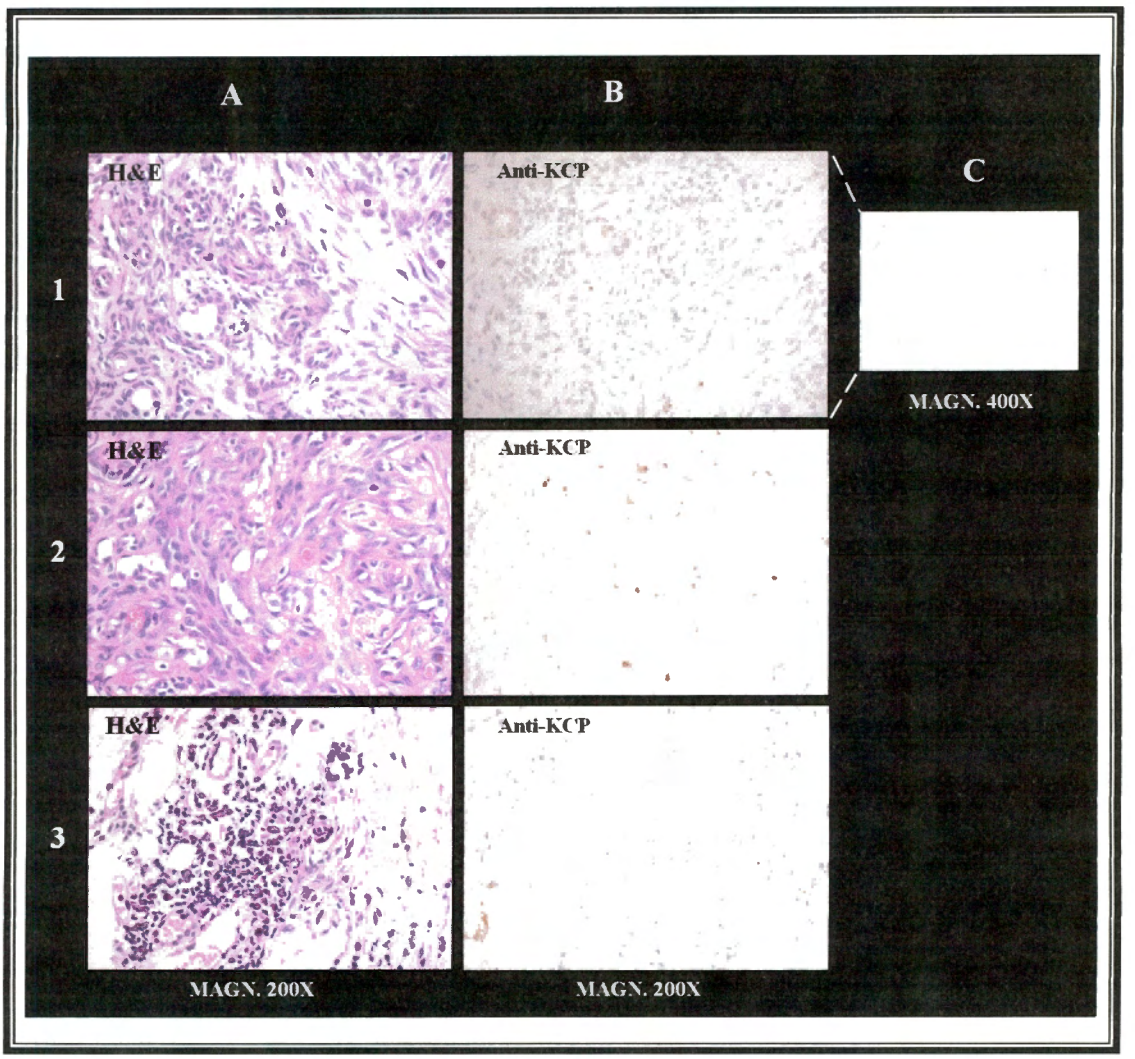

Figure 43. Immunohistochemical Analysis of Various Intermediate Plaque Stage KS with anti-KCP Peptide Primary Antibody (Immunoperoxidase, 200x)

Paraffin-embedded plaque Kaposi's sarcoma tissue sections (**1:** case no. 13132/99A1; **2:** 7973/02A1; **3:** 12830/00A1) were cut at 2-4 µm, mounted on APES-coated slides and heat fixed on a hot-plate at approximately 75°C for 30 min. **Figure 43A:** Cellular morphology by H&E staining of the intermediate plaque stage KS, showing a greater number of elongated spindle cells when compared to the early stage, dilated lymphatics, lymphocytes and plasma cells at the site of proliferation and a small number of erythrocytes can also be visualised. **Figure 43B:** Post tissue fixation, these sections underwent immunostaining by incubation with polyclonal rabbit anti-KCP primary antibody, followed by incubation with peroxidase-conjugated goat anti-rabbit secondary antibody. **Figure 43C:** Same as Figure 43B case 1 at a higher magnification showing possible endothelial staining.

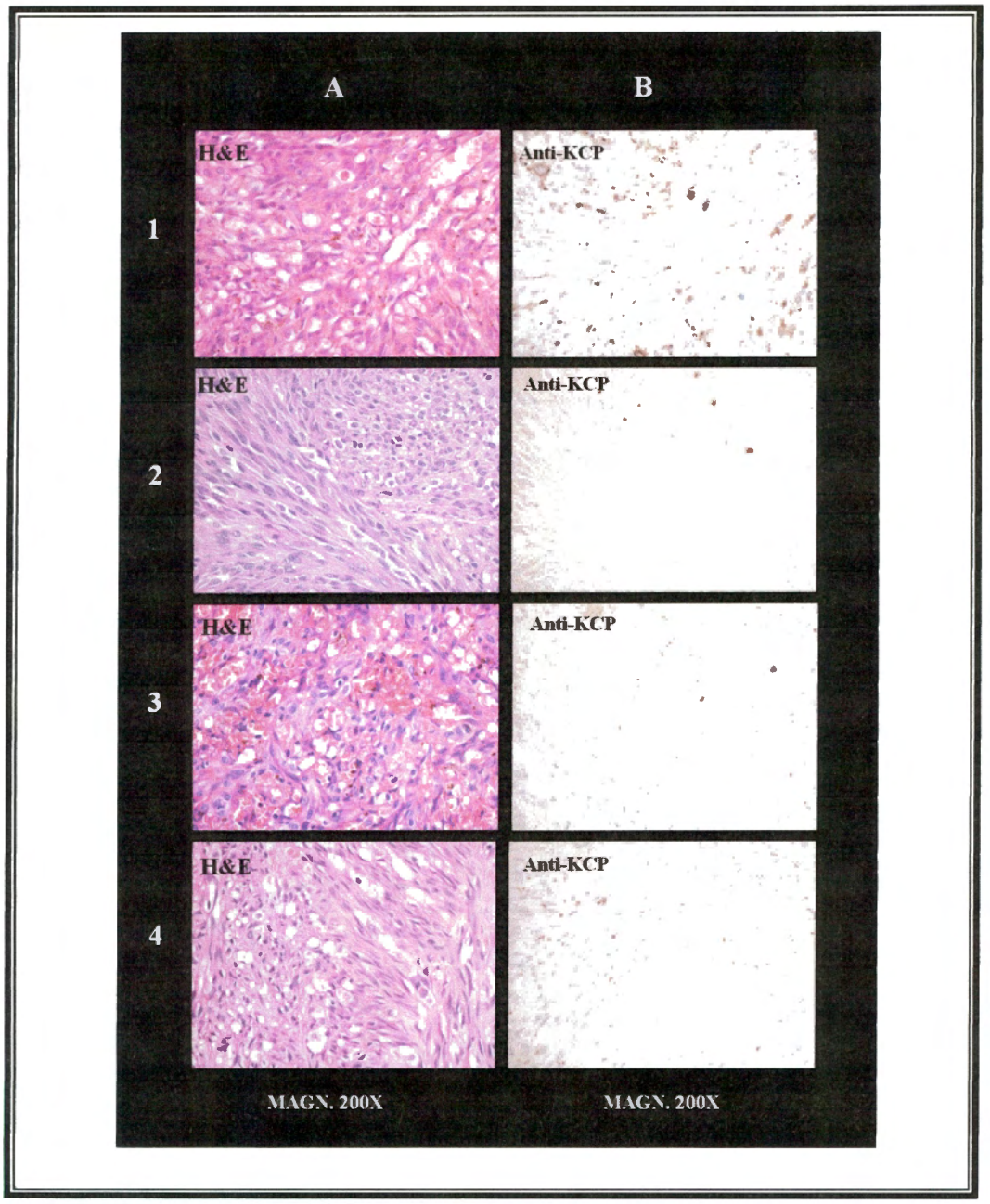

Figure 44. Immunohistochemical Analysis of Various Late/Advanced Nodular Stage KS with anti-KCP Peptide Primary Antibody (Immunoperoxidase, 200x)

Paraffin-embedded nodular Kaposi's sarcoma tissue sections (**1:** case no. 6587/01A1; **2:** 1182/01A1; **3:** 7973/02; **4:** 12362/02) were cut at 2-4 µm, mounted on APES-coated slides and heat fixed on a hot-plate at approximately 75°C for 30 min. **Figure 44A:** Cellular morphology by H&E staining of the advanced nodular stage KS tissue sections, showing fascicular growth of the more rounded-shaped spindle cells, more prominent lymphocytic infiltrates, the presence of light eosinophilic, hyaline bodies both within and between the tumour cells. Large deposits of hemosiderin can also be seen. **Figure 44B:** Post tissue fixation, these sections underwent immunostaining by incubation with polyclonal rabbit anti-KCP primary antibody, followed by incubation with peroxidase-conjugated goat anti-rabbit secondary antibody. Tissue sections were counterstained with haematoxylin, dehydrated, mounted in Entellan and visualised using light microscopy techniques.

CHAPTER FOUR

DISCUSSION

4.1 Immunohistochemical Detection of the KCP Protein in Kaposi's sarcoma

Finding a cure against HIV and a means of alleviating the pain of those infected as well as improving their quality of life is presently a national priority in South Africa. It is a known fact that often other opportunistic pathogens such as KSHV are the leading cause of death of highly immunosuppressed individuals, particularly amongst AIDS patients. KSHV causes Kaposi's sarcoma (KS), an angiogenic skin lesion originating from the tumour of endothelial cells, which has been recognized as one of the most abundant tumours found in many parts of Southern Africa and which can occasionally become highly invasive and aggressive, and capable of causing death. Apart from KS, other proliferative diseases unmistakably related to KSHV infection include some plasma cell forms of Multicentric Castleman's Disease (MCD) which is a B-cell lymphoproliferative disorder, and a body cavity-based or primary effusion lymphoma (BCBL or PEL) which also infects B-cells (Moore and Chang, 2001).

The complement system, which is part of the innate immune defence system, is composed of a group of serum proteins that interact with each other in a cascade-type reaction causing the splitting of subsequent proteins into fragments (Walport, 2001). The powerful nature of the complement system, either in the presence or absence of antibodies, can lead to virus neutralization and opsonisation, lysis of virus-infected cells and amplification of inflammatory and specific immune responses (Blom, 2004). Considering the potentially destructive nature of the complement proteins which do not have the ability to differentiate between self and non-self tissue and therefore destroy any cell including host cells (Sahu and Lambris, 2001), the host tissue have specific inhibitors/regulators of the complement system on their cell surface. Viruses are obligate intracellular parasites and ultimately depend on the cell machinery of the host to survive and propagate. Since the complement proteins implicated in the cascade activation process are not able to discriminate between self and non-self,

viruses are highly vulnerable to the complement system. Therefore, during co-evolution, viruses such as KSHV have developed and acquired clever strategies to overcome the complement system of the host in order to succeed as pathogens (Spiller *et al*, 2003a).

KSHV like other large DNA viruses encodes genes whose protein products explicitly undermine the immune system responses, including the complement cascade thereby leading to persistent infection and pathogenesis within the host. One such protein product was predicted by sequence analysis to be encoded by the ORF 4 and in order to determine if there is a link between this protein and Kaposi's sarcoma lesions, biopsies from KS-HIV patients were tested for the presence of endogenous KCP involved in complement regulation. A disruption in the cell cycle regulatory mechanism takes place when cells acquire cancerous properties and hence their uncontrollable proliferation. Therefore, to determine the localisation of endogenous KCP in response to viral-induced transformation was also a motivation for this immunohistochemical study.

The immunohistochemical studies were performed using a polyclonal anti-KCP peptide primary antibody made against a number of different epitopes situated in the N-terminus of the KCP polypeptide and designed as part of the MSc project for immunodetection and Western blot analysis of the heterologously expressed recombinant KCPs.

For every scientific experiment that is performed, it is important to have controls so that any results obtained may be regarded as significant. For this same reason, an antibody control as well as a pre-immune control as shown in Figure 38 and 39 respectively, was carried out in order to show that if any immunostaining was obtained it might indeed be regarded as specific and reliable. In addition, other appropriate controls were used for proper interpretation of results. As a positive control, it was shown that HHV-infection could be detected in all three stages of KS, namely the early patch stage, the intermediate plaque stage and the most advanced nodular stage by nuclear staining using a mouse monoclonal anti-LANA antibody (Figure 41). However, only one out of the 4 cases for each stage of the disease stained positive for HHV-8. Furthermore, three other controls namely anti-CD31, anti-CD34 and anti-Cyclin D1 (Figures 40 A-C respectively) were used as positive controls for qualitative immunohistochemistry of the paraffin-embedded tissue sections viewed by light microscopy.

EnVision+™ (DAKO) was the system of choice to perform the immunohistochemical studies. Even with the best of systems, problems can sometimes occur, such as extremely high background staining, colour development in the wrong sections, or the staining of interest may be rather weak or absent. Because most often not all the reasons for undesirable staining are clear, trying to optimize the staining and therefore solving the problem may require the testing of a number of different controls on the tissue sections.

At the beginning of the study, the immunostaining of the KS tissue sections with the polyclonal anti-KCP peptide antibody resulted in an enormous degree of inappropriate background staining (Figure 39B). All the positive controls mentioned above resulted in the expected staining: clean nuclear staining when tissue sections were incubated with anti-LANA (Figure 41) and Cyclin D1 (Figure 40C), and strong cytoplasmic staining as well as cell membrane staining with the endothelial cell markers, CD34 and CD31 as shown in Figures 40B and 40A respectively. Therefore, from these set of results it was deduced that the non-specific staining obtained with the anti-KCP peptide antibody was not due to endogenous enzyme developing the substrate, in other words, the endogenous peroxidase was appropriately blocked with aqueous 1% hydrogen peroxide and in general the immunohistochemical technique was performed successfully. Furthermore, the secondary antibody, no primary antibody negative control (Figure 38B) indicated that the background staining was not caused by cross-reactivity between the peroxidase-conjugated goat anti-rabbit secondary antibody and endogenous immunoglobulins or other tissue proteins, which may take place if the secondary antibody reacts with identical or closely related amino acid sequences of these proteins.

The first step in troubleshooting the inappropriate background staining was to optimize the concentration of primary antibody used as the optimal concentration should be the amount capable of producing clean specific staining. Therefore, a series of dilutions of the primary antibody were tested and yet no significant improvement of the improper staining took place (results not shown).

It is a possibility that the antigen of interest may have been destroyed during embedding or fixation of the tissue sections and therefore an antigen unmasking technique referred to as heat induced epitope retrieval (HIER) was carried out in order to recover antigen damaged by fixation. HIER was tried out with two different buffers EDTA (pH 8) and citrate buffer (pH 6), in order to determine at which pH the HIER

was most efficient, thereby leading to a more optimum staining pattern. After visualizing the slides using light microscopy, the buffer of choice for unmasking of the antigen was EDTA (pH 8). Further troubleshooting of the inappropriate background staining had to be continued and in case the concentration of the polyclonal IgG of interest was too low for positive immunostaining, the polyclonal IgG was enriched for using a protein-A sepharose column. SDS-PAGE analysis (Figure 31) revealed that the IgG immunoglobulins were successfully concentrated from the serum sample (starting material) using this column. Immunostaining under exactly the same conditions of a KS tissue section, incubated with polyclonal anti-KCP peptide primary antibody post protein A-sepharose purification, revealed a significant improvement in the level of background staining (Figure 39C) when compared to the same tissue section incubated with the test antibody prior to the IgG purification step (Figure 39B).

Once the background staining was substantially diminished, 4 different KS cases corresponding to the three different stages of disease progression were investigated for the presence of endogenous KCP, using the EnVision+™ system, HIER with EDTA (pH 8) and the polyclonal anti-KCP peptide primary antibody at 1:10 000.

One of the most remarkable characteristics of tumour viruses such as KSHV is their ability to express protein homologs to cellular proteins, in order to evade the host immune system as described in Chapter 1 section 1.3.2.

KSHV encodes a complement inhibitor homologue, which because of its biological function is believed to be used by the virus as an active strategy to overcome the complement system and to infect endothelial cells. As shown in panel B of Figures 42-44, endogenous KCP was not detected by the polyclonal anti-KCP peptide antibody, in the nuclei or in the cytoplasm of the spindle cells of the KS lesion vascular channels, therefore no statistical conclusions could be drawn between the three stages of KS with the use of this antibody. The fact that the anti-KCP did not detect the presence of a KCP population within the tumour cells could simply mean that the expression of this protein is ceased upon viral infection of the spindle cells. This may be attributed to the fact that the ORF 4 gene is not an essential gene for replication of the virus but only for its initial interaction with the host during infection. Furthermore, the localisation of KCP may be a rather transient process, as the protein could be quickly degraded after the virus has successfully infected its host and ceases synthesizing endogenous KCP during latent infection.

Probably by using a more sensitive detection technique such as fluorescent microscopy, and a monoclonal anti-KCP made against native KCP such as the one synthesised by Spiller *et al* (2003a), which recognises one specific epitope would have been more successful in recognising a distinct population of endogenous KCP protein within the KS tissue samples, and this may indeed be considered for future work regarding this study.

4.2 Heterologous Production of KCP in the methylotrophic yeast *Pichia* pastoris

The *P. pastoris* yeast expression system has become a very popular means for heterologous protein production. It is as easy to work with as *E. coli* or *Saccharomyces cerevisia* as it is simple to grow and manipulate in large quantities in a controlled manner. In addition, it has been both genetically and biochemically unravelled, thus providing a favourable alternative for the high-level production of foreign proteins. As a eukaryotic organism, it possesses many of the advantages of higher eukaryotic expression systems including protein processing, protein folding and posttranslational modification. As methylotrophic yeast, *Pichia* is capable of utilising methanol as its unique carbon and energy source (Sreekrishna *et al*, 1997). The metabolism of methanol takes place in the peroxisome, a specialised cell organelle, which prevents hydrogen peroxide toxicity during the oxidation of methanol to formaldehyde in the presence of molecular oxygen (Oden, 1994). Methanol oxidase, the first enzyme in the methanol utilisation pathway, has a low affinity for O_2 and as a result the yeast compensates by synthesising large quantities of this enzyme. Therefore, the highly inducible and tightly regulated methanol oxidase gene (*AOX1*) promoter has been engineered in expression vectors to drive the synthesis of foreign proteins in *Pichia* (Sreekrishna *et al*, 1997).

The 8.0 kb expression vector pPIC9 was the plasmid selected for the recombinant expression of the three different sized KCPs because it has been used successfully for the secreted expression of recombinant VCP in *P. pastoris* (Smith *et al*, 2000) and it was readily available in the laboratory.

The three DNA-portions of the KSHV ORF 4 encompassing SCRs 1 to 4 were successfully amplified from a KSHV DNA template by PCR (Figure 14) using a KSHV ORF 4-specific forward primer and three consecutive KSHV ORF 4-specific

reverse primers. For the heterologous production of the KCPs in *P. pastoris*, PCR products were inserted by ligation into pPIC9 to generate three recombinant plasmids, pPIC9/KSHV ORF 4 (735), pPIC9/KSHV ORF 4 (1436) and pPIC9/KSHV ORF 4 (1581) coding for a soluble protein comprising of the 4 sushi domains (S-), a larger protein lacking the putative transmembrane binding domain (M-) and the full-length ORF 4 (F-) respectively (Figure 20). Integration of the three different sized KSHV ORF 4 genes into the *P.* pastoris genome was carried out by homologous recombination with these pPIC9/KSHV ORF 4 DNA constructs.

Double stranded plasmid DNA template, pPIC9/KSHVORF 4 (735), pPIC9/KSHVORF 4 (1436) and pPIC9/KSHVORF 4 (1581) isolated from *E. coli* transformants was subjected to restriction endonuclease digestion and the DNA fragments were analysed by agarose gel electrophoresis (Figure 23).

Recombinant colonies with the KSHV ORF 4 gene integrated in their genomes were initially used for small expression experiments in BMMY medium. Expression and secretion of the KCP-M and KCP-F viral proteins into the media was confirmed by immunoblot using a slot-blot apparatus after blotting 100 µl of culture media supernatant onto nitrocellulose Hybond-ECL membranes (Figure 34A and 35A respectively).

Small-scale expression was followed by medium-scale production of KSHV ORF 4 proteins from recombinant *P. pastoris* colonies transformed with the three *Sac* I-digested pPIC9/KSHV ORF 4 plasmid constructs. Culture media supernatants from colonies transformed with the pPIC9 empty vector (no insert) digested with *Sac* I pre- and 96 h post-induction was included as negative controls in all of the protein expression and detection experiments, in order to show that the protein of interest was solely detected in the supernatant of recombinant strains, transformed with pPIC9 constructs expressing the genes of interest.

The time-course of expression of the KCP-S, KCP-M and KCP-F proteins was monitored by SDS-PAGE (Figure 33A, 34B and 35B respectively), and in the case of the first two recombinant proteins the induction profile was also followed by Western blot analysis, which showed that the protein could be first detected at 48 h post-induction and the amount of protein continue to build until after 72 and 96 h (Figure 33B and 34C respectively) the latter being the time chosen to harvest the cells before they begin to lyse and release unwanted proteases into the media. In addition, the

polyclonal anti-KCP peptide antibody recognised several larger and smaller bands that may represent multimer aggregates and degradation products respectively. Intensities of SDS-PAGE bands were scanned with a densitometer and the concentration of the *P. pastoris*-expressed KCP protein was quantitively estimated by comparison with a standard curve obtained with known amounts of protein (Figure 29). Under these conditions, the yield of *P. pastoris* expressed KCP-S, KCP-M and KCP-F was about 5, 6.4 and 1.76 μg per millilitre of yeast culture medium respectively. This protein concentration estimation correlates with the first two recombinant proteins, KCP-S and -M obtained from medium-scale expression [100 ml] whereas the full-length KCP-F protein was obtained from a small-scale experiment [5 ml]. In the case of the latter the amount of detectable protein in the media was very low and as a result only upon concentration of 100 μl of protein sample, a successful Western blot of the protein was obtained (Fig 35C).

Transformants expressing detectable protein varied dramatically amongst different clones even from the same transformation procedure. Several recombinant colonies were analysed for protein expression, and although the presence of insert was confirmed by PCR, not all clones expressed detectable amounts of protein. This may be explained in terms of the limitations of using the *P. pastoris* such as sensitivity to temperature, humidity and other weather elements.

On the other hand, the small-scale expressions showed that both Mut^+ and Mut^S recombinant *P. pastoris* transformants were able to express the KSHV ORF 4 protein provided that a good clone was selected and used for the expression. According to the Invitrogen manual, Mut^+ colonies are capable of producing larger quantities of protein in shorter periods of time because the *AOX1* gene is kept intact and therefore its product, which accounts for the majority of the alcohol oxidase activity, increases the cell's ability to metabolise methanol as the sole carbon source. The *AOX1* gene promoter is strictly regulated and induced by methanol to high levels and consequently it is used to drive expression of the genes of interest. Therefore, Mut^+ transformants were preferably used throughout this study.

In order to determine whether or not the *P. pastoris*-expressed recombinant KCP proteins retained their functional activity, the ability of these proteins in medium to inhibit the complement classical pathway-mediated lysis of antibody-coated sheep erythrocytes was investigated. The results obtained, noticeably demonstrate that

unlike the ammonium-sulphate precipitated-supernatant from a *Pichia* culture transformed with pPIC9/KCP-M and F, the ammonium-sulphate precipitated-supernatant from a *Pichia* culture transformed with pPIC9/KCP-S contained a functional protein capable of binding complement proteins in a concentration-dependent fashion. If taking into account the low percentage complement inhibition caused by the same volume of background control, in other words, supernatants from *Pichia* culture transformed with pPIC9 (empty vector) that underwent the same induction and concentration steps as the test samples, it is clear that a KSHV functional regulator of human complement was successfully expressed in *P. pastoris* using the pPIC9/KCP-S construct (Figure 36).

The lack of biological activity obtained in the case of the other two recombinant KCPs may be attributed to the fact that unfractionated media was used containing many native contaminating bands (Figures 34 and 35B) and therefore it is possible that something in the yeast media may have inhibited the activity of KCP-M and KCP-F. Another possibility is that these two recombinant KCPs may have been differently folded before being secreted into the media. Therefore perhaps some of the complement binding sites may have been covered or modified in some way causing insufficient biological activity (1) because of their considerable molecular sizes and (2) the three non-conservative amino acid mutations (Figure 19) probably introduced during PCR-amplification. However, it is possible that these point mutations are natural occurring polymorphisms especially since the isolate available in the database is from a different source and from a different continent. The former discussed cause of the point mutations might have been avoided if a higher fidelity polymerase such as *Pfu* was used and the PCR product was sequenced instead of the intermediate plasmid.

In addition, only the full length KCP clone was sequenced therefore unknown point mutations may have been present in the other PCR cloned regions, which may be the reason why only the truncated version of KCP was able to inhibit complement-mediated lysis of sensitised sheep red blood cells.

Furthermore, the rKCP-F should not be secreted as it contains a functional transmembrane domain (Spiller *et al*, 2003a) nevertheless it may have undergone shedding, in other words cleavage of the ectodomain may have taken place resulting in the release of a soluble but inactive protein. Ectodomain shedding is a well recognized, but not fully understood biochemical process that represents an important

and efficient strategy of activity regulation in a number of transmembrane proteins (Werb and Yan, 1998).

The presence of glycans on other proteins belonging to the RCA family has been shown to extensively influence their biological activities. For example, the MCP isoforms with a larger *O*-glycosylation domain was found to bind C4b more efficiently than the smaller and less glycosylated isoforms (Liszewski *et al*, 1998). In order to examine rKCP-S for *N*-linked glycosylation, the supernatant from culture of the recombinant strain containing partially purified protein, was treated with PNGase F and subjected to SDS-PAGE analysis. The results show a shift in molecular weight between treated and untreated KCP-S from 56 kDa to approximately 27 kDa, the protein's theoretical molecular weight (Figure 37), indicating the presence of functional *N*-glycosylation sites in the heterologously expressed truncated KCP protein, which could effectively contribute to its significant bioactivity as shown in Figure 36.

In addition, Western blot analysis with the rabbit polyclonal antibody directed against a selected KSHV ORF 4 peptide, common to all three KCP recombinant proteins, showed that the *P. pastoris*-heterologously expressed soluble-, medium- and full-length KCPs migrated electrophoretically as higher bands, which most likely is due to glycosylation of the proteins as in addition to the presence of potential *N*- and *O*-linked carbohydrate sites in the protein's primary sequence, diffused bands were obtained in all the westerns carried out, which is characteristic of glycoproteins. Protein glycosylation therefore may be another reason attributing to the lack of biological activity of the KCP isoforms besides KCP-S.

In broad terms, knowledge acquired from this study may be implemented in health and disease, in the sense that inadequate activation and regulation of the complement system is regarded as a cause of tissue destruction. This in turn, has been shown to lead to the progress of a large number of medical conditions such as Alzheimer's disease, traumatic brain injury (TBI), ischemia, arthritis, rejection of xenogeneic transplants (Daly and Kotwal, 1998; Hicks *et al*, 2002; Sacks *et al*, 2003; Low and Moore, 2005) just to name a few. Therefore, the use of CCPs and its derivatives as inhibitors of undesirable complement activation is presently a very attractive area of research.

More specifically, knowledge acquired from this expression study may provide some new insight into the utility and limitations of the *P. pastoris* system for the production

of recombinant KCP. Perhaps with the use of different vectors, expression cassettes or even different transformation techniques the heterologous production of KCP may be greatly enhanced, which can then be used in various structure-function studies. Additionally, in future a His-tag version of KCP may be considered for expression and easy purification of the protein from mammalian cells. It is however difficult to predict whether proper post-translational modifications such as glycosylation and protein folding will occur. It may be essential to remove the His-tag after purification since addition of His residues might lead to a stretch of charge on the protein, which may in turn influence its activity.

Furthermore, it is of major significance to understand how CCPs such as the KCP protein, perform their biological functions at the structural level in order to gain insight for the development of new and more efficient therapeutic inhibitors of complement.

APPENDIX A

PLASMIDS AND *PICHIA* STRAINS

Plasmid	Relevant characteristics	Source of Reference
pGEMT-Easy	3.0 kb, Amp^R, T7 promoter, SP6 promoter	Promega
pGEMT/KSHV ORF4 (735)	3.8 kb, Amp^R, T7 promoter, SP6 promoter, 735 bp KCP gene	This study
pGEMT/KSHV ORF4 (1436)	4.5 kb, Amp^R, T7 promoter, SP6 promoter, 1436 bp KCP gene	This study
pGEMT/KSHV ORF4 (1581)	4.6 kb, Amp^R, T7 promoter, SP6 promoter, 1581 bp KCP gene	This study
pPIC9	8.0 kb, Amp^R, HIS4, P_{AOX1}, α-factor signal seq	Invitrogen
pPIC9/KSHV ORF4 (735)	8.8 kb, Amp^R, HIS4, P_{AOX1}, α-factor signal seq, 735 bp KCP gene	This study
pPIC9/KSHV ORF4 (1436)	9.5 kb, Amp^R, HIS4, P_{AOX1}, α-factor signal seq, 1436 KCP gene	This study
pPIC9/KSHV ORF4 (1581)	9.6 kb, Amp^R, HIS4, P_{AOX1}, α-factor signal seq, 1581 bp KCP gene	This study
Strains	**Relevant Characteristics**	**Source of Reference**
GS115	Wildtype, genotype *his*4, phenotype Mut^+	Invitrogen
GS115/pPIC9	GS115 transformed with pPIC9	This study
GS115/pPIC9/KSHV ORF4 (735)	GS115 transformed with pPIC9/KSHV ORF4 (735)	This study
GS115/pPIC9 KSHV ORF4 (1436)	GS115 transformed with pPIC9/KSHV ORF4 (1436)	This study
GS115/ pPIC9/KSHV ORF4 (1581)	GS115 transformed with pPIC9/KSHV ORF4 (1581)	This study

APPENDIX B

LIST OF MATERIALS AND SUPPLIERS

MATERIAL	SUPPLIER
o Ampicillin	Boehringer
o Ammonium Persulphate	Boehringer
o APES	Sigma
o BM Chemiluminescence Western Blotting kit	Roche
o Broad Range Protein Molecular Weight Marker	Promega
o Coomassie brilliant blue R- 250	Sigma
o DAB liquid	Dako
o DNeasy kit for DNA purification from yeast	Qiagen
o ECL Western Blotting Kit	Amersham
o EDTA	BDH
o EnVision System	Dako
o Ethidium Bromide	Sigma
o Expand High Fidelity PCR System	Roche
o HiTrap Protein A sepharose column	Amersham
o Lamda DNA/ *Eco* RI+*Hind* III	Promega
o Lyticase	Sigma
o Miniprep plasmid isolation kit	Qiagen
o Nitrocellulose Hybond- ECL membrane	Amersham
o Normal goat serum	Dako
o PCR Nucleotide mix	Promega
o pGEM-T Easy Vector System I	Promega
o *Pichia* EasyComp kit	Invitrogen
o *Pfu* DNA Polymerase	Promega
o PNGase F	Sigma
o Ponceau S	Sigma
o Restriction endonucleases	Roche
o *Taq* DNA Polymerase	Promega
o Tween-20	Merck
o X-ray film	Amersham
o Wizard SV gel and PCR clean-up system	Promega

REFERENCES

Alagiozoglou L, Sitas F and Morris L (2000) Phylogenetic analysis of human herpesvirus-8 in South Africa and identification of a novel subgroup. *J of General Virology* **81:**2029-2038

Alberts B, Bray D, Lewis J, Raff M, Roberts K and Watson JD (1994) Molecular Biology of the cell (3rd edition), pp860- 879. Garland Publishing, Inc., New York

Albrecht JC and Fleckenstein B (1992) New member of the multigene family of complement control proteins in herpesvirus saimiri. *J Virol* **66:** 3937-3940.

Albrecht J-C, Nicholas J, Biller D, Cameron KR, Biesinger B, Newman C, Wittmann S, Craxton MA, Coleman H, Fleckenstein B and Honess RW (1992) Primary structure of the herpesvirus Saimiri genome. *J. Virol* **66:** 5047-5058

Altschul SF, Madden TL, Schäffer AA, Zhang J, Zhang Z, Miller W and Lipman DJ (1997) Gapped BLAST and PSI-BLAST: a new generation of protein database search programs. *Nucleic Acids Res* **25:** 3389-3402

Ballestas ME, Chatis PA and Kaye KM (1999) Efficient persistence of extrachromasomal KSHV DNA mediated by latency-associated nuclear antigen. *Science* **284:** 641-644

Barbera AJ, Ballestas ME and Kaye KM (2004) The Kaposi's sarcoma-associated herpesvirus latency-associated nuclear antigen 1 N terminus is essential for chromosome association, DNA replication and episome persistence. *J. Virol* **78:** 294-301

Barilla-LaBarca ML, Liszewski MK, Lambris JD, Hourcade D and Atkinson JP (2002) Role of membrane cofactor protein (CD46) in regulation of C4b and C3b deposited on cells. *The Journal of Immunology* **168:** 6298-6304

Barlow PN, Steinkasserer A, Norman DG, Kieffer B, Wiles AP, Sim RB, Campbell ID (1993) Solution structure of a pair of complement modules by nuclear magnetic resonance. *J Mol Biol* **232:** 268-284.

Blom AM, Webb J, Villoutreix BO and Dahlbäck B (1999) A cluster of positively charged amino acids in the C4BP α-chain is crucial for C4b binding and factor I cofactor function. *The Journal of Biological Chemistry* **274:** 19237-19245

Blom AM (2004) Strategies developed by bacteria and virus for protection from the human complement system. *Scand J Clin Lab Invest* **64:** 479-496

Boshoff C and Weiss R (2002) AIDS- related malignancies. *Nature Reviews* **2:** 373-382

Boshoff C (2003) Kaposi's sarcoma scores cancer coup. *Nature medicine* **9:** 261-262

Bower M, Fox P, Fife K, Gill J, Nelson M and Gazzard B (1999) Highly active anti-retroviral therapy (HAART) prolongs time to treatment failure in Kaposi's sarcoma. *AIDS* **13:** 2105-2111

Bradford, MM (1976) A rapid and sensitive method for the quantification of microgram quantities of protein utilising the principle of protein- dye binding. *Anal Biochem* **72:** 248-254

Cannon MJ, Laney AS and Pellett PE (2003) Human Herpesvirus 8: Current Issues. *Emerging Infections* **37:** 82-87

Cesarman E, Moore PS, Rao PH, Inghirami G, Knowles DM, Chang Y (1995) *In vitro* establishment and characterization of two AIDS-related lymphoma cell lines containing Kaposi's sarcoma-associated herpesvirus-like (KSHV) DNA sequences. *Blood* **86:** 2708-2714

Cesarman E, Nador RG, Bai F, Bohenzky RA, Russo JJ, Moore PS, Chang Y and Knowles DM (1996) Kaposi's sarcoma-associated herpesvirus contains G protein-coupled receptor and cyclin D homologs which are expressed in Kaposi's sarcoma and malignant lymphoma. *J of Virology* **70:** 8218-8223

Chang Y, Cesarman E, Pessin MS, Lee F, Culpepper J, Knowles DM and Moore PS (1994) Identification of herpesvirus-like DNA sequences in AIDS-associated Kaposi's sarcoma. *Science* **266:**1865-1869

Chaston TB and Lidbury BA (2001) Genetic "budget" of viruses and the cost to the infected host: a theory on the relationship between the genetic capacity of viruses, immune evasion, persistence and disease. *Immunol Cell Biol* **79:** 62-66

Chor PJ and Santa Cruz DJ (1992) Kaposi's sarcoma: a clinicopathologic review and differential diagnosis. *J Cutan Pathol* **19:** 6-20

Ciufo DM, Cannon JS, Poole LJ, Wu FY, Murray P, Ambinder RF and Hayward GS (2001) Spindle cell conversion by Kaposi's sarcoma associated herpesvirus: formation of colonies and plaques with mixed lytic and latent gene expression in infected primary dermal microvascular endothelial cell cultures. *J. Virol* **75:** 5614-5626

Coscoy L and Ganem D (2000) Kaposi's sarcoma-associated herpesvirus encodes two proteins that block cell surface display of MHC class I chains by enhancing their endocytosis. *Proc Natl Acad Sci USA* **94:** 8051-8056

Curreli F, Robles MA, Friedman-Kien AE and Flore O (2003) Detection and quantization of Kaposi's sarcoma-associated herpesvirus (KSHV) by a single competitive-quantitative polymerase chain reaction. *Journal of Virological Methods* **107:** 261-267

Dahlabäck B and Müller-Eberhard (1984) Ultrastructure of C4b-binding protein fragments formed by limited proteolysis using chymotrypsin. *J Biol Chem* **259:** 11631-11634

Dietz M (2000) Viral Cytokines. *Stem Cells* **18:** 69-72

Daly J and Kotwal GJ (1998) Pro-inflammatory complement activation by the Aβ peptide of Alzheimer's disease is biologically significant and can be blocked by vaccinia virus complement control protein. *Neurobiology of Aging* **19:** 619-627

Dupin N, Fisher C, Kellam P, Ariad S, Tulliez M, Franck N, van Marck E, Salmon D, Gorin, I, Escande JP, Weiss RA, Alitalo K and Boshoff C (1999) Distribution of human herpesvirus-8 latently infected cells in Kaposi's sarcoma, multicentric castleman's disease and primary effusion lymphoma. *Proc Natl Acad Sci USA* **96:** 4546-4551

Fishelson Z, Donin N, Zell S, Schultz S and Kirscfink M (2003) Obstacles to cancer immunotherapy: expression of membrane complement regulatory proteins (mCRPs) in tumours. *Molecular Immunology* **40:** 109-123

Friborg J Jr, Kong WP, Hottiger M and Nabel G (1999) p53 inhibition by the LANA protein of KSHV protects against cell death. *Nature* **402:** 889-94

Friedman HM, Cohen GH, Eisenberg RJ, Seidel CA and Cines DB (1984) Glycoprotein C of herpes simplex virus 1 acts as a receptor for the C3b complement component on infected cells. *Nature* **309:** 633-635

Fujimuro M, Wu FY, apRhys C, Kajumbula H, Young DB, Hayward GS and Hayward SD (2003) A novel viral mechanism for deregulation of β-catenin in Kaposi's sarcoma-associated herpesvirus latency. *Nature medicine* **9:** 300-306

Gaidano G, Cechova K, Chang Y, Moore PS, Knowles DM and Dalla-Favera R (1996) Establishment of AIDS-related lymphoma cell lines from lymphomatous effusions. *Leukemia* **10:** 1237-1240

Gaidano G, Gloghini A, Gattei V, Rossi MF, Cilia AM, Godeas C, Degan M, Perin T, Canzonieri V, Aldinucci D, Saglio G, Carbone A and Pinto A (1997) Association of Kaposi's sarcoma-associated herpesvirus-positive primary effusion lymphoma with expression of the CD138/syndecan-1 antigen. *Blood* **90:** 4894-4900

Gao S-J, Boshoff C, Jayachandra S, Weiss RA, Chang Y and Moore PS (1997) KSHV ORF K9 (vIRF) is an oncogene which inhibits interferon signalling pathway. *Oncogene* **15:** 1979-1985

Geraminejad P, Memar O, Aronson I, Rady PL, Hengge U and Tyring K (2002) Kaposi's sarcoma and other manifestations of human herpesvirus-8. *J Am Acad Dermatol* **47:** 641-55

Hartwell LH and Weinert TA (1989) Checkpoints: Controls that ensure the order of cell cycle events. *Science* **246:** 629-634

Hengel H, Brune W and Koszinowski UH (1998) Immune evasion by cytomegalovirus-survival strategies of a highly adapted opportunist. *Trends Microbiol* **6:** 190-197

Hermans P (2000) Opportunistic AIDS-associated malignancies in HIV-infected patients. *Biomed & Pharmacother* **54:** 32-40

Hicks RR, Keeling KL, Yang M-Y, Smith SA, Simons AM and Kotwal GJ (2002) Vaccinia virus complement control protein enhances functional recovery after traumatic brain injury. *Journal of Neurotrauma* **19:** 705-714

Hideshima T, Chauhan D, Teoh G, Rage N, Treon SP, Tai YT, Shima Y and Anderson KC (2000) Characterisation of signalling cascades triggered by human interleukin-6 versus Kaposi's sarcoma-associated herpes virus-encoded viral interleukin 6. *Clin Cancer Res* **6:** 1180-1189

Higgins D, Thompson J, Gibson T, Thompson JD, Higgins DG and Gibson TJ (1994) CLUSTAL W: Improving the sensitivity of progressive multiple sequence alignment through sequence weighting, position-specific gap penalties and weight matrix choice. *Nucleic Acids Res* **22:** 4673- 4680

Hong A, Davies S and Lee CS (2003) Immunohistochemical detection of the human herpes virus 8 (HHV-8) latent nuclear antigen-1 in Kaposi's sarcoma. *Pathology* **35:** 448-450

Hourcade D, Holers VM and Atkinson JP (1989) The regulators of complement activation (RCA) gene cluster. *Adv Immunol* **45:** 381- 416

Hourcade D, Garcia AD, Post TW, Taillon Miller P, Holers VM, Wagner LM, Bora NS, Atkinson JP (1992) Analysis of the human regulators of complement activation (RCA) gene cluster with yeast artificial chromosomes (YACs). Genomics **12:** 289-300

Jenner RG, Alba MM, Boshoff C and Kellam P (2001) Kaposi's sarcoma-associated herpesvirus latent and lytic gene expression as revealed by DNA arrays. *J Virol* **75:** 891-902

Jenner RG and Boshoff C (2002) The molecular pathology of Kaposi's sarcoma-associated herpesvirus. *Biochimica et Biophysica Acta* **1602:** 1-22

Judde JG, Lacoste V, Briere J, Kassa-Kelembho E, Clyti E, Couppie P, Buchrieser C, Tulliez M, Morvan J and Gessain A (2000) Monoclonality or oligoclonality of human herpesvirus 8 terminal repeat sequences in Kaposi's sarcoma and other diseases. *J. Natl. Cancer Inst.* 92: 729-736

Kapadia SB, Molina H, van Berkel V, Speck SH and Virgin HW (1999) Murine gammaherpesvirus 68 encodes a functional regulator of complement activation. *J Virol* **73:** 7658-7670.

Kirkitadze MD and Barlow PN (2001) Structure and flexibility of the multiple domain proteins that regulate complement activation. *Immunol Rev* **180:** 146-61.

Kojima A, Iwata K, Seya T, Matsumoto M, Ariga H, Atkinson JP and Nagasawa S (1993) Membrane cofactor protein (CD46) protects cells predominantly from alternative complement pathway- mediated C3-fragment deposition and cytolysis. *J Immunol* **151:** 1519-1527

Kotwal GJ (2000) Poxviral mimicry of complement and chemokine system components: what's the end game? *Rev Immun Today* **21:** 242-248

Kotwal GJ, Hugin AW and Moss B (1989) Mapping and insertional mutagenesis of a vaccinia virus gene encoding a 13.800-Da secreted protein. *Virology* **171:** 579-587

Kotwal GJ, Isaacs SN, McKenzie R, Frank MM and Moss B (1990) Inhibition of the complement cascade by the major secretory protein of vaccinia virus. *Science* **250:** 827-30

Kotwal GJ, Miller CG and David EJ (1998) The inflammation modulatory protein (IMP) of cowpox virus drastically diminishes the tissue damage by down-regulating cellular infiltration resulting from complement activation. *Molecular and Cellular Biochemistry* **185:** 39-46

Kotwal GJ and Moss B (1988) Vaccinia virus encodes a secretory polypeptide structurally related to complement control proteins. *Nature* **335:** 176-178

Kotwal GJ and Moss B (1989) Vaccinia virus encodes two proteins that are structurally related to members of the plasma serine protease inhibitor superfamily. *J. Virol* **63:** 600-606

Laemmli, UK (1970) Cleavage of structural proteins during the assembly of the head of bacteriophage T4. *Nature* **227:** 680-685

Laman H and Boshoff C (2001) Is KSHV lytic growth induced by a methylation-sensitive switch? *Trends in Microbiology* **9:** 464-66

Lambris JD, Sahu A and Wetsel R (1998) The chemistry and biology of C3, C4 and C5; in *The human complement system in health and disease* (eds) JE Volanakis and M Frank (New York: Marcel Dekker) pp 83-118

Liszewski MK, Leung M, Cui W, Subramanian VB, Parkinson J, Barlow PN, Manchester M and Atkinson JP (2000) Dissecting sites important for complement

regulatory activity in membrane cofactor protein (MCP; CD46). *J Biol Chem* **275:** 37692-37701

Low JM and Moore TL (2005) A role for the complement system in rheumatoid arthritis. *Curr Pharm Des.* **11:** 655-670

Lubinski J, Wang L, Mastellos D, Sahu A, Lambris JD, Friedman HM (1999) In vivo role of complement interacting domains of herpes simplex virus type 1 glycoprotein gC. *J Exp Med* **190:** 1637-1646

Luttichau HR, Stine J, Boesen TP, Johnsen AH, Chantry D, Gerstoft J and Schwartz TW (2000) A highly selective CC chemokine receptor (CCR) 8 antagonist encoded by the poxvirus molluscum contagiosum. *J Exp Med* **191:** 171-18

Madigan MT, Martinko JM and Parker J (2000) *Brock Biology of Microorganisms.* (9th Edition). Prentice Hall International, New Jersey, 269-270

Maley F, Trimble RB, Tarentino AL and Plummer TH Jr (1989) Characterisation of glycoproteins and their associated oligosaccharides through the use of endoglycosidases. *Analy Biochem* **180:** 195-204

Mann DJ, Child ES, Swanton C, Laman H and Jones N (1999) Modulation of p27 (Kip1) levels by the cyclin encoded by Kaposi's sarcoma-associated herpesvirus. *EMBO J* **18:** 654-663

Masumi A, Wang IM, Lefebvre B Yang XJ, Nakatani Y and Ozato K (1999) The histone acetylase PCAF is a phorbol-ester-inducible coactivator of the IRF family that confers enhanced interferon responsiveness. *Mol Cell Biol* **19:** 1810-1820

Matolcsy A, Nador RG, Cesarman E and Knowles DM (1998) Immunoglobulin VH gene mutational analysis suggests that primary effusion lymphomas derive from different stages of B cell maturation. *Am J Pathol* **153:** 1609-1614

McGeer PL and McGeer EG (1992) Complement proteins and complement inhibitors in Alzheimer's disease. *Research in Immunology* **143:** 624-630

McKenzie R, Kotwal GJ, Moss B, Hammer CH and Frank MM (1992) Regulation of complement activity by vaccinia virus complement-control protein. *JID* **166:** 1245-1250

Medof ME, Walter EI, Roberts WL, Haas R and Rosenberry TL (1986) Decay accelerating factor is anchored to cells by a C- terminal glycolipid. *Biochemistry* **25:** 6740-6747

Meri S, Morgan BP, Davies A, Daniels RH, Olavesen MG, Waldmann H and Lachmann PJ (1990) Human protectin (CD59), an 18000-20000 MW complement lysis restricting factor, inhibits C5b-8 catalysed insertion of C9 into lipid bilayers. *Immunology* **71:** 1-9

Miller CG, Shchelkunov SN and Kotwal GJ (1997) The cowpox virus-encoded homolog of the vaccinia virus complement control protein is an inflammation modulatory protein. *Virology* **229:** 126-133

Miller G, Heston L, Grogan E, Gradoville L, Rigsby M, Sun R, Shedd D, Kushnaryov VM, Grossberg S and Chang Y (1997) Selective switch between latency and lytic replication of Kaposi's sarcoma herpesvirus and Epstein-Barr virus in dually infected body cavity lymphoma cells. *J. Virol* **71:** 314-324

Milligan S, Robinson M, O'Donnell E and Blackbourn DJ (2004) Inflammatory Cytokines inhibit Kaposi's sarcoma-associated herpesvirus lytic gene transcription in *In Vitro*-infected endothelial cells. *J Virol* **78:** 2591-2596

Montefiori DC, Cornell RJ, Zhou JY, Zhou JT, Hirsch VM and Johnson PR (1994) Complement control proteins, CD46, CD55, and CD59, as common surface constituents of human and simian immunodeficiency viruses and possible targets for vaccine protection. *Virology* **205:** 82-92.

Moore PS and Chang Y (2001) Kaposi's sarcoma-associated herpesvirus. *In* Knipe DM and Howley PM (ed.), Fields Virology (4th edition, Vol.2). Lippincott Williams and Wilkins, USA. pp 2803-2833

Moore PS, Gao S-J, Dominguez E, Cesarman O, Lungu DM, Knowles R, Garber DJ, McGeoch P, Pellett P and Chang Y (1996) Primary characterization of a herpesvirus-like agent associated with Kaposi's sarcoma. *J. Virol* **70:** 549-558

Muller-Eberhard HJ (1986) The membrane attack complex of complement. *Annu Rev Immunol* **4:** 503-528

Mullick J, Bernet J, Singh AK, Lambris JD and Sahu A (2003) Kaposi's sarcoma-associated herpesvirus (human herpesvirus 8) open reading frame 4 protein (Kaposica) is a functional homolog of complement control proteins. *J. Virol* **77:** 3878-3881

Murthy KHM, Smith SA, Ganesh VK, Judge KW, Mullin N, Barlow PN, Ogata CM and Kotwal GJ (2001) Crystal structure of a complement control protein that regulates both pathways of complement activation and binds heparan sulfate proteoglycans. *Cell* **104:** 301-311

Nagashunmugam T, Lubinski J, Wang L, Goldstein LT, Weeks BS, Sundaresan P, Kang EH, Dubin G, Friedman HM. (1998) In vivo immune evasion mediated by herpes simplex virus type 1 immunoglobulin G Fc receptor. *J. Virol* **72:** 5351-5359

Neipel F, Albrecht JC and Fleckenstein B (1997) Cell-homologous genes in the Kaposi's sarcoma-associated rhadinovirus human herpesvirus 8: determinants of its pathogenicity. *J. Virol* **71:** 4187-4192

Nicholas J, Zong JC, Alcendor DJ, Ciufo DM, Poole IJ, Saeisky RT, Chiou CJ, Zhang X, Wan X, Guo HG, Reitz MS and Hayward GS (1998) Novel organizational features, captured cellular genes, and strain variability within the genome of KSHV/HHV8. *J Natl Cancer Inst Monogr* **23:** 79-88

Nicholson-Weller A and Wang CE (1994) Structure and function of decay accelerating factor CD55. *J Lab Clin Med* **123:** 485-491

Nielsen CH, Fischer EM, and Leslie RG (2000) The role of complement in the acquired immune response. *Immunology* **100:** 4-12

Oden KL (1994) A manual of methods for expression of recombinant proteins in *Pichia pastoris*. Version 3.0 Invitrogen Corporation, San Diego.

O' Farrel, PH (1975) High resolution two-dimensional electrophoresis of proteins. *J Biol Chem* **250:** 4007- 4021

Pan L, Malligan L, Michaeli J, Cesarman E and Knowles DM (2001) Polymerase chain reaction of Kaposi's sarcoma-associated herpesvirus-optimised protocols and their application to myeloma. *JMD* **3:** 32-38

Parravinci C, Corbellino M, Paulli M, Magrini U, Lazzarino M, Moore PS and Chang Y (1997) Expression of a virus-derived cytokine, KSHV vIL-6, in HIV-seronegative Castleman's disease. *Am J Pathol* **151:** 1517-1522

Pozhaarskaya VP, Weakland LL and Offermann MK (2004) Inhibition of infectious human herpesvirus 8 production by gamma interferon and alpha interferon in BCBL-1 cells. *J Gen Virol* **85:** 2779-2787

Renne R, Lagunoff M, Zhong W and Ganem D (1996) The size and conformation of Kaposi's sarcoma-associated herpesvirus (HHV-8) DNA in infected cells and virions. *J. Virol* **70:** 8151-8154

Romanos MA, Scorer CA and Clare JJ (1992) Foreign gene expression in yeast: a review. *Yeast* **8:** 423-488

Rother RP, Rollins SA, Fodor WL, Albrecht JC, Setter E, Fleckenstein B and Squinto SP (1994) Inhibition of complement-mediated cytolysis by the terminal complement inhibitor of herpesvirus saimiri. *J Virol* **68:** 730-737

Russo JJ, Bohenzky RA, Chien M-C, Chen J, Yan M, Maddalena D, Parry JP, Peruzzi D, Edelman IS, Chang Y and Moore PS (1996) Nucleotide sequence of the Kaposi sarcoma-associated herpesvirus (HHV8). *Proc Natl Acad Sci USA* **93:** 14862-14867

Sacks SH, Chowdhury P and Zhou W (2003) Role of the complement system in rejection. *Current opinion in Immunology* **15:** 487-492

Sahu A and Lambris JD (2001) Structure and biology of complement protein C3, a connecting link between innate and acquired immunity. *Immunol Rev* **180:** 35-48

Sahu A, Isaacs SN, Soulika AM and Lambris JD (1998a) Interaction of vaccinia virus complement control protein with human complement proteins: factor I-mediated degradation of C3b to iC3b1 inactivates the alternative complement pathway. *J Immunol* **1:** 5596-5604

Sahu A, Morikis D and Lambris JD (2000) Complement inhibitors targeting C3, C4 and C5 in *Therapeutic interventions in the complement system* (eds) JD Lambris and VM Holers (Totowa: Humana Press) pp 75-112

Sahu A, Sunyer JO, Moore WT, Sarrias MR, Soulika AM and Lambris JD (1998b) Structure, functions, and evolution of the third complement component and viral molecular mimicry. *Immunol Res* **17:** 109-121

Sanger F, Nicklen S and Coulson AR (1977) DNA sequencing with chain terminating inhibitors. *Proc Natl Acad Sci USA* **74:** 5463-5467

Sato N and Torigoe T (1998) The molecular chaperones in cell cycle control. *Annals of the New York Academy of Sciences* **851:** 61-66

Sarid R, Flore O, Bohenzky RA, Chang Y and Moore PS (1998) Transcription mapping of the Kaposi's sarcoma-associated herpesvirus (Human herpesvirus 8) genome in a body cavity-based lymphoma cell line (BC-1). *J. Virol* **72:** 1005-1012

Sellers WR and Kaelin WG (1996) pRB as a modulator of transcription. *Biochem Biophys Act* **1288:** M1- M5

Sewada R, Ohashi K, Anaguchi H, Okazaki H, Hattori M, Minato N, and Naruto M (1990) Isolation and expression of the full- length cDNA encoding CD59 antigen of human lymphocytes. *DNA Cell Biol* **9:** 213- 220

Shulz TF, Sheldon J and Greensill J (2002) Kaposi's sarcoma associated herpesvirus (KSHV) or human herpesvirus 8 (HHV8). *Virus Research* **82:** 115-126

Smith SA and Kotwal GJ (2001) Virokines: novel immunomodulatory agents. *Expert Opin Biol Ther* **1:** 343-357

Smith SA, Mullin NP, Parkinson J, Shchelkunov SN, Totmenin AV, Loparev VN, Spiller OB, Morgan BP, Tufaro F and Devine DV (1996) Altered expression of host-encoded complement regulators on human cytomegalovirus-infected cells. *Eur J Immunol* **26:** 1532-1538.

Smith SA, Mullin NP, Parkinson J, Shchelkunov SN, Totmenin AV, Loparev VN, Srisatjaluk R, Reynolds DN, Keeling KL, Justus DE, Barlow PN and Kotwal GJ (2000)

Conserved surface-exposed K/R-X-K/R motifs and net positive charge on poxvirus complement control proteins serve as putative heparin binding sites and contribute to inhibition of molecular interactions with human endothelial cells: a novel mechanism for evasion of the host defence. *J. of Virol* **74:** 5659-5666

Smith SA, Krishnasamy G, Murthy KHM, Cooper A, Bromek K, Barlow PN and Kotwal, GJ (2002) Vaccinia virus complement control protein is monomeric, and retains structural and functional integrity after exposure to adverse conditions. *Biochimica et Biophysica Acta* **1598:** 55-64

Smith SA, Screenivasan R, Krishnasamy G, Judge KW, Murthy KH, Arjunwadkar SJ, Pugh DR and Kotwal GJ (2003) Mapping of regions within the vaccinia virus complement control protein involved in dose-dependent binding to key complement components and heparin using surface plasmon resonance. *Biochimica et Biophysica Acta* **1650:** 30-39

Spiller OB, Blackbourn DJ, Mark L, Proctor DG and Blom AM (2003b) Functional activity of the complement regulator encoded by Kaposi's sarcoma associated herpesvirus. *J Biol Chem* **278:** 9283-9289

Spiller OB, Robinson M, O'Donnell E, Milligan S, Morgan BP, Davison AJ and Blackbourn DJ (2003a) Complement regulation by Kaposi's sarcoma-associated herpesvirus ORF4 protein. *J. Virol* **77:** 592-599

Sreekrishna K, Brankamp RG, Kropp KE, Blankenship DT, Tsay J, Smith PL, Wierschke JD, Subramaniam A and Birkenberger LA (1997) Strategies for optimal synthesis and secretion of heterologous proteins in the methylotrophic yeast *Pichia pastoris*. *Gene* **190:** 55-62

Srisatjaluk R, Reynolds DN, Keeling KL, Justus DE, Barlow PL and Kotwal GJ (2000) Conserved Surface-exposed K/R-X-K/R motifs and net positive charge on poxvirus complement control proteins serve as putative heparin binding sites and contribute to inhibition of molecular interactions with human endothelial cells: a novel mechanism for evasion of host defence. *J. Virol* **74:** 5659-5666

Swanton C, Mann DJ, Fleckenstein B, Neipel F, Peters G and Jones N (1997) Herpes viral cyclin/Cdk6 complexes evade inhibition by CDK inhibitor proteins. *Nature* **390:** 184-187

Taraboletti G, Benelli R, Borsotti P, Rusnati M, Presta M, Giavazzi R, Ruco L and Albini A (1999) Thrombospondin-1 inhibits Kaposi's sarcoma (KS) cell and HIV-1 Tat-induced angiogenesis and is poorly expressed in KS lesions. *J Pathol* **188:** 76-81

Thompson J D, Higgins DJ, and Gibson TJ (1994) CLUSTAL W: improving the sensitivity of progressive multiple sequence alignment through sequence weighting, positions-specific gap penalties and weight matrix choice. *Nucleic Acids Research* **22:** 4673-4680.

Upton C, Mossman K and McFadden G (1992) Encoding of a homolog of the IFN-gamma receptor by myxoma virus. *Science* **258:** 1369-1372

Van der Heuvel S and Harlow E (1993) Distinct roles for cyclin-dependent kinases in cell cycle control. *Science* **262:** 2050-2053

Vanderplasschen A, Mathew E, Hollinshead M, Sim RB and Smith GL (1998) Extracellular enveloped vaccinia virus is resistant to complement because of incorporation of host complement control proteins into its envelope. *Proc Natl Acad Sci USA* **95:** 7544-7549

Varthakavi V, Smith RM, Deng H, Sun R and Spearman P (2002) Human immunodeficiency virus typl-1 activates lytic cycle replication of Kaposi's sarcoma-associated herpesvirus through induction of KSHV Rta. *Virology* **297:** 270-280

Walport MJ (2001) Complement. *N Engl J Med* **344:** 1140-1144

Wang JY (1997) Retinoblastoma protein in growth suppression and death protection. *Curr Opin Genet Dev* **7:** 39- 45

Wang SE, Wu FY, Fujimuro M, Zong J, Hayward SD and Hayward GS (2003) Role of CCAAT/Enhancer-binding protein alpha (C/EBPα) in activation of the Kaposi's sarcoma-associated herpesvirus (KSHV) lytic-cycle replication-associated protein (RAP) promoter in cooperation with the KSHV replication and transcription activator (RTA) and RAP. *J. Virol* **77:** 600-623

Wang X-P and Gao S-J (2003) Auto-activation of the transforming viral interferon regulatory factor encoded by Kaposi's sarcoma-associated herpesvirus (HHV-8). *J Gen Virol* **84:** 329-336

Weiß HM, Haase W, Michel H and Reiländer H (1995) Expression of functional mouse 5-HT_{5A} serotonin receptor in the methylotrophic yeast *Pichia pastoris*: pharmacological characterisation and localization. *FEBS Letters* **377:** 451-456

Zong J, Ciufo DM, Viscidi R, Alagiozoglou L, Tyring S, Rady P, Orenstein J, Boto W, Kalumbuja H, Romano N, Melbye M, Kang GH, Boshoff C and Hayward GS (2002) Genotypic analysis at multiple loci across Kaposi's sarcoma herpesvirus (KSHV) DNA molecules: clustering patterns, novel variants and chimerism. *J. Clinical Virology* **23:** 119-148